# Small x physics

*Anna Staśto*

Penn State University

# Outline

**Lecture 1:**

Introduction to Deep Inelastic Scattering
Parton model
Collinear framework: factorization
DGLAP evolution equations
Parton distribution functions from DGLAP
Nuclear structure functions
Nuclear PDFs
EIC prospects for inclusive DIS and nPDFs

**Lecture 2:**

Regge theory and Pomeron
Outline of BFKL construction:
- Effective Lipatov vertex
- Gluon reggeizeation: trajectory

BFKL equation
Eigenvalue.  Collinear structure
Properties of the solution:
- Diffusion
- Increase with energy

Small x anomalous dimension

**Lecture 3:**

BFKL at NLL: large correction
Collinear limit of NLL BFKL
Resummation:
- Kinematical constraint, shifts of poles
- DGLAP anomalous dimension

Resummed result in Mellin space
Resummed result in momentum space
Improved small x  splitting function
Phenomenology examples

**Lecture 4:**

Dipole model: GBW example
BFKL revisited: Mueller dipole evolution
Multiple rescattering: BK evolution
Properties of solution to BK equation
Saturation scale
Impact parameter dependence
Phenomenology examples: structure functions, diffraction, angular decorelations

# Literature

Completely incomplete list of useful resources:

**Collinear factorization**

*S. Catani, Introduction to QCD ( CERN lectures)*

**BFKL**:

*J. R. Forshaw & D. A. Ross, Quantum Chromodynamics and the Pomeron*

*V. del Duca, hep-ph/9503226, An introduction to the perturbative QCD pomeron and to jet physics at large rapidities*

(+ other topics) *V. Barone & E. Predazzi, High Energy Particle Diffraction*

(BFKL in the dipole formalism) *A.H. Mueller, Soft gluons in the infinite momentum wave function and the BFKL pomeron*

**Saturation, nonlinear evolution**:

*Y.V. Kovchegov, hep-ph/9901281,Small x F(2) structure function of a nucleus including multiple pomeron exchanges*

*I. Balitsky, hep-ph/9509348, Operator expansion for high-energy scattering*

*Y.V. Kovchegov & E. Levin, Quantum Chromodynamics at High Energy*

**Resummation:**

*G.P. Salam, hep-ph/9910492, An Introduction to leading and next-to-leading BFKL*

*+ papers by Ciafaloni et.al*

# Motivation: high energy particle collisions

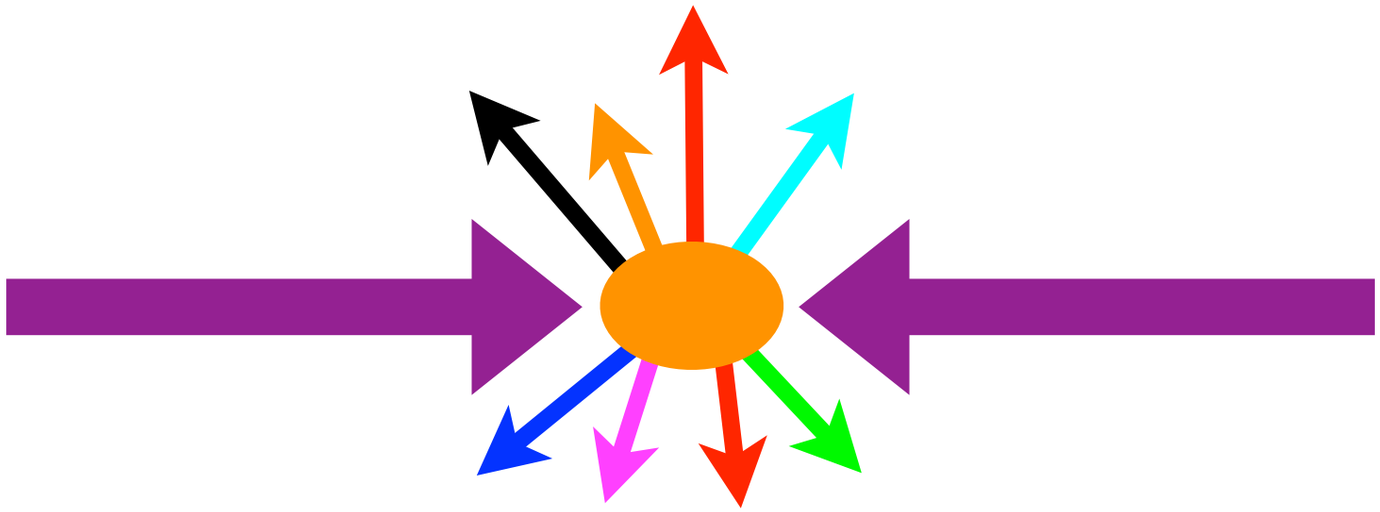

High energy of collision: $\sqrt{s} \gg m, \Lambda_{QCD}$

*Standard Model of Particle Physics*

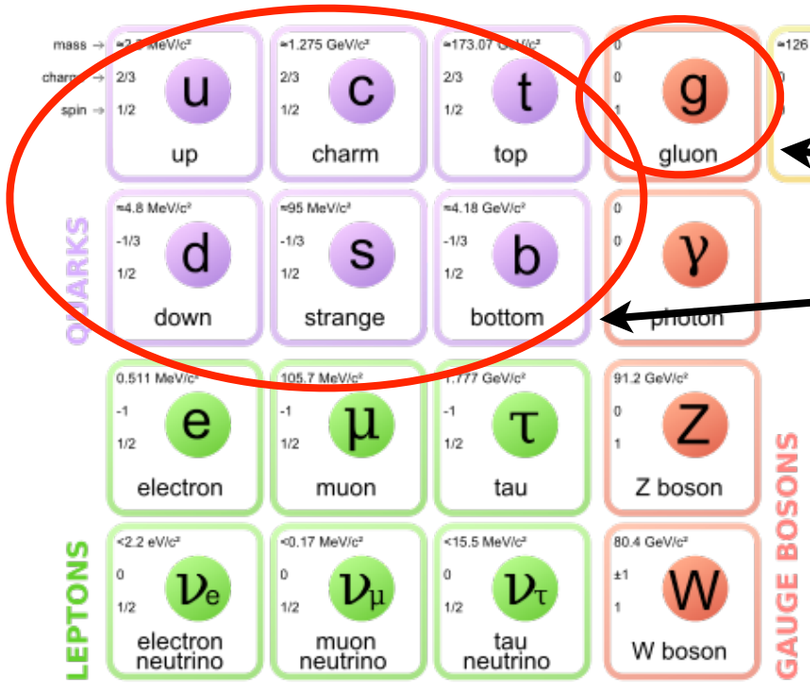


*strongly interacting sector of SM: Quantum Chromodynamics (QCD)*

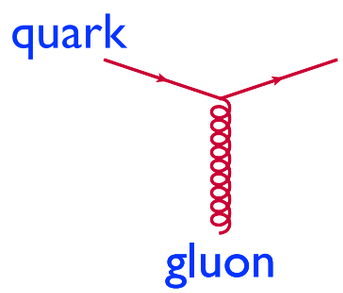


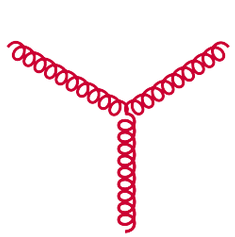

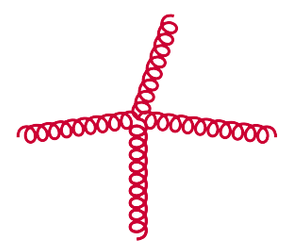

gluon interactions

# Motivation: what is high energy (small x) regime of QCD ?

Understand the regime of **high energy QCD** in particle collisions.

Test the **universality** of this regime in **different processes/collisions**.

Important in itself and for applications: eg. initial state in **heavy ion** collisions, **astroparticle** physics.

Structure function $F_2$
**electron-proton**

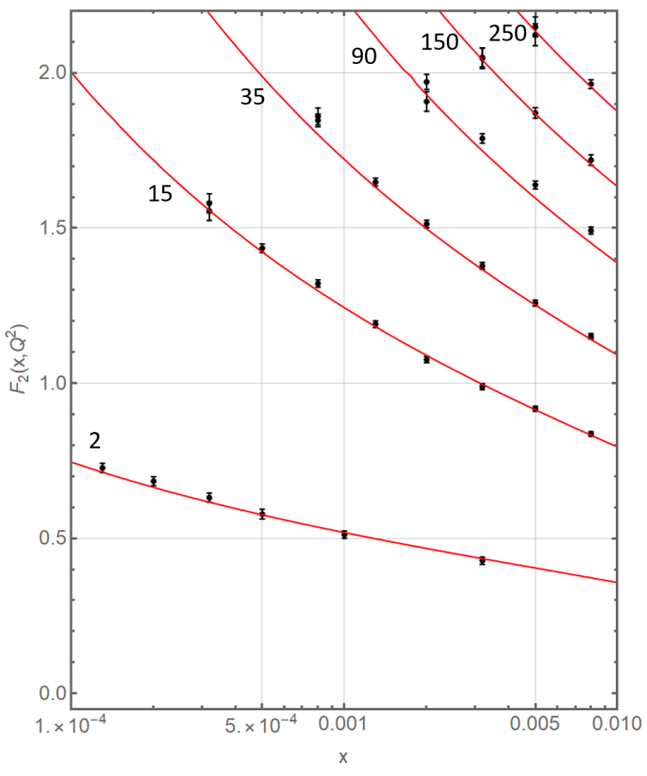


Exclusive vector-meson: **electron-proton**

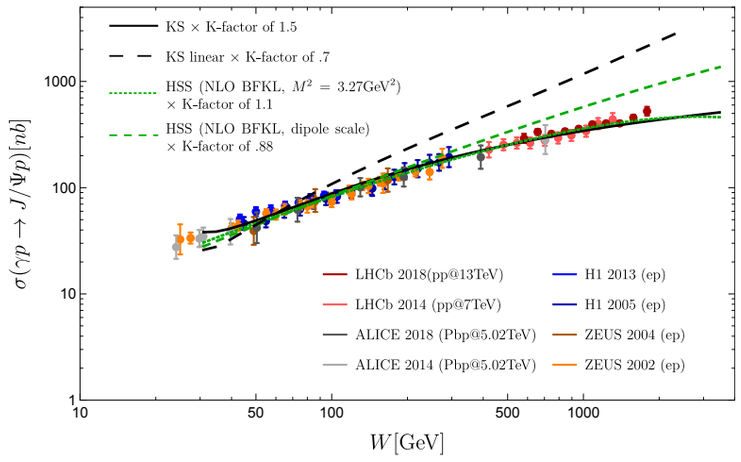


Virtual photon scattering
**electron-positron**

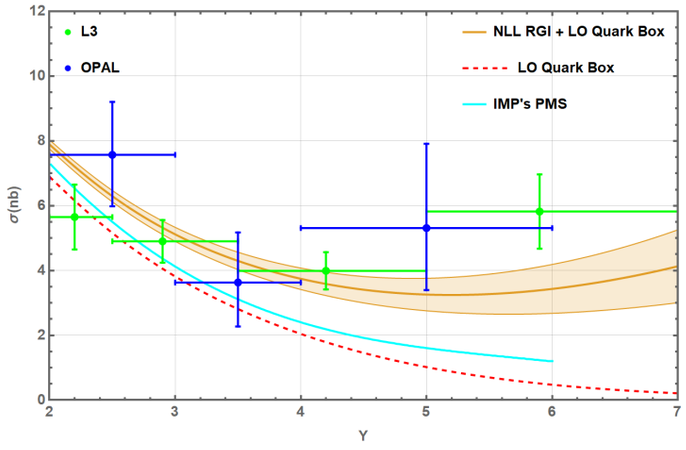


Heavy quark: **proton-proton**

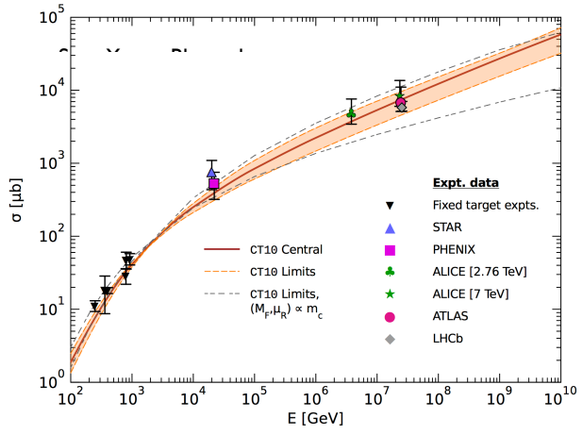


Cross section **neutrino-nucleon**

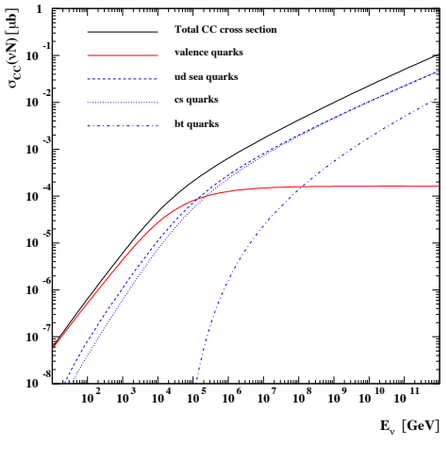


***What all these processes have in common?***

# Motivation: proton structure at high energy

*Relevant for EIC !*

Focus first on **electron-proton** scattering :

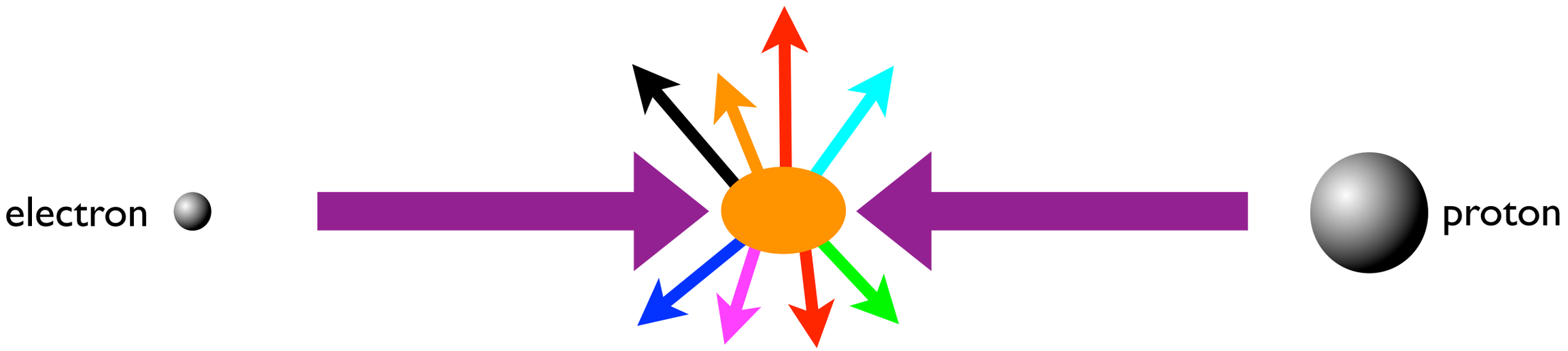


High energy of collision: $\sqrt{s} \gg m, \Lambda_{QCD}$

**High energy** limit of electron-proton/nucleus collisions

**Proton/nucleus structure** at high energies

# Observation of deep inelastic electron–proton scattering

VOLUME 23, NUMBER 16 PHYSICAL REVIEW LETTERS 20 OCTOBER 1969

OBSERVED BEHAVIOR OF HIGHLY INELASTIC ELECTRON-PROTON SCATTERING

M. Breidenbach, J. I. Friedman, and H. W. Kendall
Department of Physics and Laboratory for Nuclear Science,*
Massachusetts Institute of Technology, Cambridge, Massachusetts 02139

and

E. D. Bloom, D. H. Coward, H. DeStaebler, J. Drees, L. W. Mo, and R. E. Taylor
Stanford Linear Accelerator Center,† Stanford, California 94305
(Received 22 August 1969)

20 GeV electron beam scattering off protons

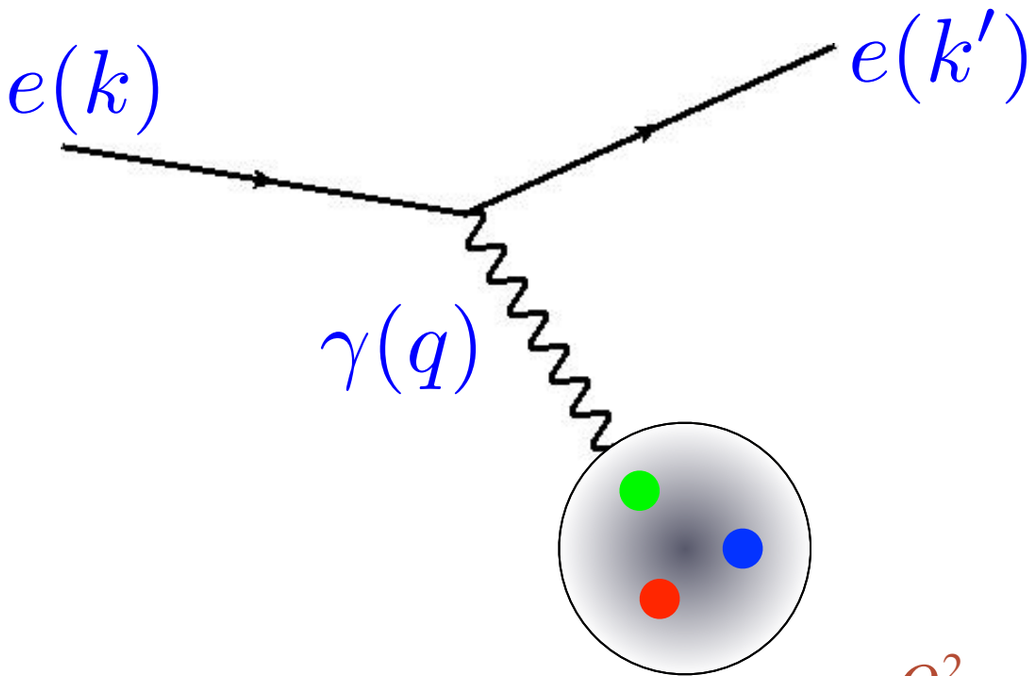


elastic scattering
form factor included

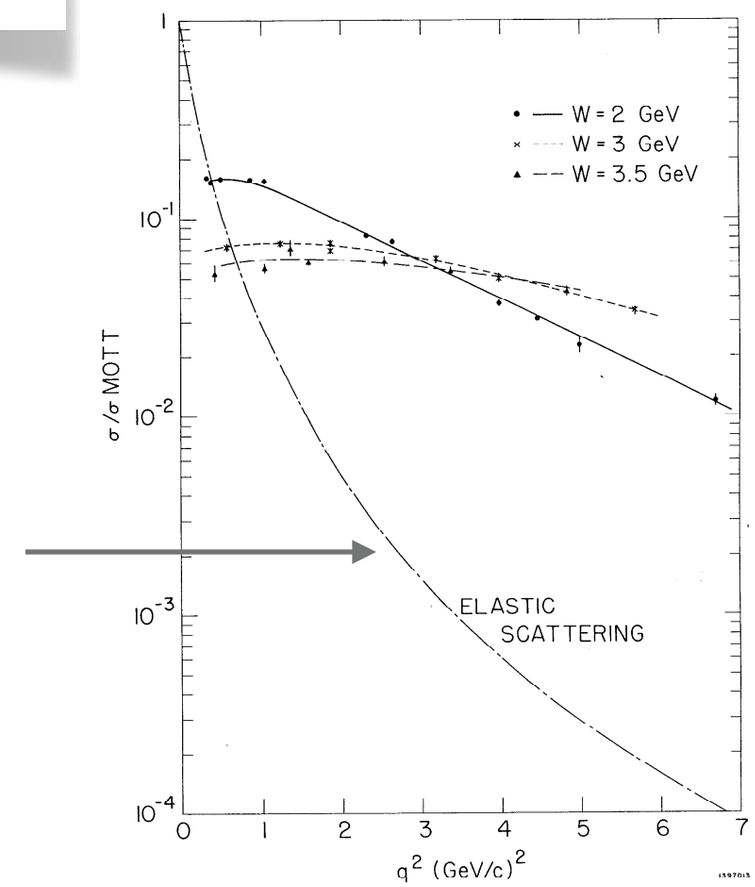


**$Q^2 = -q^2$: resolving power of interaction**

# Deep Inelastic lepton-hadron scattering

Inelastic scattering off proton

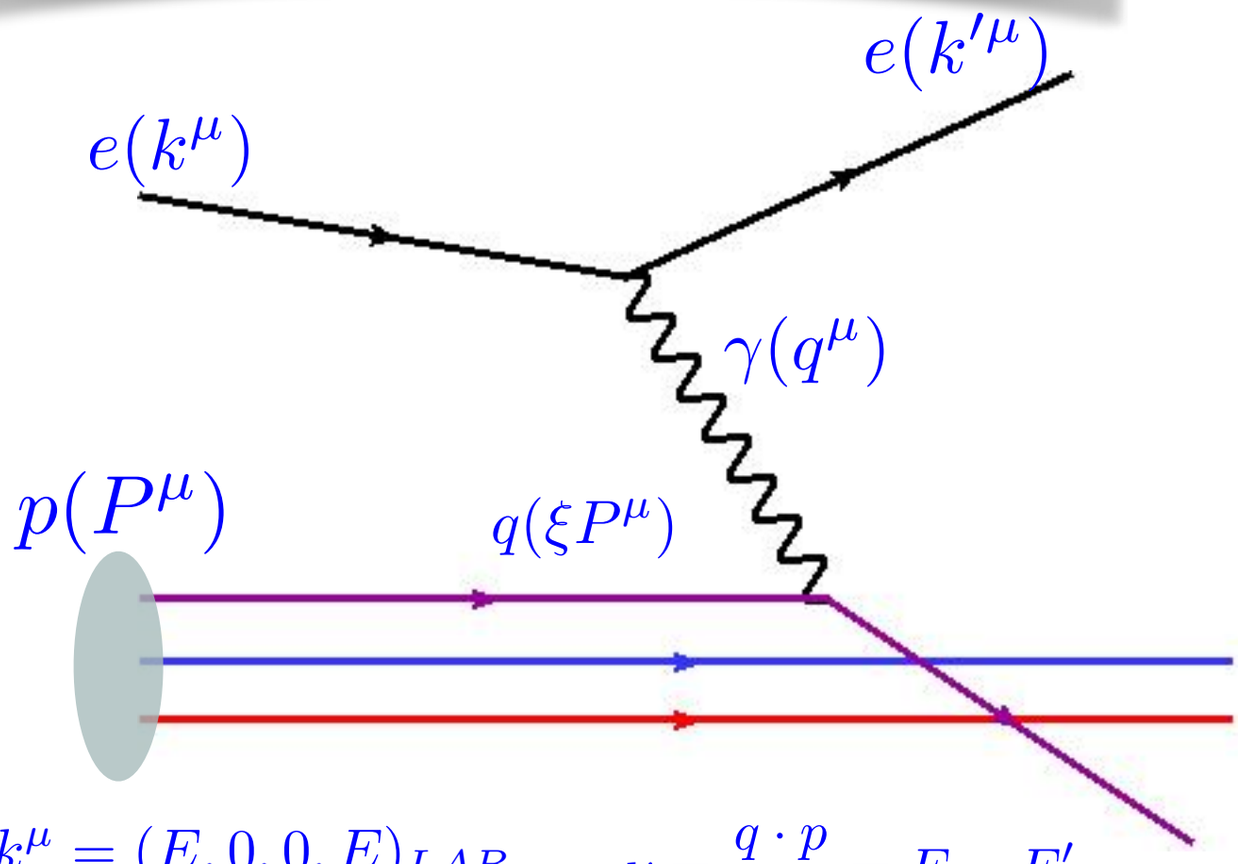


$k^{\mu} = (E, 0, 0, E)_{LAB}$

$k'^{\mu} = (E', 0, 0, E')_{LAB}$

$\nu = \frac{q \cdot p}{M} = E - E'$

Lepton energy loss in nucleon rest frame

Deep $Q^2 \gg M^2_{\text{hadron}}$

Inelastic $W^2 \gg M^2_{\text{hadron}}$

Elastic scattering off parton

$q = k - k'$ lepton momentum transfer

$Q^2 = -q^2$ photon virtuality: resolving power

$x = \frac{Q^2}{2P \cdot q} \simeq \frac{Q^2}{Q^2 + W^2}$ Bjorken x

$W^2 = (p + q)^2$ total energy² of photon-proton system

$s = (p + k)^2$ total cms energy²

$y = \frac{p \cdot q}{p \cdot k} = \frac{\nu}{E}$

**Inelasticity**: fraction of lepton energy loss in the nucleon rest frame

# DIS preliminaries

**Scattering amplitude:**

$$\mathcal{M} = e^2 \bar{u}(k', \lambda') \gamma^\mu u(k, \lambda) \frac{1}{q^2} < X | J_\mu^{em}(0) | N, \sigma >$$

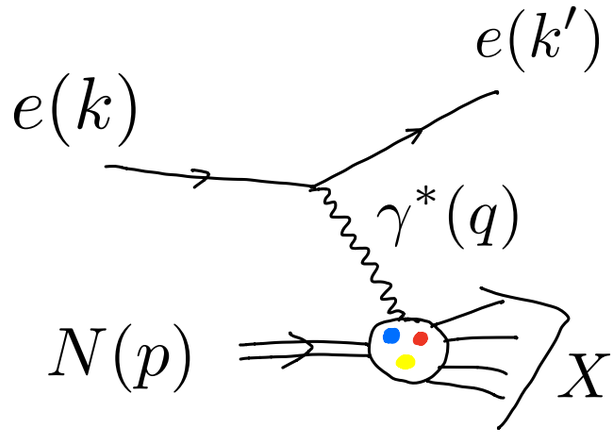


$\langle X|$ Hadronic final state

$|N, \sigma\rangle$ Nucleon/nucleus initial state

$J_\mu^{\rm em}(0)$ Electromagnetic current

**Cross section:**

$$d\sigma = \frac{1}{F} \frac{d^3 k'}{2E'(2\pi)^3} \frac{1}{4} \sum_{\sigma \lambda \lambda'} |\mathcal{M}|^2$$

**Flux factor:**

$$F = 4p \cdot k$$

Sum performed over the polarization states

# DIS preliminaries

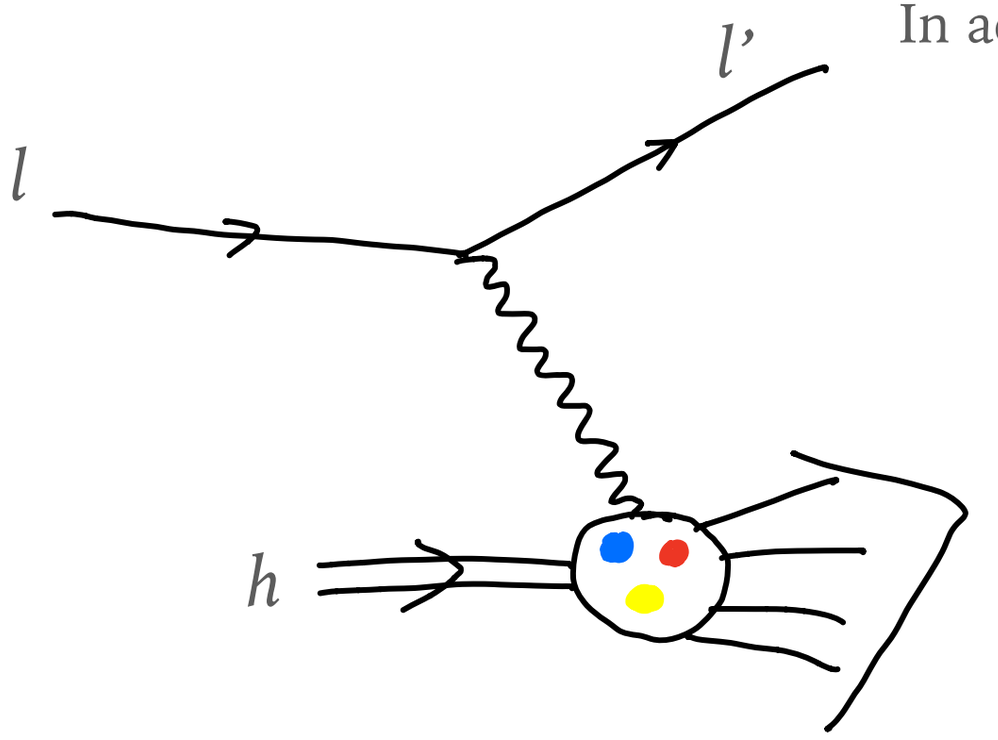


In addition to exchanged photon one can have

Neutral Weak Current (NC)

$Z$

Charged Current (CC)

$W^{\pm}$

( neutrino scattering)

*Consider only one photon exchange*
*Masses of leptons and hadron are neglected*

$$d\sigma \sim \left| \quad \right|^2 =$$

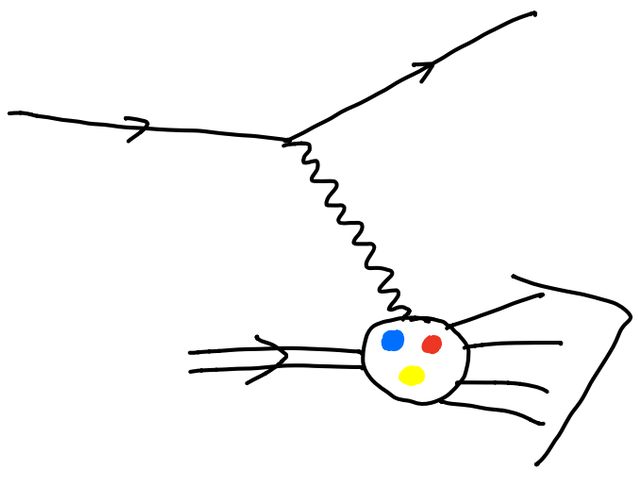

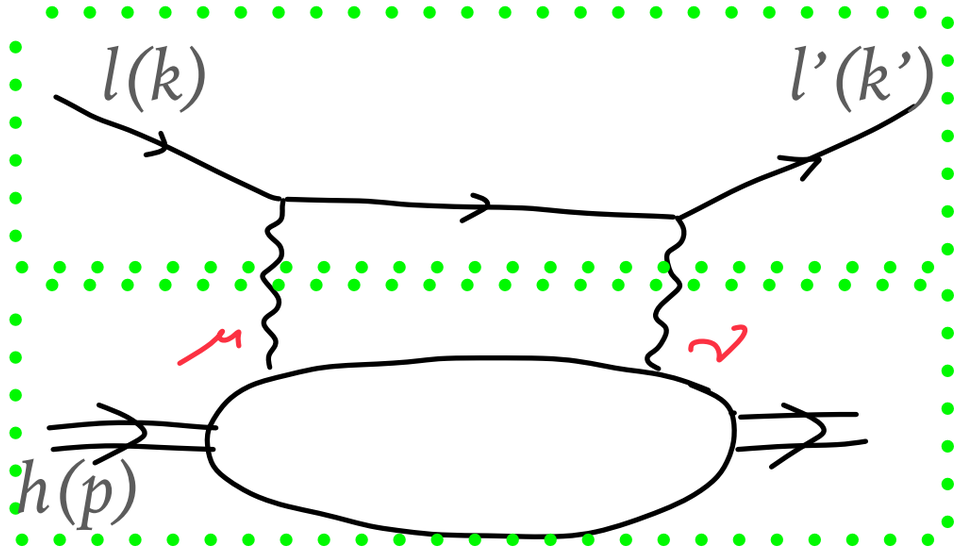


$L^{\mu\nu}$ lepton tensor

$\sim L^{\mu\nu} W_{\mu\nu}$

$W_{\mu\nu}$ hadron tensor

# DIS preliminaries

*Consider only photon exchange*
*Masses of leptons and hadron are neglected*

DIS cross section can be written in the factorized way:

*lepton tensor*

*hadron tensor*

$$\frac{d^2\sigma}{dE'd\Omega} = \frac{\alpha_{em}^2}{Q^4}\frac{E'}{E}L_{\mu\nu}^{em}W^{\mu\nu}$$

**Leptonic tensor:** can be evaluated straightforwardly

$$L_{\rm em}^{\mu\nu} = \frac{1}{2}\sum_{s'}\bar{u}_\alpha^{(s')}(k')\gamma_{\alpha\beta}^\mu\sum_s u_\beta^{(s)}(k)\bar{u}_\gamma^{(s)}(k)\gamma_{\gamma\delta}^\nu u_\delta^{(s')}(k')$$

Final result:

$$L_{\rm em}^{\mu\nu} = \frac{1}{2}Tr(\not{k}'\gamma^\mu\not{k}\gamma^\nu) = 2(k^\mu k'^\nu + k'^\mu k^\nu - \frac{1}{2}Q^2 g^{\mu\nu})$$

Note that it only depends on 4-momenta of initial, final leptons and photon 4-momentum

# DIS preliminaries


**Hadronic tensor** contains all the information about the hadron involved in the process.

Depends on the 4-momenta of the incoming nucleon and the photon

Definition of the hadronic tensor:

$$W_{\mu\nu}(p,q) = \frac{1}{4M}\sum_{\sigma}\sum_{X}(2\pi)^4\delta^4(p_X - p - q) < N\sigma|J^{em}_{\mu}(0)|X >< X|J^{em}_{\nu}(0)|N\sigma >$$

$$W_{\mu\nu}(p,q) = \frac{1}{4M}\sum_{\sigma}\int\frac{d^4\xi}{2\pi}e^{iq\xi} < N\sigma|J^{em}_{\mu}(\xi)\, J^{em}_{\nu}(0)|N\sigma >$$

Decomposition of the hadronic tensor:

$$W_{\mu\nu}(p,q) = -W_1(g_{\mu\nu} - \frac{q_\mu q_\nu}{q^2}) + \frac{W_2}{M^2}(p_\mu - \frac{p\cdot q}{q^2}q_\mu)\cdot(p_\nu - \frac{p\cdot q}{q^2}q_\nu)$$

Two independent **structure functions** (unpolarized, only photon exchange):

$$MW_1 = F_1 \qquad \frac{Q^2}{2Mx}W_2 = F_2$$

Dimensionless

# Parton model – Bjorken scaling

If proton consisted  of pointlike constituents which do not interact, then the scattering off proton will be just an **incoherent scattering** off the pointlike constituents.

**DIS cross section**

$$\frac{d^2\sigma}{d\Omega dE'} = \frac{\alpha^2}{4E^2 \sin^4 \frac{\Theta}{2}} (2W_1 \sin^2 \frac{\Theta}{2} + W_2 \cos^2 \frac{\Theta}{2})$$

$\Theta$ Lepton scattering angle in the hadron rest frame

Compare with **electron-muon** cross section

$$\frac{d^2\sigma^{e\mu\to e\mu}}{d\Omega dE'} = \frac{\alpha^2}{4E^2 \sin^4 \frac{\Theta}{2}} [\cos^2 \frac{\Theta}{2} - \frac{q^2}{2M^2} \sin^2 \frac{\Theta}{2}] \delta(\nu + \frac{q^2}{2M})$$

Can read off structure functions in this case immediately

$$2MW_1^p(\nu, Q^2) = 2F_1 = \frac{Q^2}{2M\nu} \delta(1 - \frac{Q^2}{2M\nu})$$
$$\nu W_2^p(\nu, Q^2) = F_2 = \delta(1 - \frac{Q^2}{2M\nu})$$

# Parton model

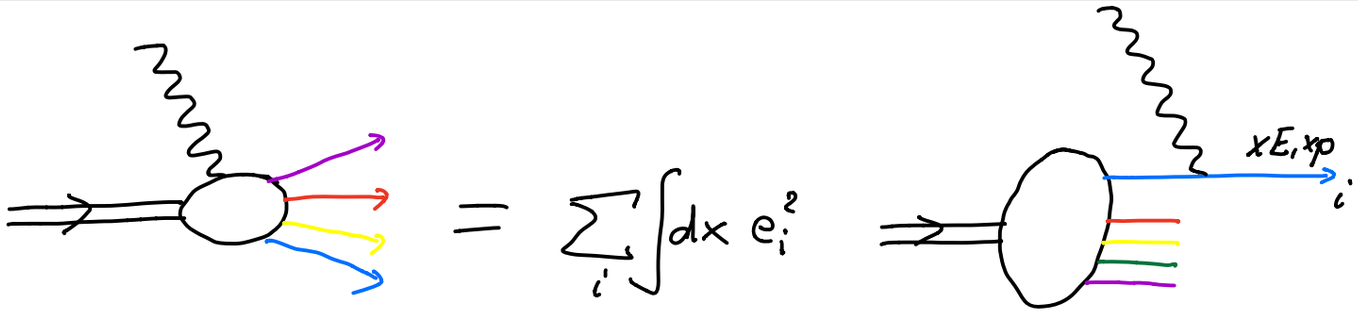


x: longitudinal momentum fraction of the proton carried by the struck parton

**Parton distribution function**

$$f_i(x) = \frac{dP_i}{dx} =$$

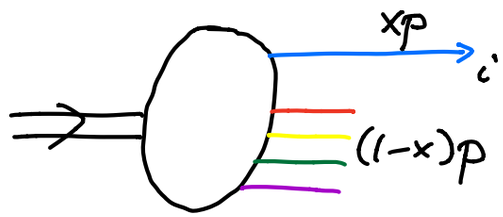


**Momentum sum rule**

$$\sum_k \int_0^1 dx\, x f_k(x) = 1$$

**Structure functions:**

$$\nu W_2^p(\nu, Q^2) = F_2 = \sum_i \int_0^1 d\beta e_i^2 f_i(\beta)\beta\delta(\beta - \frac{1}{\omega}) = \sum_i e_i^2 x f_i(x)$$

$$MW_1^p(\nu, Q^2) = F_1 = \frac{\omega}{2} F_2$$

$$x = \frac{Q^2}{2M\nu} = \frac{Q^2}{2p\cdot q} = \frac{1}{\omega}$$

$$F_2(x) = \sum_i e_i^2 x f_i(x) \quad F_1(x) = \frac{1}{2x} F_2(x)$$

# Parton model – Bjorken scaling

The structure functions for scattering on **pointlike parton**
have the property that they depend only on one dimensionless variable:

$$x = \frac{Q^2}{2M\nu} = \frac{Q^2}{2p \cdot q}$$

$$F_1(x, Q^2) \to F_1(x) \qquad F_2(x, Q^2) \to F_2(x)$$

No dependence on $Q^2$: **Bjorken scaling**

$$\omega = \frac{1}{x}$$

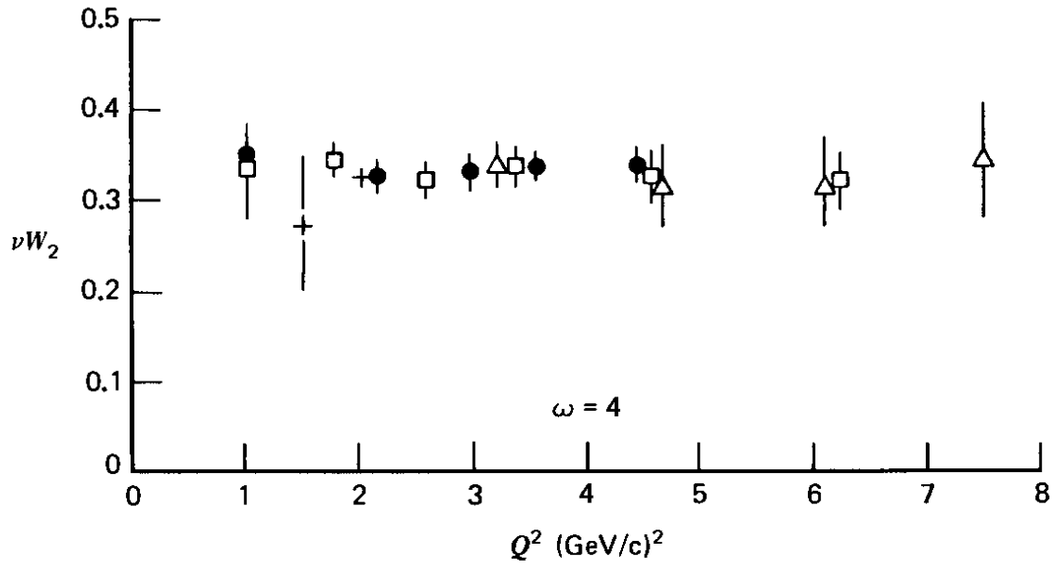


**Fig. 9.2** The structure function $\nu W_2$ determined by electron–proton scattering as a function of $Q^2$ for $\omega = 4$. Data are from the Stanford Linear Accelerator.

# Callan-Gross relation

In the parton model there is a relation

$$F_1(x) = \frac{1}{2x} F_2(x)$$

**Longitudinal** structure function has to vanish in the scaling limit

Consequence of parton model and spin 1/2 quarks

$$F_L(x) = F_2(x) - 2xF_1(x)$$

Parton model assumptions:

- **Incoherent** scattering on **pointlike** constituents
- **Transverse** momenta of the partons are **vanishing**

# Parton model

$$\nu W_2^p(\nu, Q^2) = F_2 = \sum_i \int_0^1 d\beta e_i^2 f_i(\beta)\beta\delta(\beta - \frac{1}{\omega}) = \sum_i e_i^2 x f_i(x)$$

$x = \frac{Q^2}{2M\nu} = \frac{Q^2}{2p \cdot q} = \frac{1}{\omega}$

How the structure function shape reflects the parton distribution inside the proton:

- One valence quark
- Three, non-interacting valence quarks, sharing equal momentum
- Three quarks interacting, changing the momentum
- Many sea quarks

# Revealing partonic structure of the proton

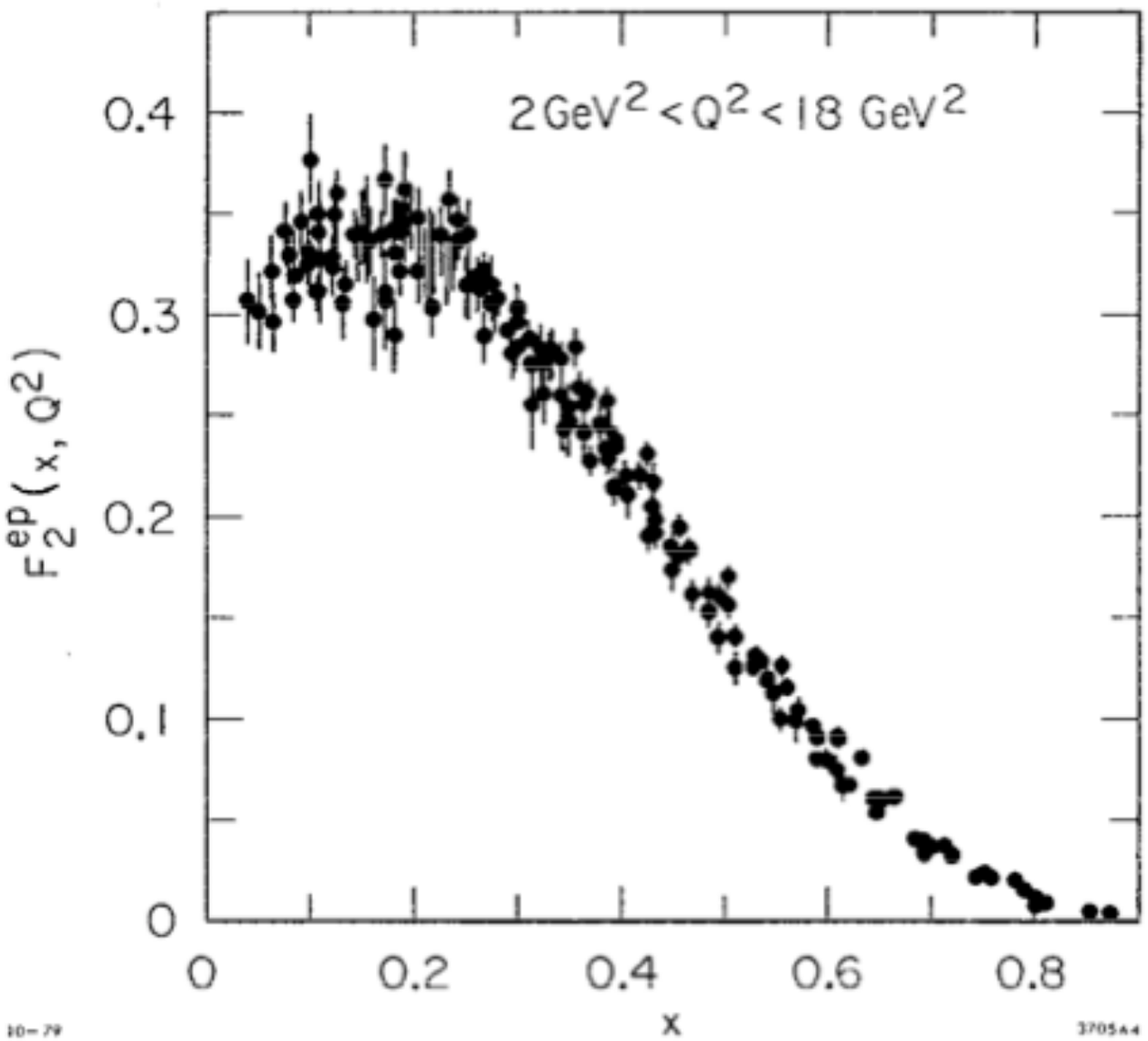


Measured cross section

Momentum distribution of partons

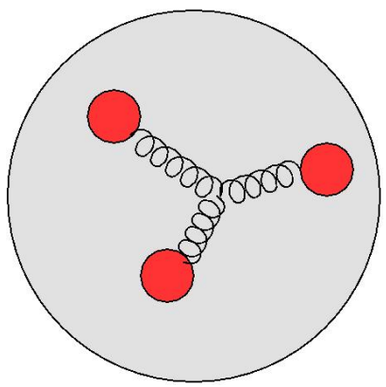

# Summarizing: DIS structure functions

Inclusive DIS cross section for $lp \to lX$ ($l$ charged lepton, $Q^2 \ll M_Z^2$, $s \gg M_p^2$)

$$\frac{d^2\sigma}{dxdQ^2} = \frac{2\pi\alpha_{\rm em}^2}{Q^4 x}\left[(1+(1-y)^2)F_2(x,Q^2) - y^2 F_L(x,Q^2)\right]$$

structure functions

$$y = \frac{p\cdot q}{p\cdot k} = Q^2/(sx)$$ inelasticity

Can use $(x, Q^2, s)$ or $(x, Q^2, y)$

**Structure functions** encode all the information about the **proton(hadron) structure**

$F_T(x,Q^2) = F_2(x,Q^2) - F_L(x,Q^2)$ transversely polarized photons

$F_L(x,Q^2)$ longitudinally polarized photons

Often experiments give **reduced cross section**

$$\sigma_{r,NC} = \frac{d^2\sigma_{NC}}{dxdQ^2}\frac{Q^4 x}{2\pi\alpha_{\rm em} Y_+} = F_2 - \frac{y^2}{Y_+}F_L \qquad Y_+ = 1+(1-y)^2$$

Dominated by the $F_2$ structure function except for large $y$
$F_L$ structure function non-zero due to QCD corrections

In order to measure $F_L$ & $F_2$ need to vary y, perform measurements at various energies

**At EIC: variable energies, can extract $F_L$ & $F_2$ independently**

# Exploring proton structure at higher energy

DESY - Hamburg
HERA Collider
1992-2007


The only electron(positron)-proton collider ever built: EIC will be the next !

*Center of mass energy:*

$$E_{\mathrm{cm}} = 320\ \mathrm{GeV}$$

equivalent to 50 TeV electron beam on a fixed proton target...about 2500 times more than at SLAC

# Deep Inelastic Scattering at large $Q^2$

- Lepton undergoes wide angle scattering at high $Q^2$
- DIS: probing small distance scales $\lambda \sim \frac{1}{Q} \ll \frac{1}{M_{\text{hadron}}}$

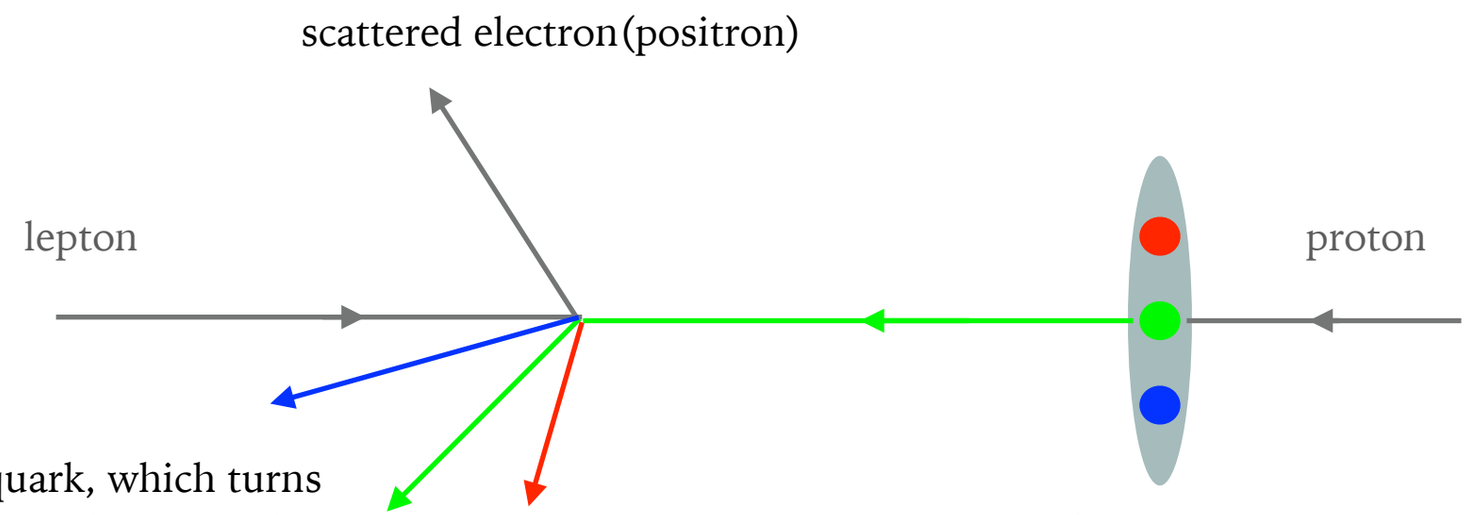


Schematic picture of the DIS scattering

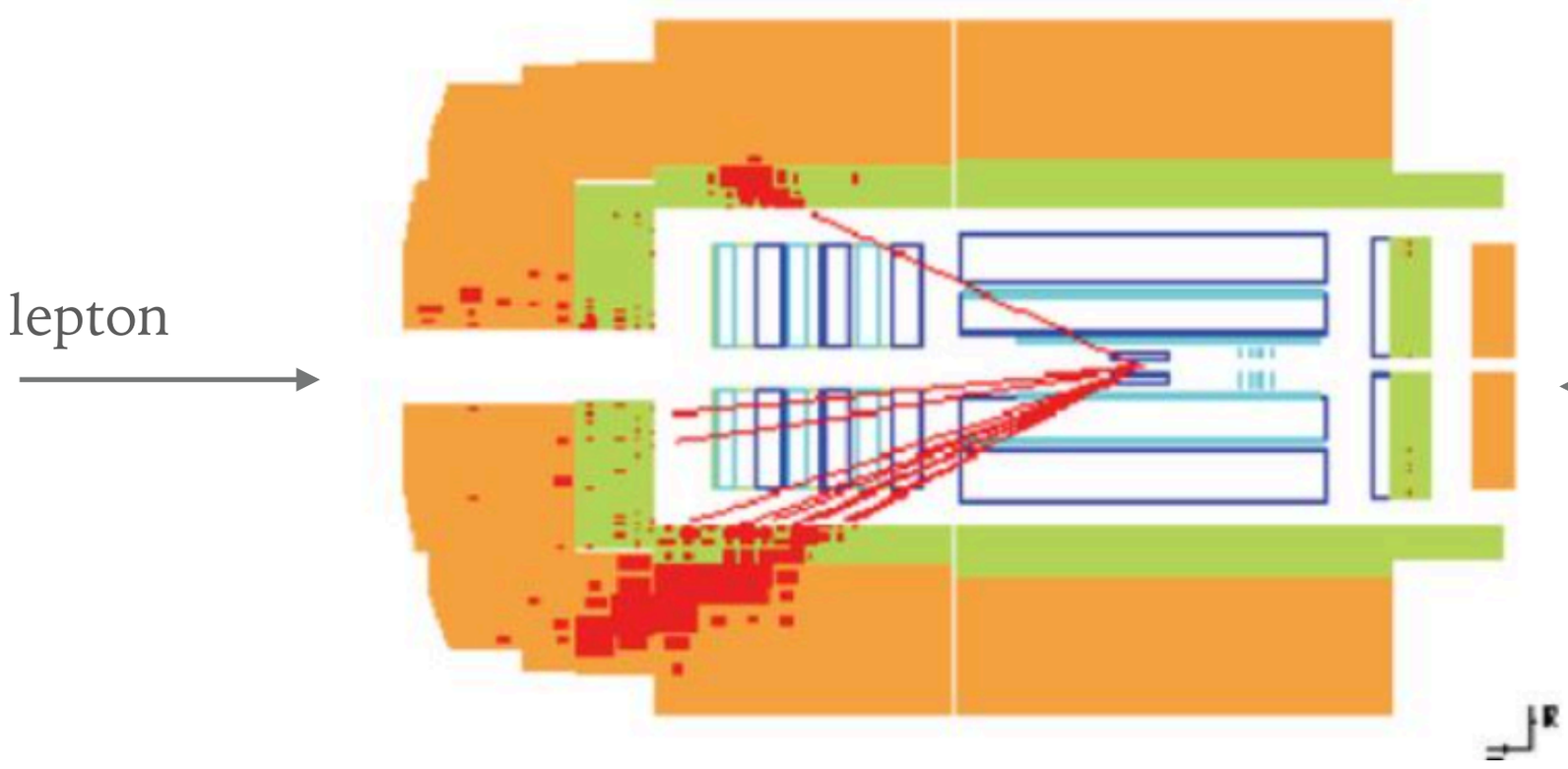


Actual DIS event at H1 at HERA

# Measurements of proton structure function

*low energy*

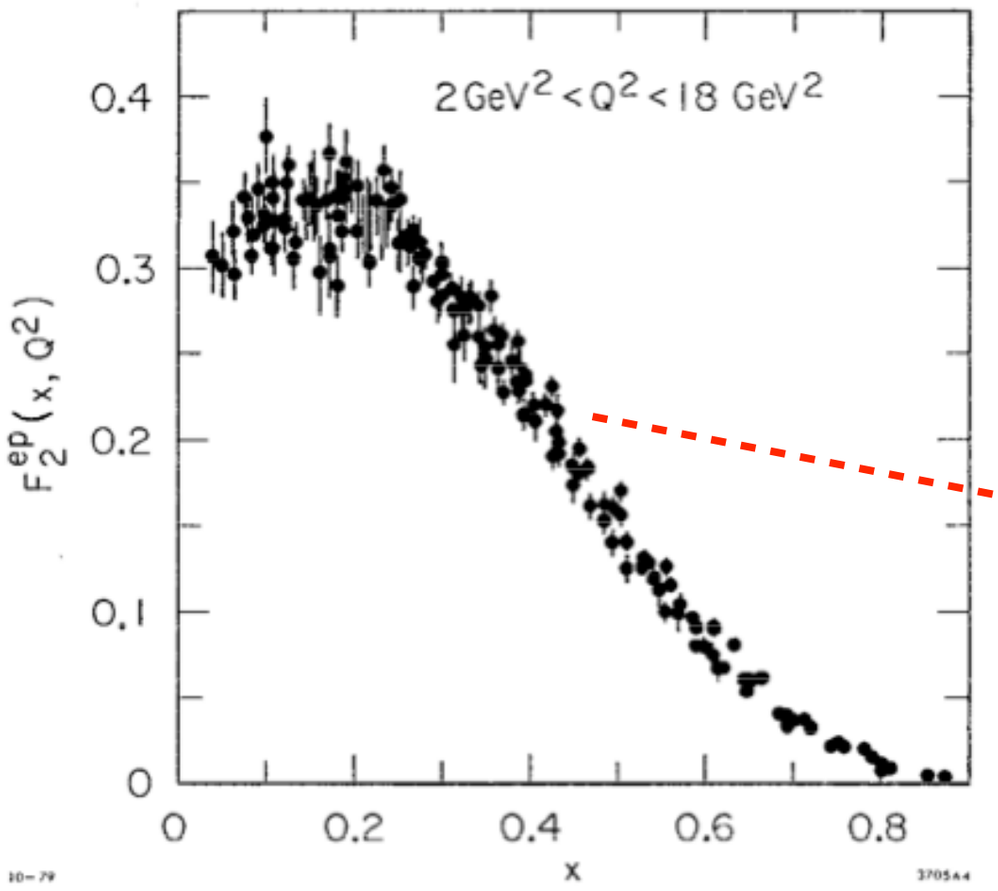


*high energy*

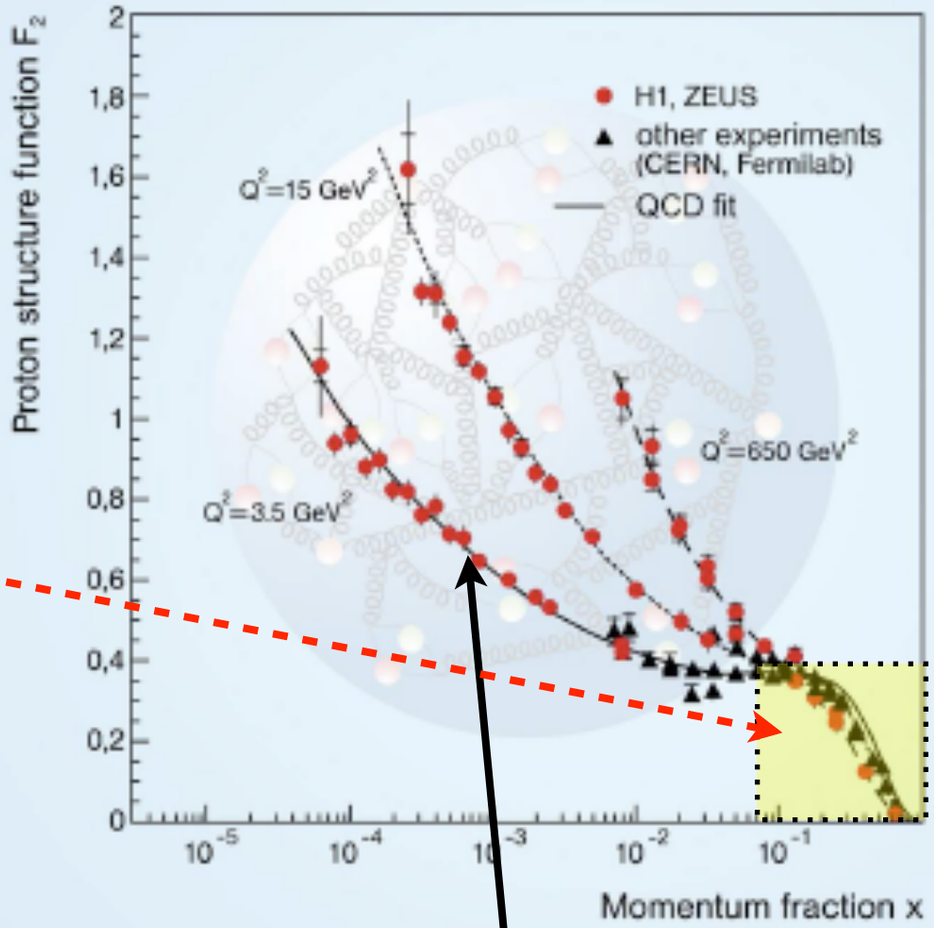


Cross section and that means parton density **increases**:

- with **decreasing x** (fraction of long. mom.)
- with **increasing scale Q** (resolving power)

Where does this rise come from?

Answer: QCD radiation

# Collinear framework

*See lectures by S.Catani, Introduction to QCD*

**Parton model**

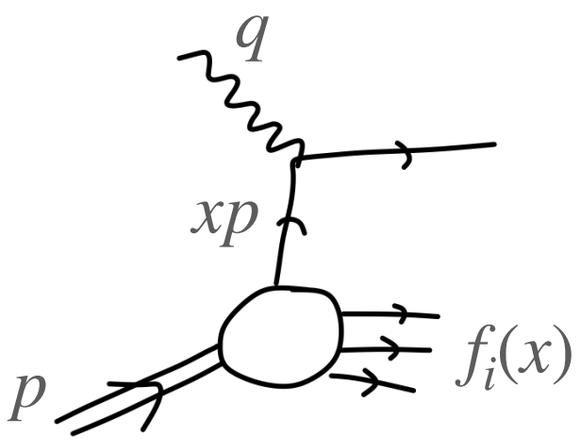


parton distribution

**Including the QCD corrections**

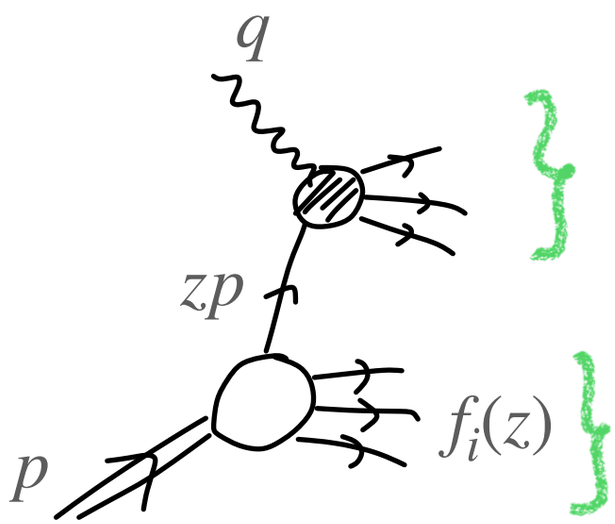


partonic cross section

parton distribution

**Lowest order corrections to the partonic cross section**

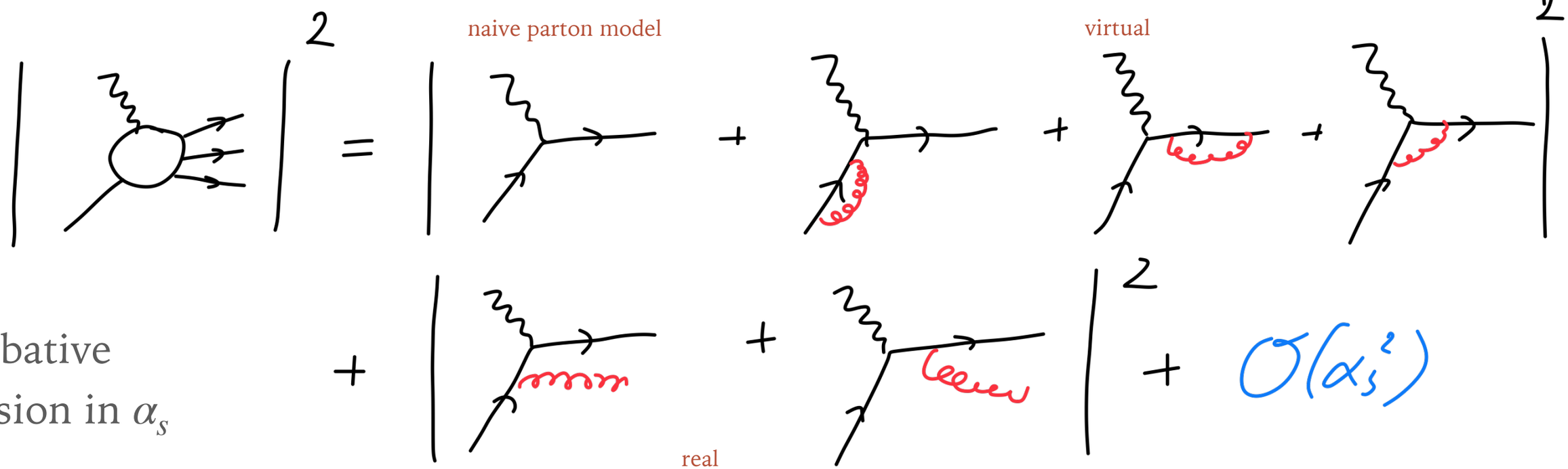


Perturbative expansion in $\alpha_s$

# Collinear framework

- Perturbative calculation will lead to **soft** and **collinear** singularities
- **Final** state completely inclusive: **soft** and **final** state collinear singularities cancel
- Only one parton in the initial state, so not fully inclusive: uncanceled initial collinear singularities

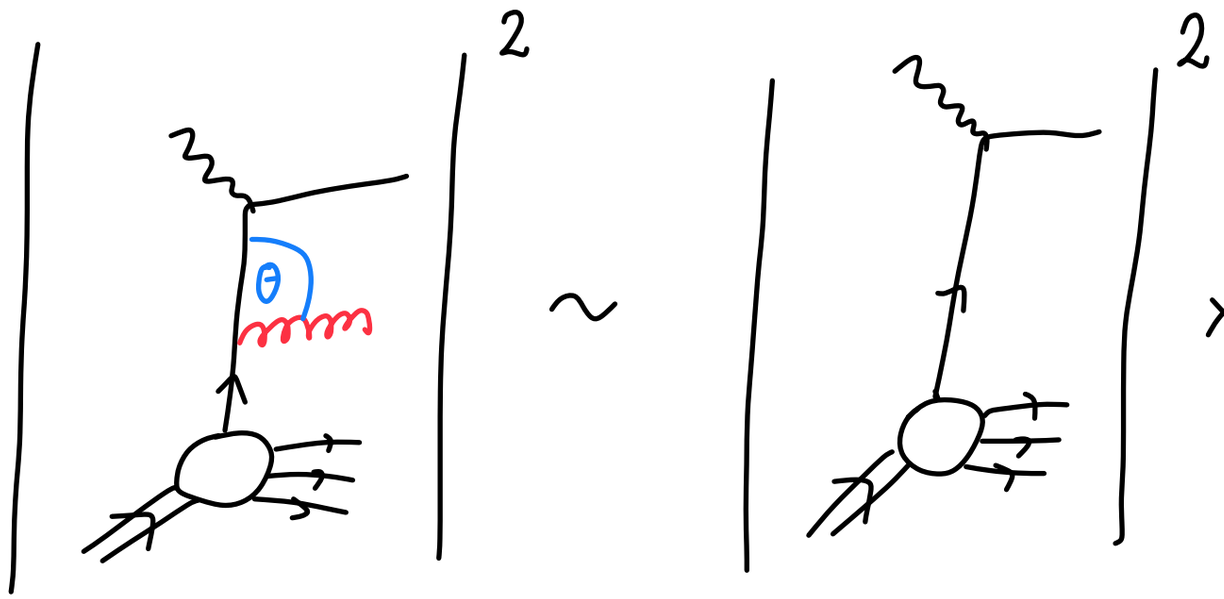


$$\sim \times \alpha_s \int_0^1 \frac{d\theta^2}{\theta^2}$$

logarithmic integration over the angle

$k_T \sim \theta p$

transverse momentum

$$\alpha_s \int_0^1 \frac{d\theta^2}{\theta^2} \to \alpha_s \int_0^{Q^2} \frac{dk_T^2}{k_T^2} \to \alpha_s \int_{Q_0^2}^{Q^2} \frac{dk_T^2}{k_T^2}$$

Collinear divergence regularized by the hadronic scale $Q_0^2$

$1/Q_0$ average distance between partons in the hadron

**Large collinear logarithm**

# Collinear framework

- Regularization gives dependence on the IR cutoff: dependence on **long distance** physics
- Need to identify the **short distance** part of the cross section
- However, there are also **higher order corrections**

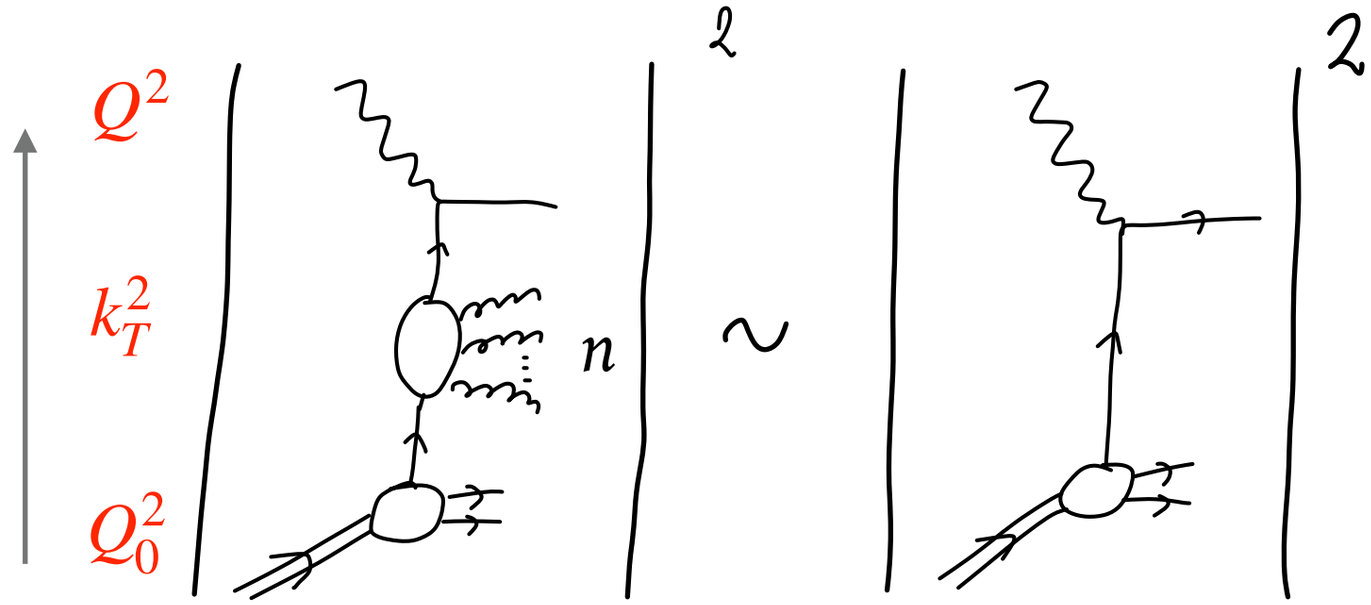


$$\sim \times \left[\alpha_s(Q^2)\int_{Q_0^2}^{Q^2}\frac{dk_T^2}{k_T^2}\right]^n$$

*Parton emission over large region of $k_T$*

*Enhancement from collinear logarithms*

$$\alpha_s(Q^2)\int_{Q_0^2}^{Q^2}\frac{dk_T^2}{k_T^2} = \alpha_s(Q^2)\ln\frac{Q^2}{Q_0^2} \sim \mathcal{O}(1) \quad \text{not} \quad \mathcal{O}(\alpha_s) \qquad \ln\frac{Q^2}{Q_0^2} \sim \frac{1}{\alpha_s(Q^2)}$$

- Strong coupling is compensated by a **large logarithm**
- Need **resummation of collinear logarithms**

$Q_0 \sim M_{\text{hadron}} \sim \Lambda_{QCD}$

# Factorization of collinear singularities

- There is sensitivity to IR cutoff and need for resummation of collinear logarithms
- Both problems can be solved by: **universal factorization of collinear singularities**
- Define parton density from parton model as bare parton density

*parton density in naive parton model* $f(x) \longrightarrow f^{(0)}(x)$ *bare parton density*

Absorb collinear singularities into the redefinition (renormalization) of the parton density

true parton density $$f(x,Q^2) = f^{(0)}(x)\,\Gamma(\alpha_s(Q^2), \ln Q^2/Q_0^2)$$

Factor $\Gamma(\alpha_s(Q^2), \ln Q^2/Q_0^2)$ contains all the collinear logarithms $\left[\alpha_s(Q^2)\int_{Q_0^2}^{Q^2}\frac{dk_T^2}{k_T^2}\right]^n$

- This factor and therefore corresponding parton density should be **universal**, i.e. does not depend on the process but only on the proton
- It should be **factorizable** from the hard process

# Universal factorization of collinear singularities

**Argument based on power counting for collinear singularites in physical gauge**

Consider an emission of collinear parton of momentum $k$

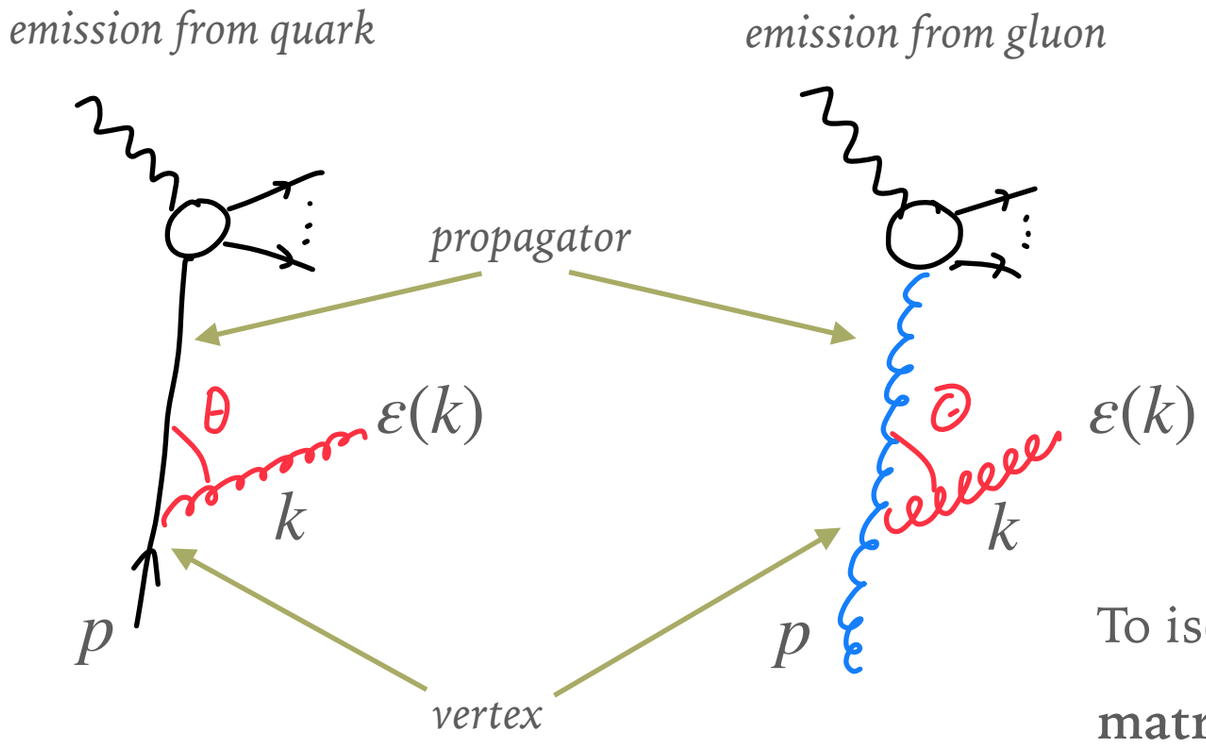


**phase space factor**

$$\frac{d^3k}{2k_0} \sim k_0 dk_0 d\phi \sin\theta d\theta$$

$\phi$ azimuthal angle

$\theta$ emission angle

$$\sin\theta d\theta \sim d\theta^2 \quad \text{when} \quad \theta \to 0$$

To isolate the collinear singularity need $\frac{1}{\theta^2}$ in **squared matrix** element

**In matrix element:**

**propagator**

$$\frac{1}{(p-k)^2} = \frac{1}{-2p\cdot k} = \frac{1}{-2p_0k_0(1-\cos\theta)} \sim \frac{1}{\theta^2}$$

**vertex**

$$p_i \cdot \varepsilon(p_j) \sim \theta \quad \textit{where} \quad p_i, p_j \to p, k, p-k$$

*in the collinear limit*

$$\textit{and} \quad p\cdot\varepsilon(p) = 0$$ *physical polarization is transverse*

# Universal factorization of collinear singularities

## Squaring the matrix element in the DIS case

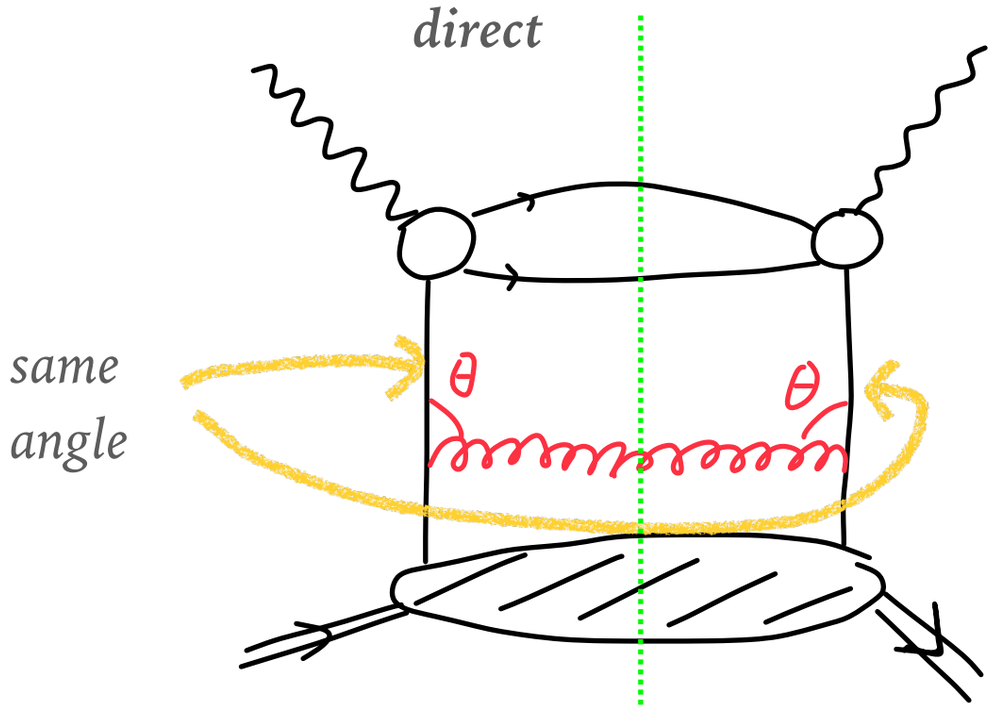


$$\frac{\theta}{\theta^2}\,\frac{\theta}{\theta^2} \sim \frac{1}{\theta^2}$$

giving logarithmic singularity

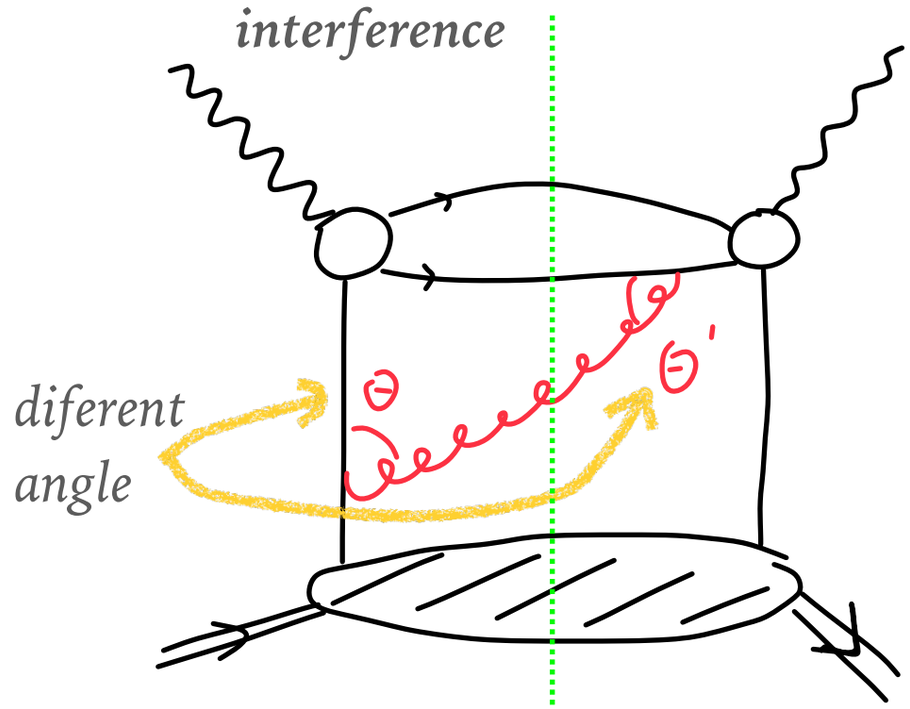


$$\frac{\theta}{\theta^2}\,\frac{\theta'}{\theta'^2} \sim \frac{1}{\theta\theta'} \xrightarrow{\theta\to 0} \frac{1}{\theta}$$

not sufficiently singular

Only **direct** diagrams contribute to the collinear singularities.
**Interference** diagrams do not contribute to the collinear singularities.

# Universal factorization of collinear singularities

2PI cannot be disjoint by cutting 2 lines

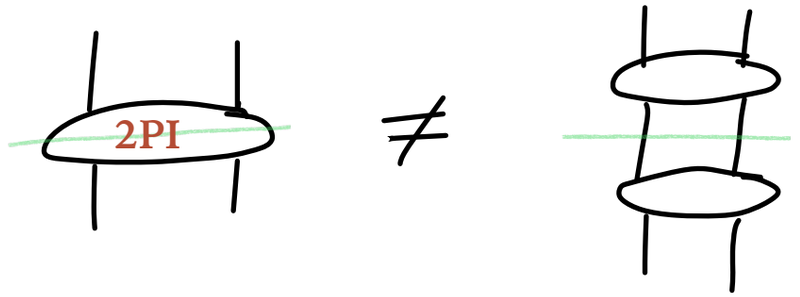


Perform decomposition into 2PI
(two particle irreducible graphs)

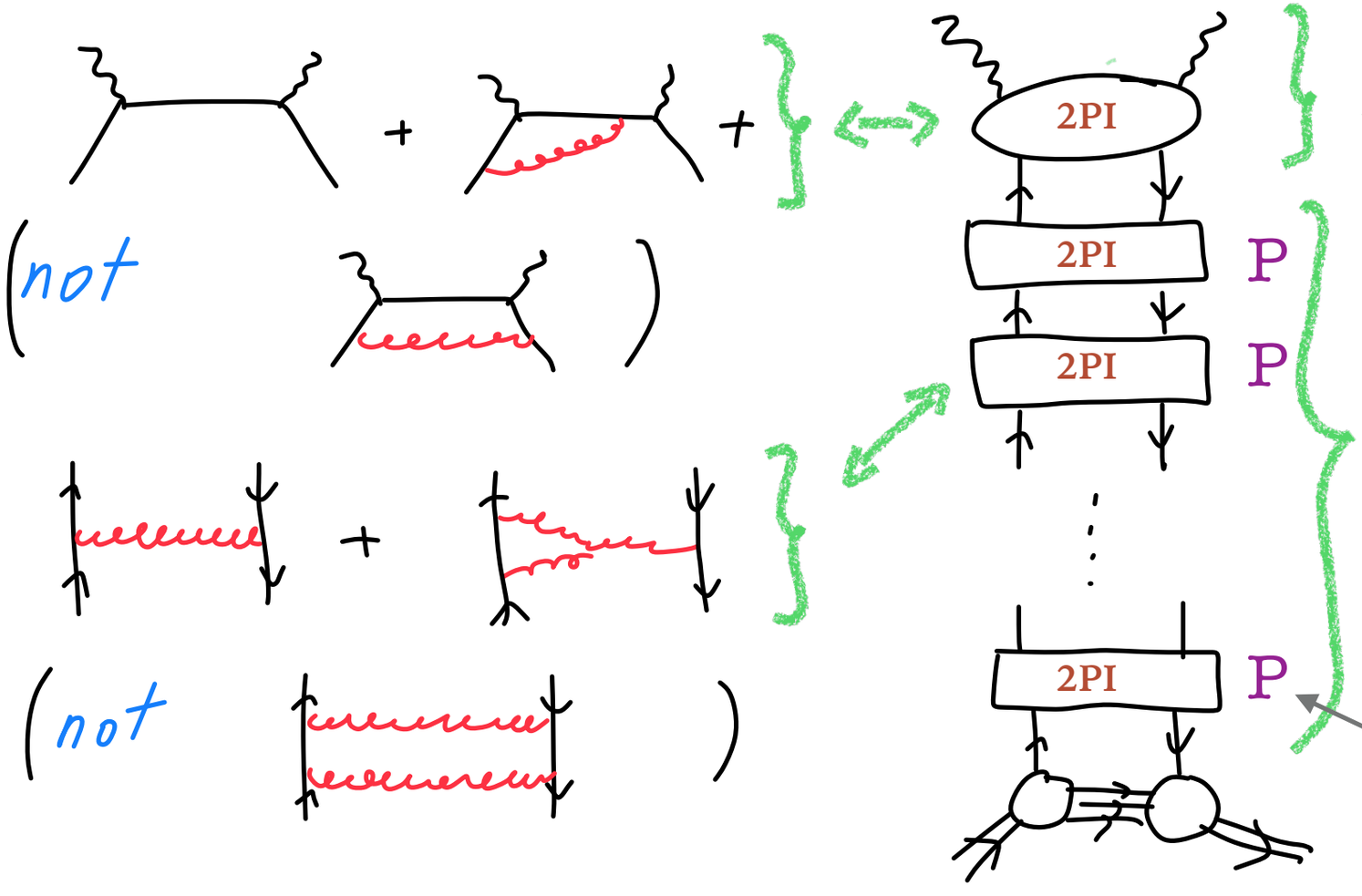


process dependent

process independent
resums all collinear logarithms

kernel

# Collinear factorization formula

Introduce factorization scale $\mu_F$ and split last integration: $k_T < \mu_F$ and $k_T > \mu_F$

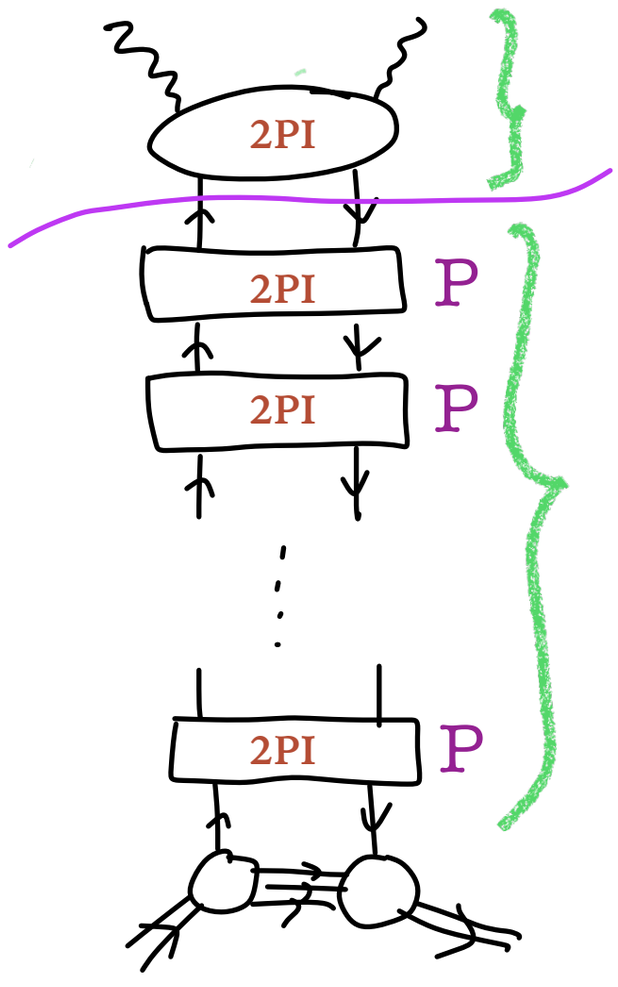


$$\int_{\mu_F^2}^{Q^2} \frac{dk_T^2}{k_T^2} \rightarrow \hat{\sigma}_{\rm hard}(\mu_F^2)$$

$$\int_{Q_0^2}^{\mu_F^2} \frac{dk_T^2}{k_T^2} \rightarrow \Gamma(\mu_F^2/Q_0^2) f^{(0)} \\ \| \\ f(\mu_F^2)$$

contains all collinear logarithms from integrations

## Collinear factorization formula

$$\sigma(p, Q^2) = \sum_j \int_x^1 dz\, \hat{\sigma}_{\rm hard,j}(zp, Q, \mu_F^2, \alpha_s)\, f_j(z, \mu_F^2)$$

*hadronic cross section* — *partonic cross section* — *parton density*

# Collinear factorization

In summary: can write collinear factorization formula for structure functions

$$F_{2,L}(x,Q^2) = x\sum_q e_q^2 \sum_j \int_x^1 \frac{dz}{z} C^j_{2,L}(x/z, Q^2/\mu_F^2, \alpha_s)\, f_j(z,\mu^2) \quad +\mathcal{O}(\frac{\Lambda^2}{Q^2})$$

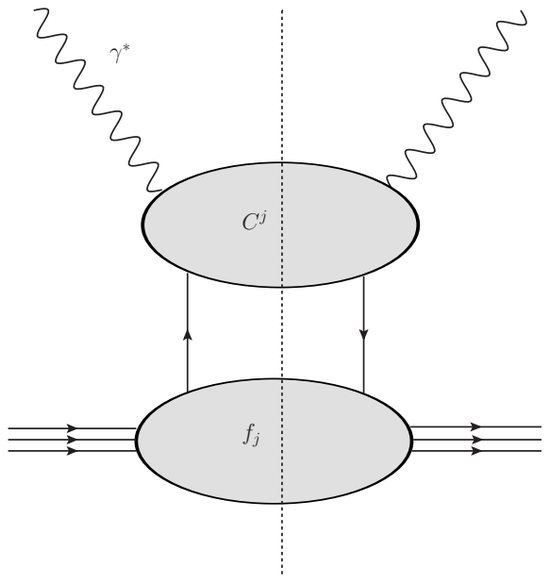


$C^j_{2,L}(x/z, Q^2/\mu_F^2, \alpha_s)$

**Coefficient functions:** calculable order by order in perturbation theory

$f_j(z,\mu_F^2)$

**Parton densities:** non-perturbative distributions in longitudinal momentum fractions $z$ at a given factorization scale $\mu_F^2$

$\mathcal{O}(\frac{\Lambda^2}{Q^2})$

Power corrections.
Control the onset of the regime where the factorization in violated
The scale could be determined experimentally, can depend on energy (saturation scale) and target type

# Factorization scale (in)dependence

Appearance of the arbitrary **factorization scale** $\mu_F$ that divides **parton density** from the **hard scattering cross section**

Physical cross section cannot depend on $\mu_F$, therefore the scale dependence should cancel between hard partonic cross section and parton density

$$\sigma(p, Q^2) = \hat{\sigma}_{\rm hard}(\alpha_s(Q^2), \mu_F^2) \otimes f(\mu_F^2)$$

Therefore in principle one can choose arbitrary $\mu_F$

However: $\hat{\sigma}_{\rm hard}(\alpha_s(Q^2), \mu_F^2) = \hat{\sigma}^{(0)} + \alpha_s \hat{\sigma}^{(1)}(Q/\mu_F) + \alpha_s^2 \hat{\sigma}^{(2)}(Q/\mu_F) + \dots$

Higher order terms will contain logarithmic enhancements $\alpha_s^n (\ln Q/\mu_F)^n$

They appear because of the integration of the collinear spectrum above for $k_T > \mu_F$

Thus if factorization scale is very different from Q, then $\ln Q/\mu_F \gg 1$ we would need to resum many orders in the hard scattering cross section and reliability of fixed order expansion is spoiled.

In order to avoid it set: $\mu_F = aQ$ where $a \sim 1$

Can vary a to test the stability of the expansion, estimate of higher orders

Common choices: a=0.5,1,2

# Scale dependence of the PDFs

Parton distribution functions become scale dependent $f_i(x, Q^2)$ due to the resummation of large collinear logarithms. As a consequence, the structure functions exhibit scaling violations

$$F_2(x) \to F_2(x, Q^2)$$

With increasing $Q^2$ the resolution is increased.

The quarks can emit more partons, and thus at high $Q^2$ and one sees more partons with small values of x.

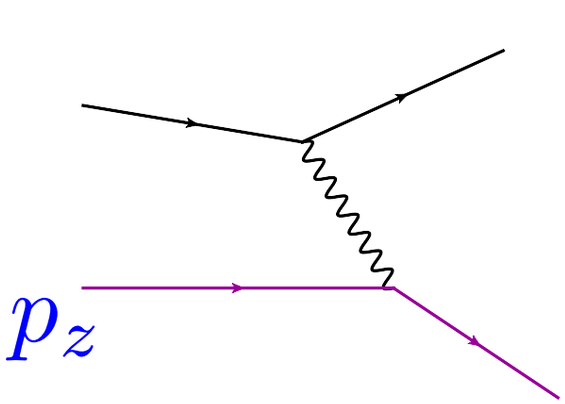


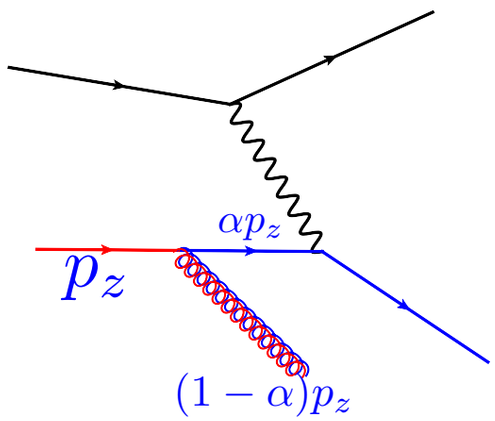


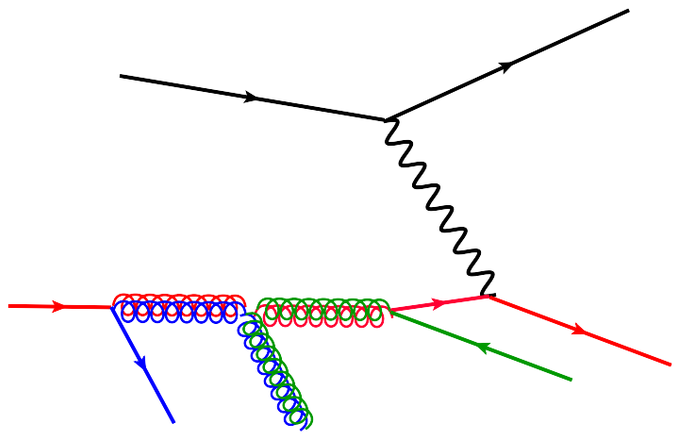

# DGLAP evolution equations

Scale dependent parton densities: non-perturbative objects, cannot compute in perturbative QCD (other methods: lattice)

Scale dependence predicted by perturbative QCD

**Dokshitzer-Gribov-Lipatov-Altarelli-Parisi (DGLAP) evolution equations**

**Strong ordering in transverse momenta**

$$Q^2 \gg k_{n\perp}^2 \gg \cdots \gg k_{i\perp}^2 \gg \cdots \gg k_{1\perp}^2$$

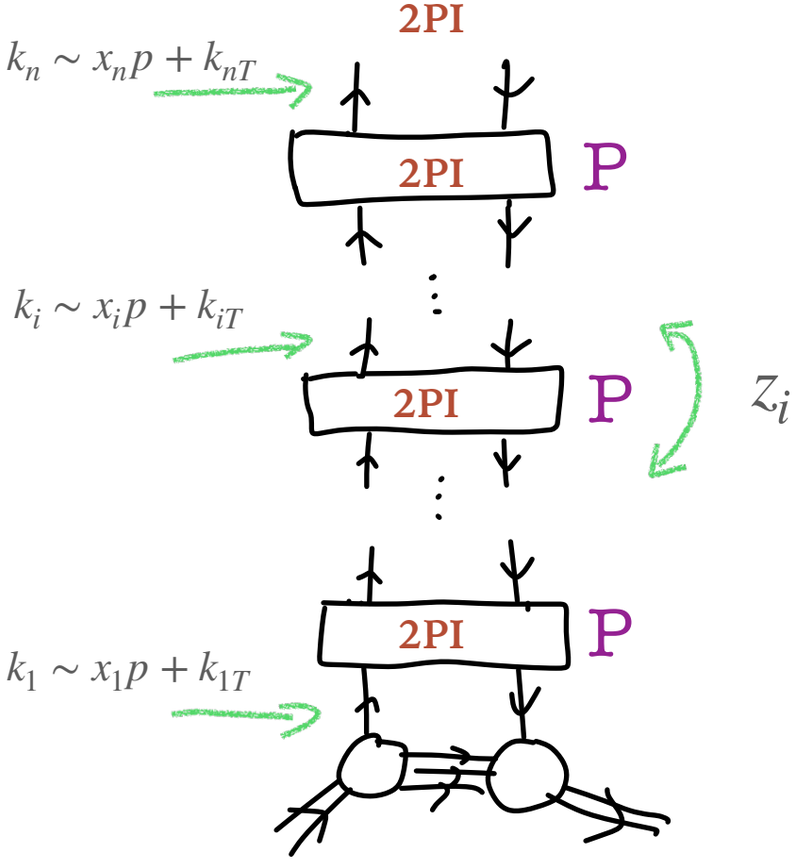


P kernel: splitting function $P(\alpha_s, z_i)$, calculable in pQCD

$z_i$ fraction of longitudinal momentum transferred along the cascade

$$f(x,Q^2) = f^{(0)}(x) + \int_{Q_0^2}^{Q^2} \frac{dk_{nT}^2}{k_{nT}^2} \int_x^1 \frac{dz_n}{z_n} P_n(\alpha_s(k_{nT}^2), z_n) f(\frac{x}{z_n}, k_{nT}^2)$$

Taking derivative with respect to $Q^2$

$$Q^2 \frac{d}{dQ^2} f(x,Q^2) = \int_x^1 \frac{dz}{z} P(\alpha_s(Q^2), z) f(\frac{x}{z}, Q^2)$$

**Differential** equation, provides evolution in $Q^2$

**Needs an input at initial scale $Q_0^2$**

# Collinear approximation: DGLAP evolution

DGLAP evolution: system of equations for parton densities, quarks and gluons

$$\mu^2 \frac{\partial}{\partial \mu^2} \begin{pmatrix} q_i(x,\mu^2) \\ g(x,\mu^2) \end{pmatrix} = \sum_j \int_x^1 \frac{dz}{z} \begin{pmatrix} P_{q_i q_j}(\alpha_s, z) & P_{q_i g}(\alpha_s, z) \\ P_{g q_j}(\alpha_s, z) & P_{gg}(\alpha_s, z) \end{pmatrix} \begin{pmatrix} q_j(\frac{x}{z},\mu^2) \\ g(\frac{x}{z},\mu^2) \end{pmatrix}$$

$q_j$ : quark density, $g$ : gluon density

**Splitting functions**
calculated perturbatively

LO NLO NNLO N³LO

$$P_{ab}(\alpha_s, z) \equiv P_{b\to a}(\alpha_s, z) = \frac{\alpha_s}{2\pi} P_{ab}^{(0)}(z) + \left(\frac{\alpha_s}{2\pi}\right)^2 P_{ab}^{(1)}(z) + \left(\frac{\alpha_s}{2\pi}\right)^3 P_{ab}^{(2)}(z) + \left(\frac{\alpha_s}{2\pi}\right)^4 P_{ab}^{(3)}(z) + \dots$$

$$\frac{d}{d \ln Q^2}$$

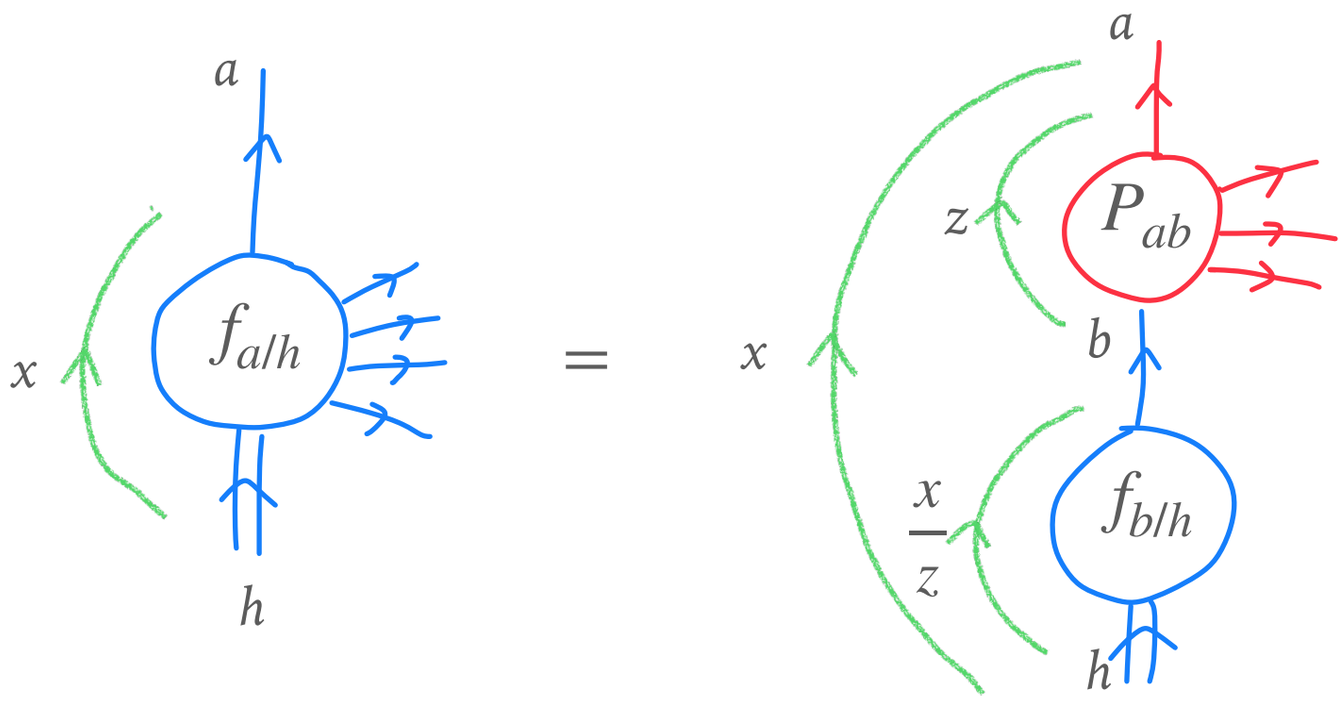


$P_{ab}$: describe splitting of parton b into parton a

# Splitting functions

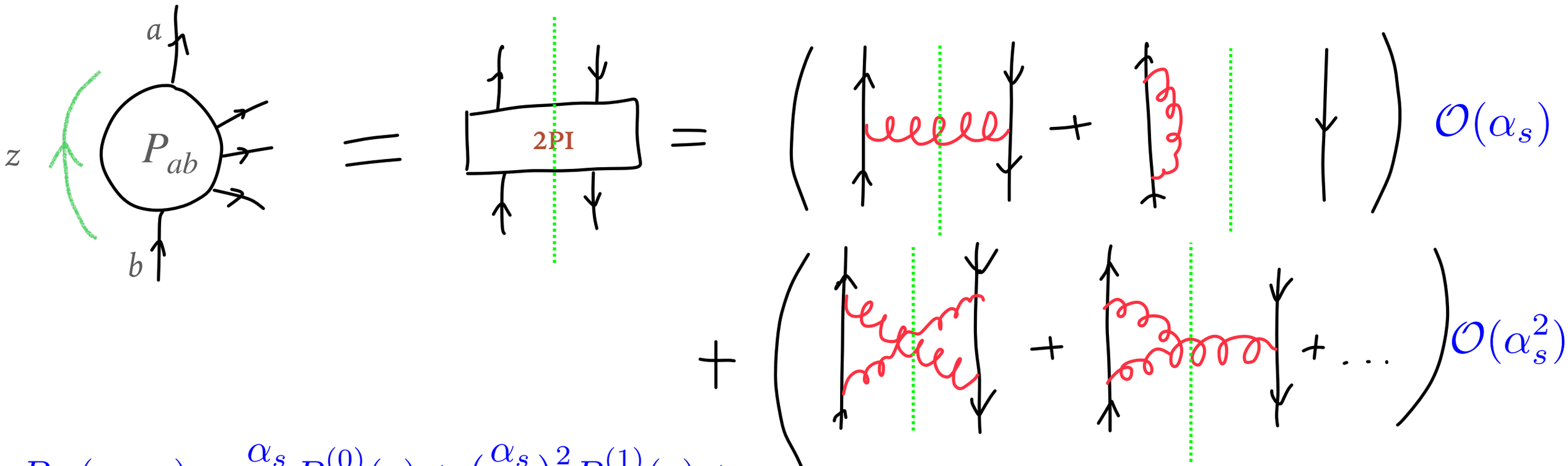


$$P_{ab}(\alpha_s, z) = \frac{\alpha_s}{2\pi} P_{ab}^{(0)}(z) + \left(\frac{\alpha_s}{2\pi}\right)^2 P_{ab}^{(1)}(z) + \ldots$$

Solving DGLAP with LO, NLO,… is equivalent to summing towers of large logarithms:

$$\alpha_s^n \left(\ln \frac{Q^2}{Q_0^2}\right)^n \quad , \quad \alpha_s^n \left(\ln \frac{Q^2}{Q_0^2}\right)^{n-1}$$

Emission of additional parton without $k_T$ ordering, adds power of $\alpha_s$ without accompanying collinear logarithm

# Splitting functions

## Leading order splitting functions

$$P_{qg}^{(0)}(z) = T_R\left[z^2 + (1-z)^2\right]$$

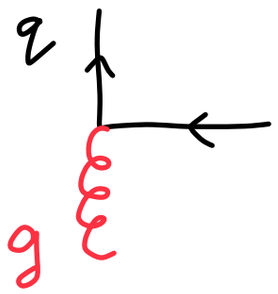


$$P_{gq}^{(0)}(z) = C_F\left[\frac{z^2 + (1-z)^2}{z}\right]$$

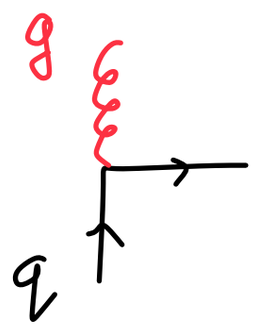


$$P_{qq}^{(0)}(z) = C_F\left[\frac{1+z^2}{(1-z)_+} + \frac{3}{2}\delta(1-z)\right]$$

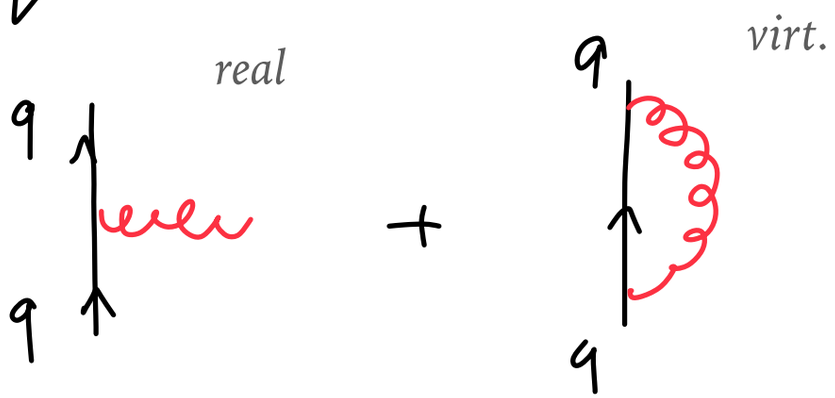


$$\int_0^1 dz f(z)\left(\frac{1}{1-z}\right)_+ \equiv \int_0^1 dz \frac{f(z)-f(1)}{1-z}$$

$$P_{gg}^{(0)}(z) = 2C_A\left[\frac{z}{(1-z)_+} + \frac{1-z}{z} + z(1-z) + \delta(1-z)\frac{11C_A - 4n_f T_R}{6}\right]$$

dominant at small z(x)

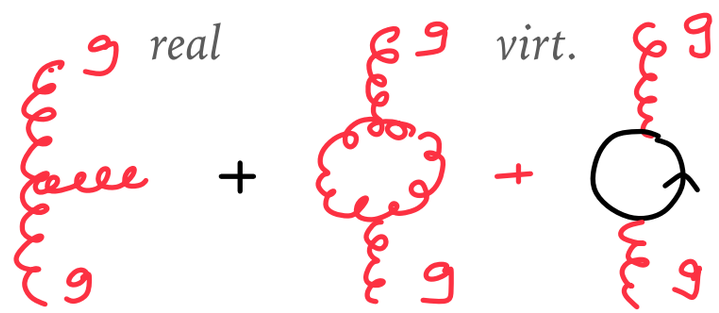

# Momentum sum rule in DGLAP

$$\mu^2 \frac{\partial}{\partial \mu^2} \begin{pmatrix} q_i(x,\mu^2) \\ g(x,\mu^2) \end{pmatrix} = \sum_j \int_x^1 \frac{dz}{z} \begin{pmatrix} P_{q_i q_j}(z,\alpha_s) & P_{q_i g}(z,\alpha_s) \\ P_{g q_j}(z,\alpha_s) & P_{gg}(z,\alpha_s) \end{pmatrix} \begin{pmatrix} q_j(\frac{x}{z},\mu^2) \\ g(\frac{x}{z},\mu^2) \end{pmatrix}$$

The DGLAP evolution equations satisfy the momentum sum rule

$$1 = \int_0^1 dx[xg(x,Q^2) + \sum_{j=q,\bar{q}} x f_j(x,Q^2)]$$

Valid at any value of $Q^2$

Which translates into conditions on the integrals of splitting functions

$$\int_0^1 dx x[P_{qq(x)} + P_{gq}(x)] = 0 \qquad \int_0^1 dx x[2N_F P_{qg(x)} + P_{gg}(x)] = 0$$

In addition the flavor sum rule holds

$$\int_0^1 dx[f_{q_i}(x,Q^2) - f_{\bar{q}_i}(x,Q^2)] = N_i$$

number of valence quarks i

# DGLAP anomalous dimensions

Define anomalous dimension via Mellin moment of the splitting function

$$\gamma_{ij}(\omega) = \int_0^1 dx\, x^\omega P_{ij}(x)$$

Example: gluon anomalous dimension at LO:

$$\gamma^{(0)}(\omega) = 2C_A\left(\frac{1}{\omega} - \frac{1}{\omega+1} + \frac{1}{\omega+2} - \frac{1}{\omega+3} - \psi(2+\omega) - \gamma_E + \frac{11}{12} - \frac{N_f}{18}\right)$$

Singularities at $\omega \to 0$ inform about small x limit

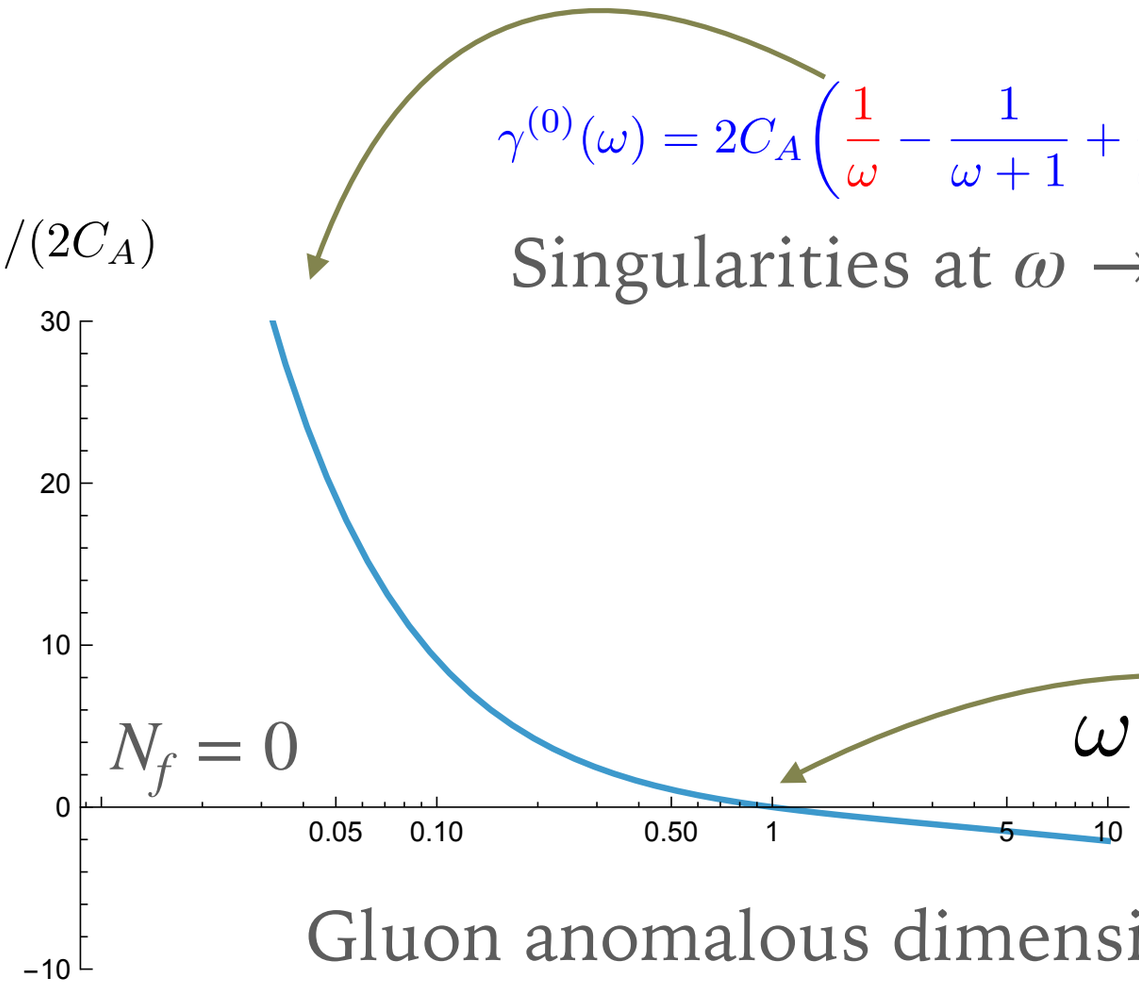


Momentum sum rule in terms of anomalous dimensions

$$\gamma_{qq}(\omega = 1) + \gamma_{gq}(\omega = 1) = 0$$

$$2N_f\gamma_{qg}(\omega = 1) + \gamma_{gg}(\omega = 1) = 0$$

Gluon anomalous dimension (at $N_f = 0$) **vanishes** at $\omega = 1$

Pure gluodynamics satisfies momentum sum rule

# Approximate solution: large x

$f_a(x,Q^2) =$ 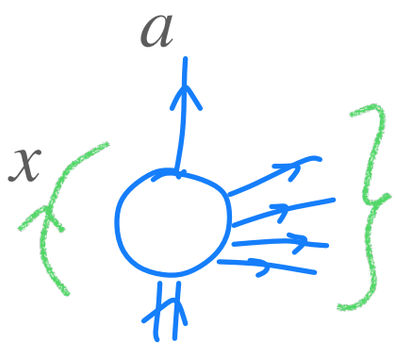


Quark/gluon retains most momentum
Many soft gluons radiated
Evolution dominated by terms with $\left(\frac{1}{1-z}\right)_+$

$$P_{qq}(z) \simeq C_F \frac{2}{(1-z)_+} \qquad P_{gg}(z) \simeq 2C_A \frac{1}{(1-z)_+}$$

$$\int_x^1 dz \left(\frac{1}{1-z}\right)_+ = -\int_0^x \frac{dz}{1-z} = \ln(1-x)$$

Iteration of DGLAP with $P_{aa}(z)$

$$\exp\left[\int_x^1 dz \frac{2C_a}{(1-z)_+} \int_{Q_0^2}^{Q^2} \frac{dq^2}{q^2} \frac{\alpha_s(q^2)}{2\pi}\right] = \exp(p_a \ln(1-x)) = (1-x)^{p_a}$$

where $p_a = \frac{C_a}{\pi\beta_0} \ln \frac{\alpha_s(Q_0^2)}{\alpha_s(Q^2)}$ and we have $p_a > 0$ for $Q_0^2 < Q^2$

The resulting parton distribution will behave as:

where initial distribution
$f_a(x,Q_0^2) \sim (1-x)^\eta,\ \eta > 0$

$f_a(x,Q^2) \simeq f_a(x,Q_0^2)\,(1-x)^{p_a}$
More suppression at large x, with increasing $Q^2$

*(can obtain this solution also by using Mellin space)*

# Approximate solution: small x

$f_a(x, Q^2) =$

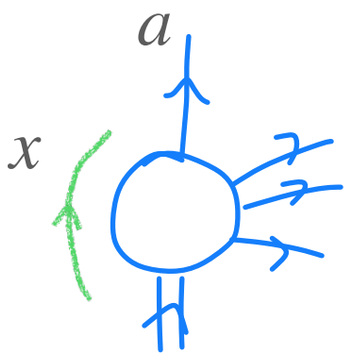


$x \to 0$

can emit many gluons

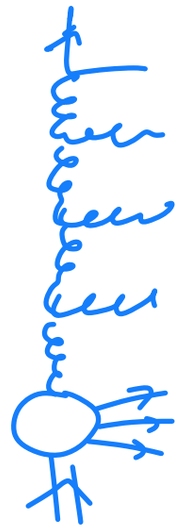

many gluons emitted over the large rapidity range:

$$\Delta y \simeq \ln 1/x$$

Dominated by the evolution of the gluon density

$$P_{gg}(z) \simeq 2C_A \frac{1}{z}$$

$$z \to 0$$

*(can obtain this solution also by using Mellin space)*

Solution as $x \to 0$:

$$x f_g(x, Q^2) \simeq x f_g(x, Q_0^2) \exp\left[\sqrt{\frac{2C_A}{\pi\beta_0} \ln\frac{\alpha_s(Q_0^2)}{\alpha_s(Q^2)} \ln\frac{1}{x}}\right]$$

- **Strong rise of gluon density** (and in consequence of structure functions) with **decreasing** $x$
- Faster than any power of $\ln 1/x$ but slower than any power of $1/x$ *(however if input distribution behaves as a power than it could dominate)*
- Steepness of this distribution increases with $Q^2$
- Characteristic property of non-abelian theory: **self-interacting gluons**

# Example : DGLAP evolution of the gluon density

Example of the DGLAP evolution (LO): gluon density

Valence-like input: $xg(x, Q_0^2) = N_g x^{0.5}(1-x)^5$

linear scale

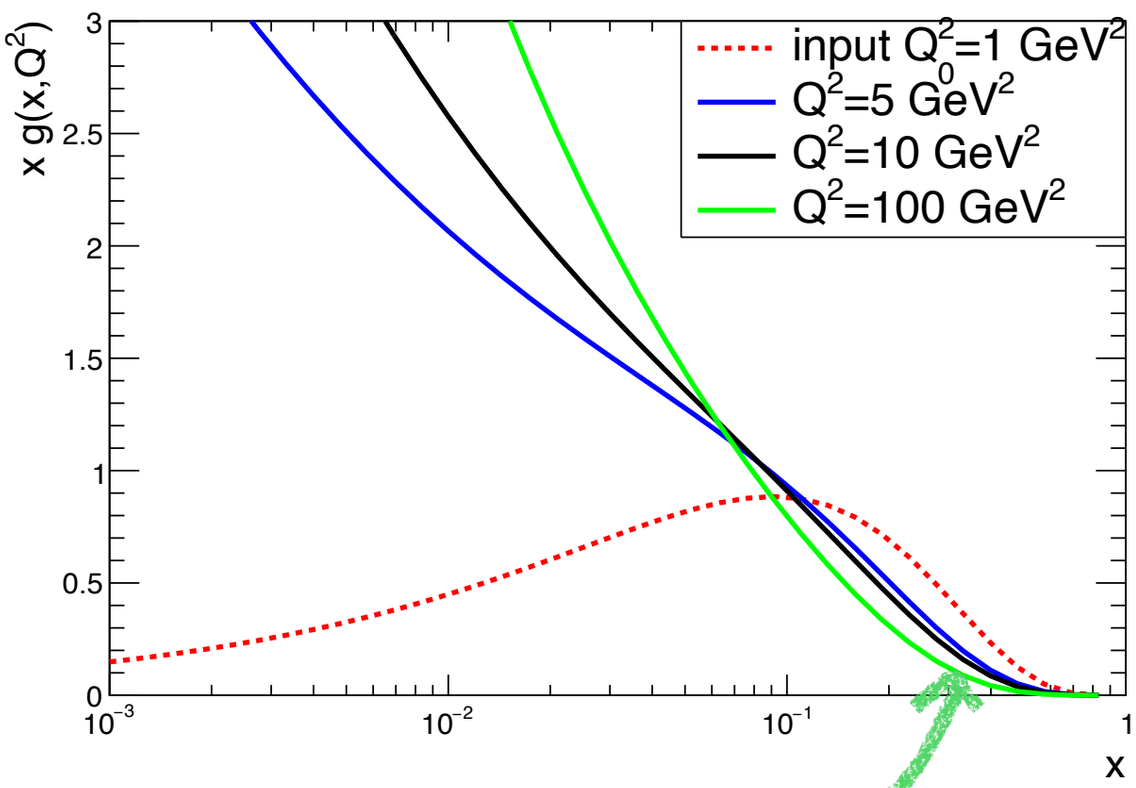


logarithmic scale

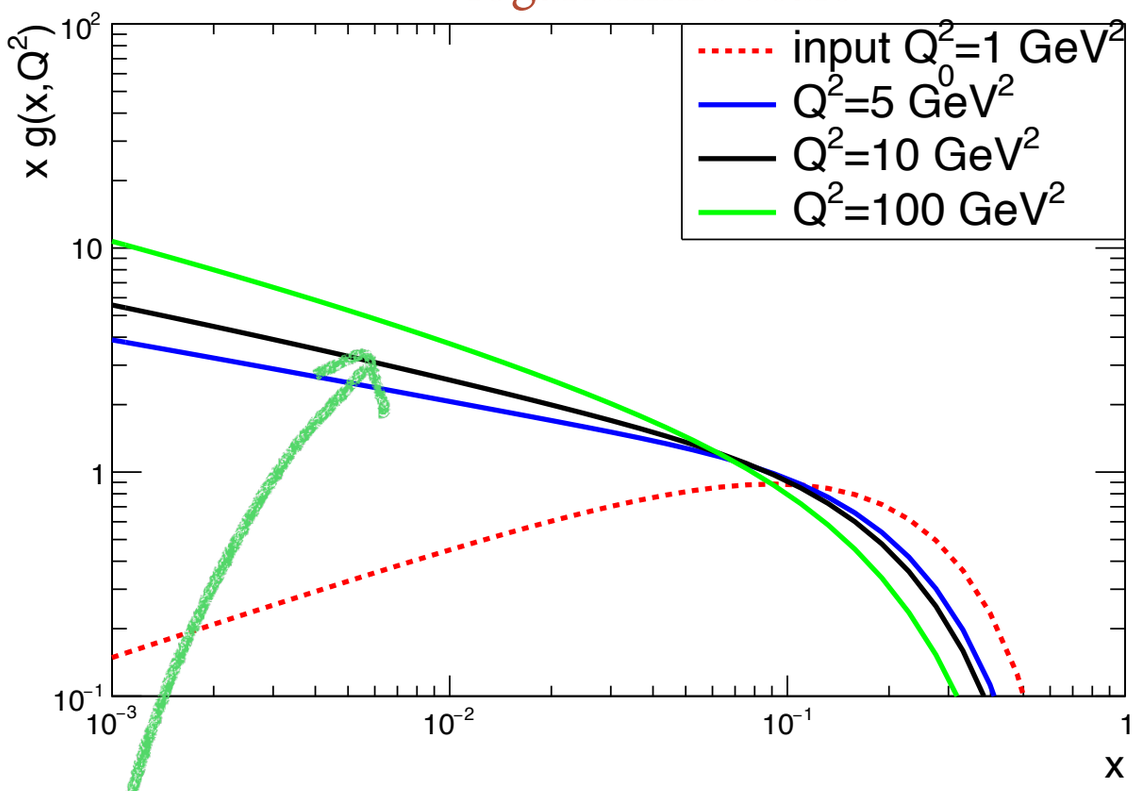


Depletion at large x, growth at small x

Valence-like input modified to increase at small x

# Proton PDFs

## Parametrization

$$xf(x) = Ax^B(1-x)^C(1+Dx+Ex^2)$$

- There is no particular reason to limit the analysis to this form, but pragmatically this is what works
- The power on (1-x) terms is positive and ensures that the distribution vanishes for x=1
- The power at x term can be positive or negative, depending on whether the distribution is valence like or sea
- Note that gluons at this order are initially valence-like
- They can become negative. Formally this is not a problem since this is not observable quantity. Practically this is a problem since the cross section can turn negative and this is then unphysical

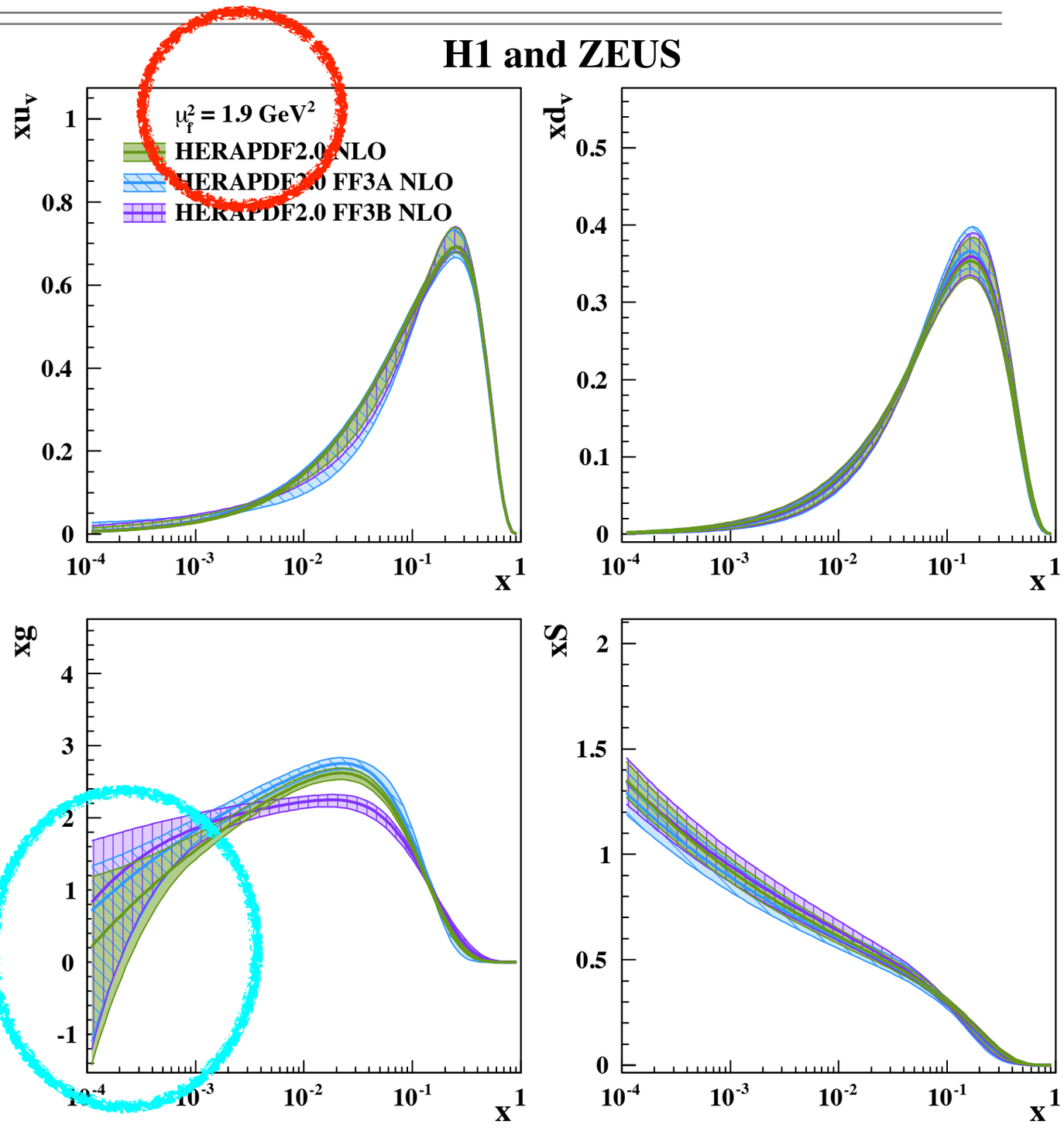

# Parton densities from DGLAP

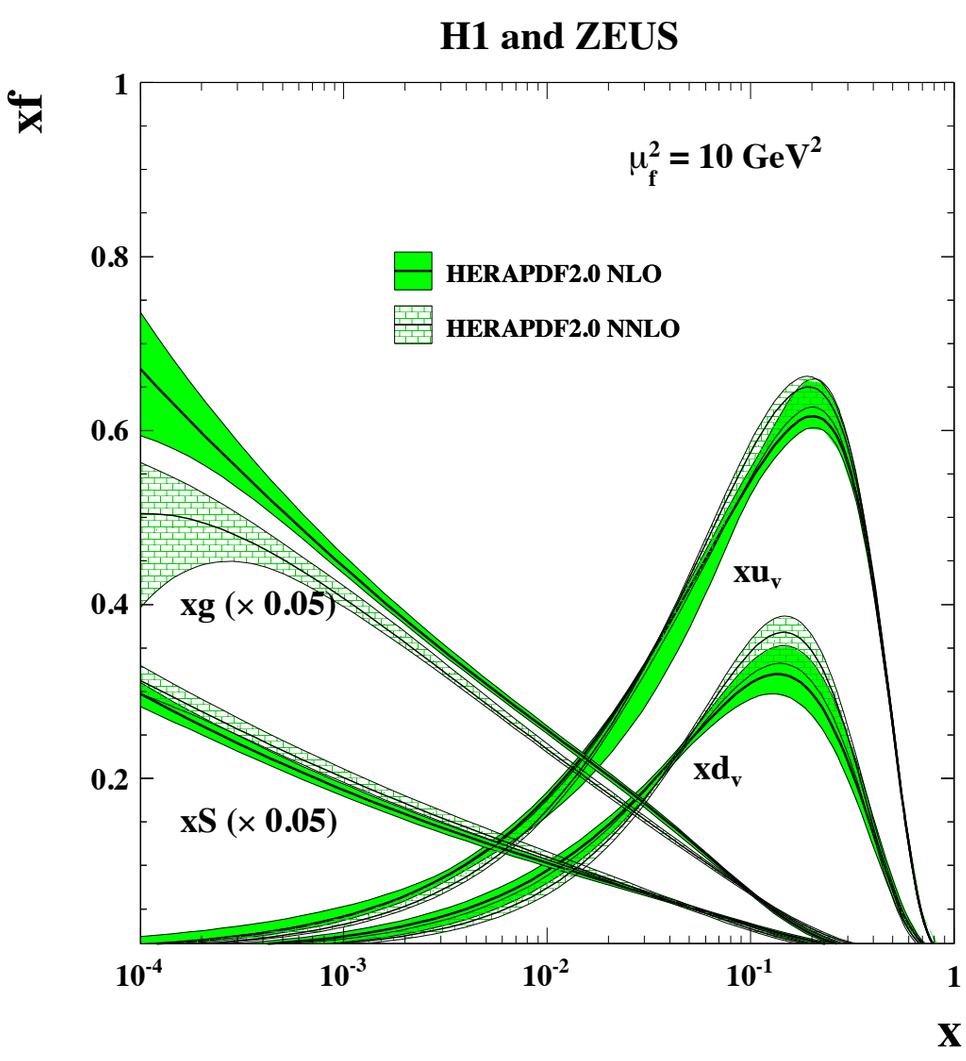


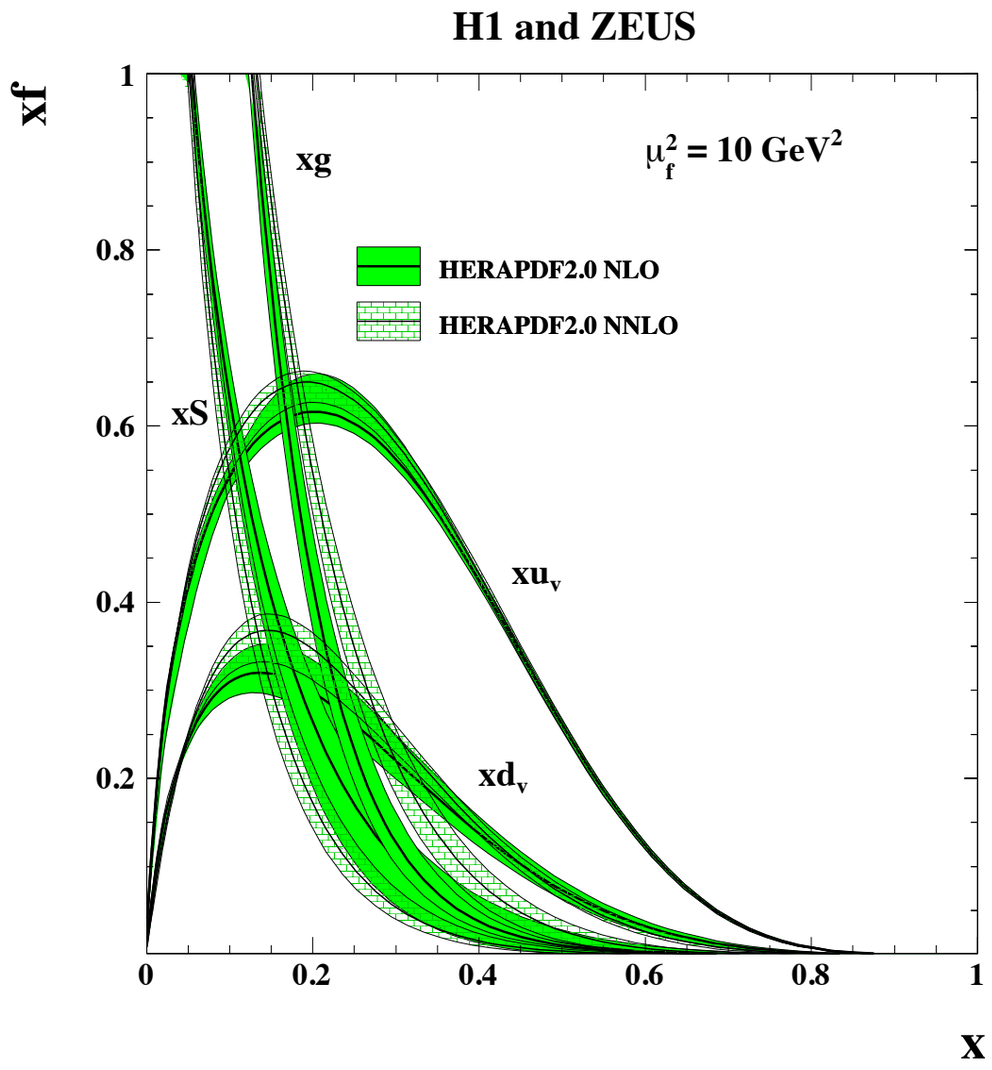


Gluon density dominates at small $x$

Valence distribution have peak around 0.1

NLO vs NNLO small $x$ behavior

Small $x$ : large energy

$$x = \frac{Q^2}{Q^2 + W^2}$$

$$W^2 = s_{\gamma^* p}$$

# PDFs and structure function

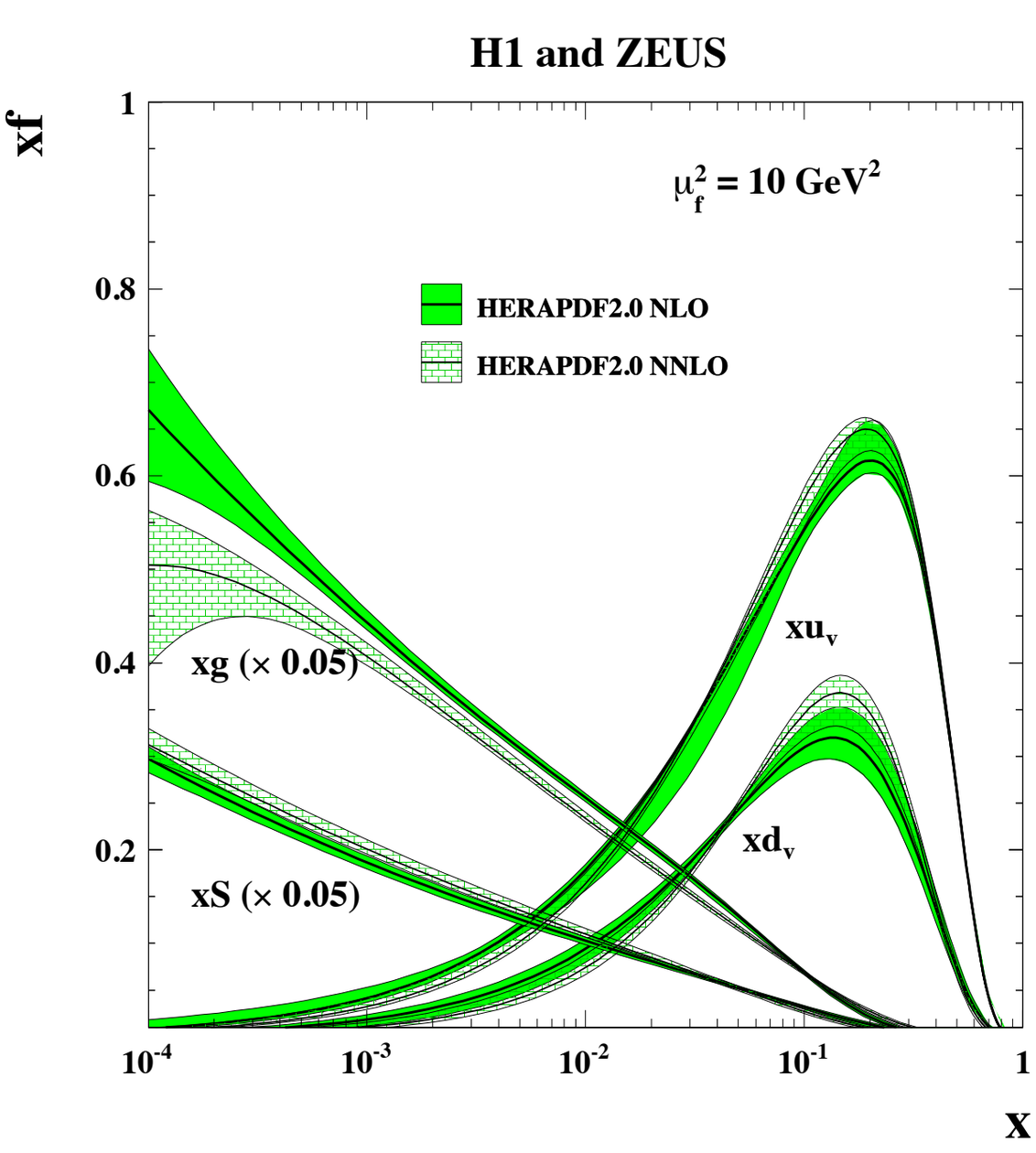


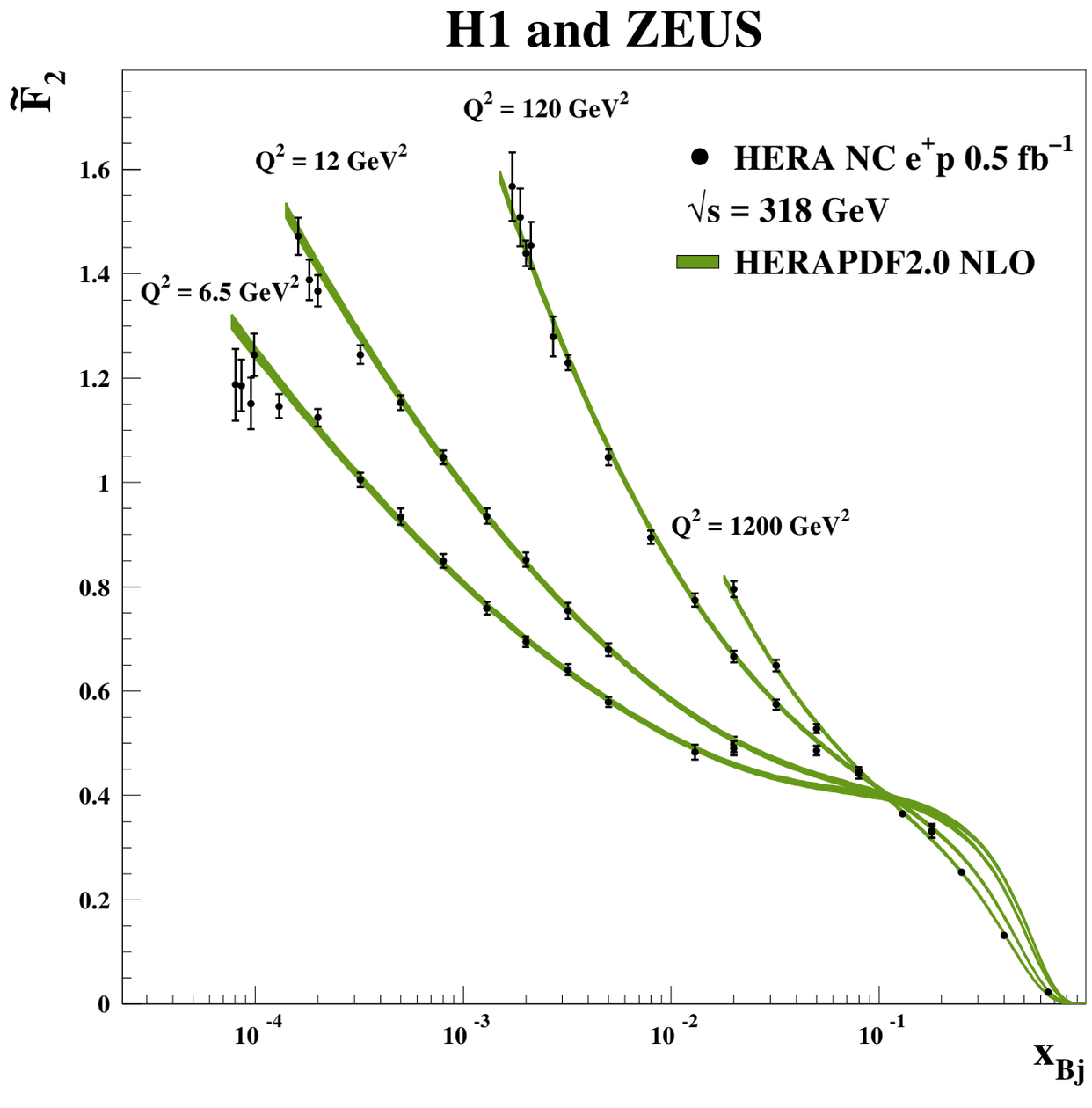

# DGLAP fits of cross section for the proton

DGLAP based fits of the structure function for proton work very well

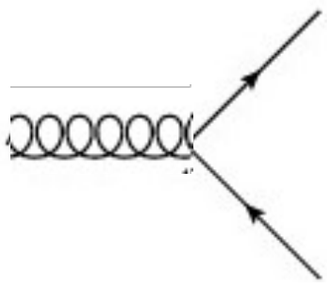

@ low x

QCD scaling violations

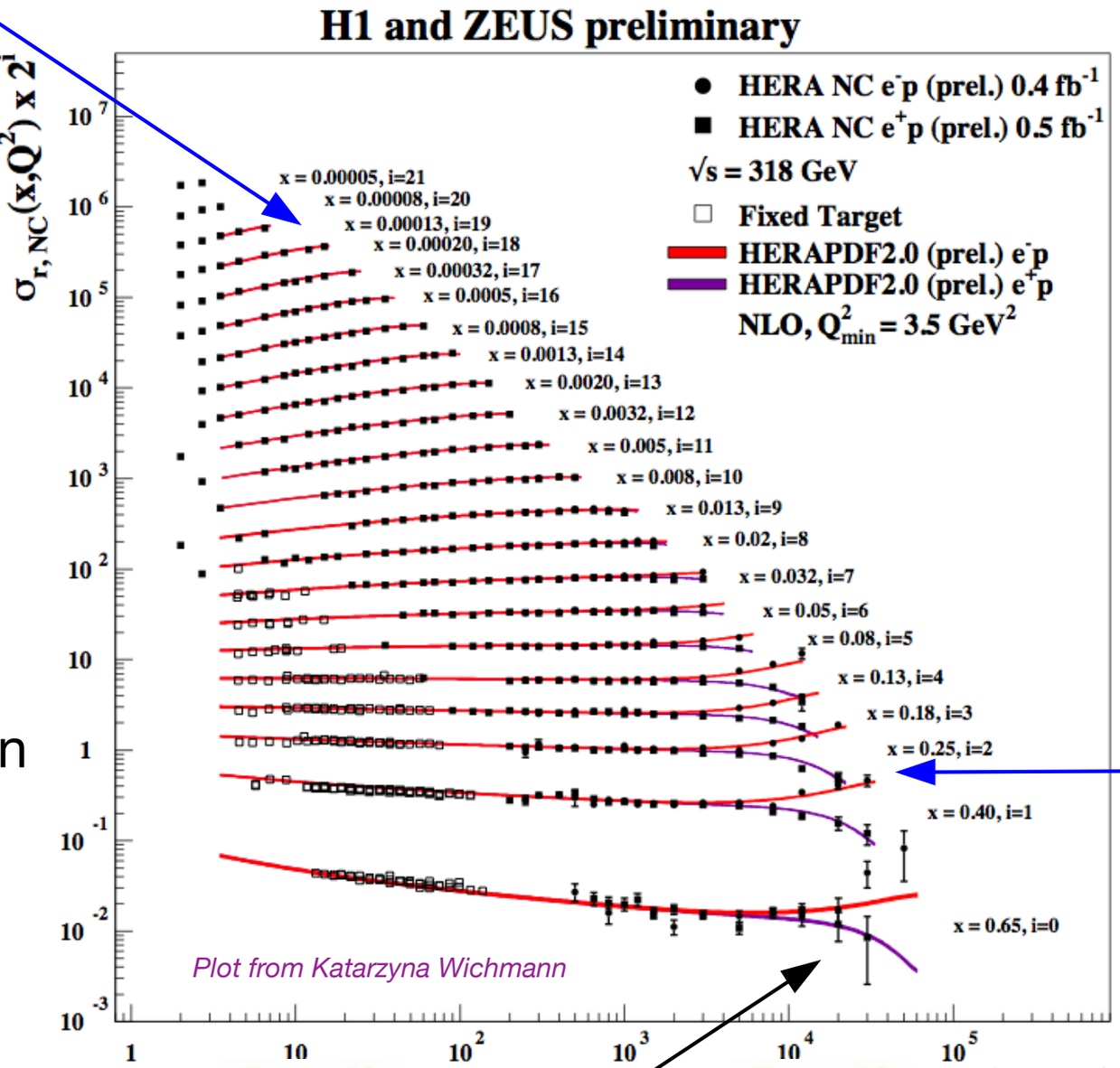


Plot from Katarzyna Wichmann

Bjorken scaling region

@ high Q²

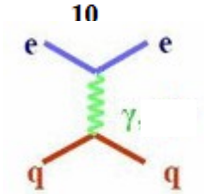


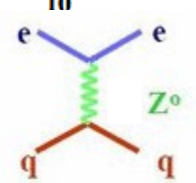


Reduced cross section

$$\sigma_{r,NC} = F_2 - \frac{y^2}{Y+} F_L$$

$$Q^2 \ll M_Z^2$$



@ high x

# DGLAP fits of $F_2$ for the proton

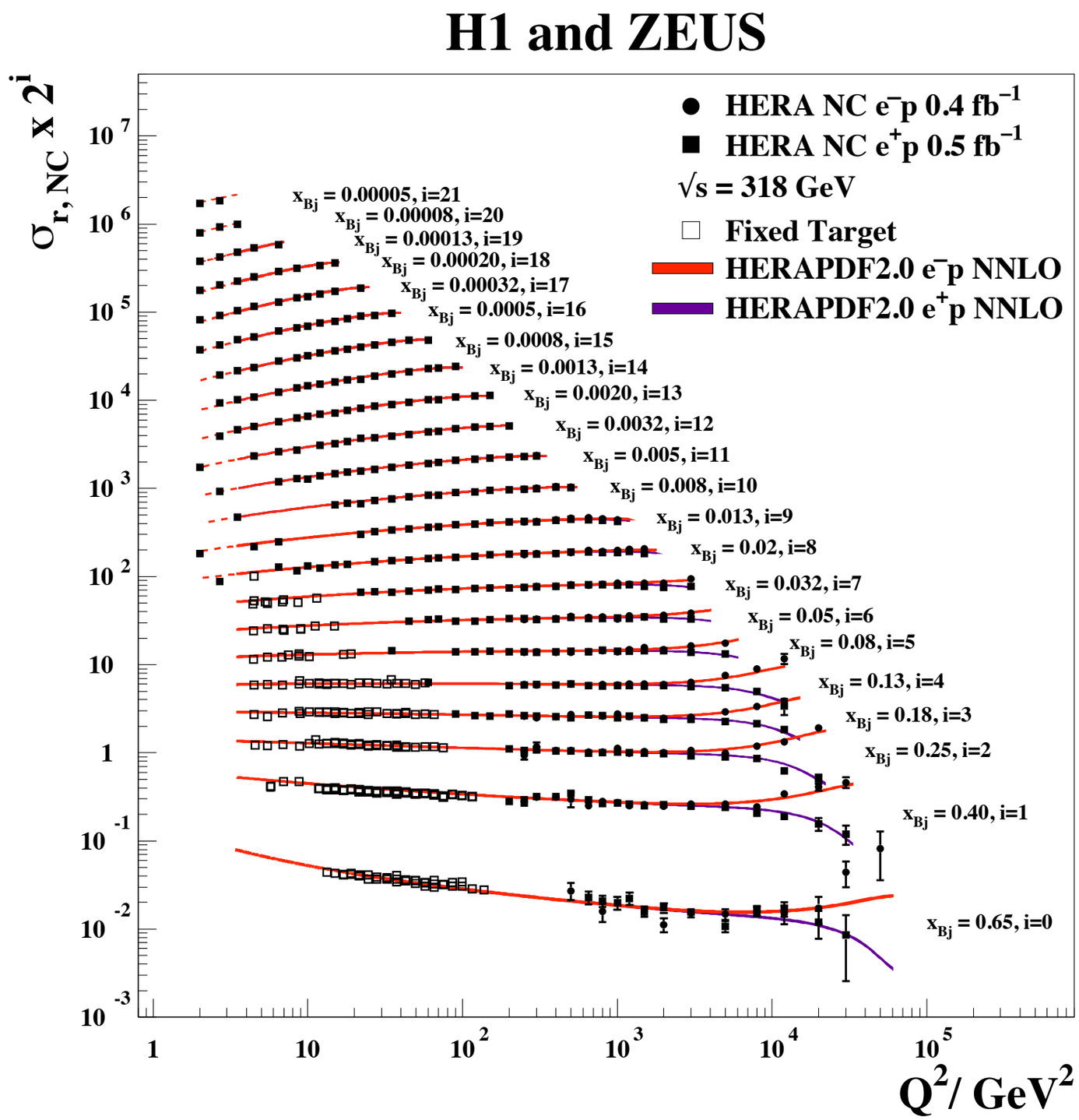


Similar quality of NNLO fit

Collinear description works very well

# Longitudinal structure function $F_L$

In parton model $F_L = 0$. Callan-Gross relation. In QCD it becomes non-zero

$$\sigma_{r,NC} = \frac{d^2\sigma_{NC}}{dxdQ^2}\frac{Q^4 x}{2\pi\alpha_{\rm em} Y_+} = F_2 - \frac{y^2}{Y_+}F_L \qquad Y_+ = 1 + (1-y)^2$$

Need various y values for fixed (x,$Q^2$)

Measurement for various energies

HERA: 920, 575, 460 GeV

In each bin of (x,$Q^2$) perform linear fit

to $\sigma_r$ as a function of $\frac{y^2}{Y_+}$

Intercept and slope give $F_2$ & $F_L$

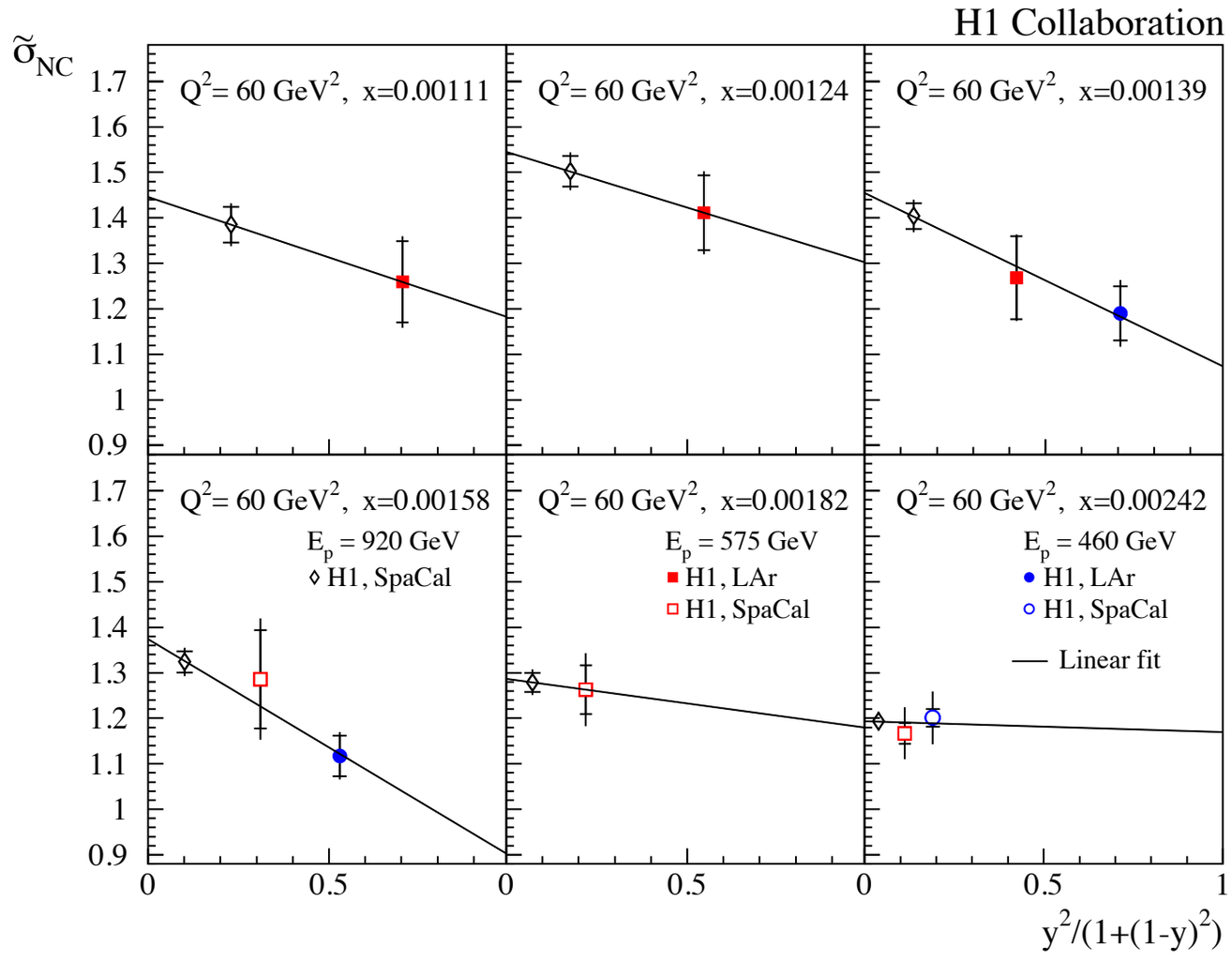


*Note: here* $\tilde{\sigma}_r = \sigma_r - \frac{Y_-}{Y_+}xF_3$ *$xF_3$ negligible for* $Q^2 < 800\ \mathrm{GeV}^2$

# Longitudinal structure function $F_L$

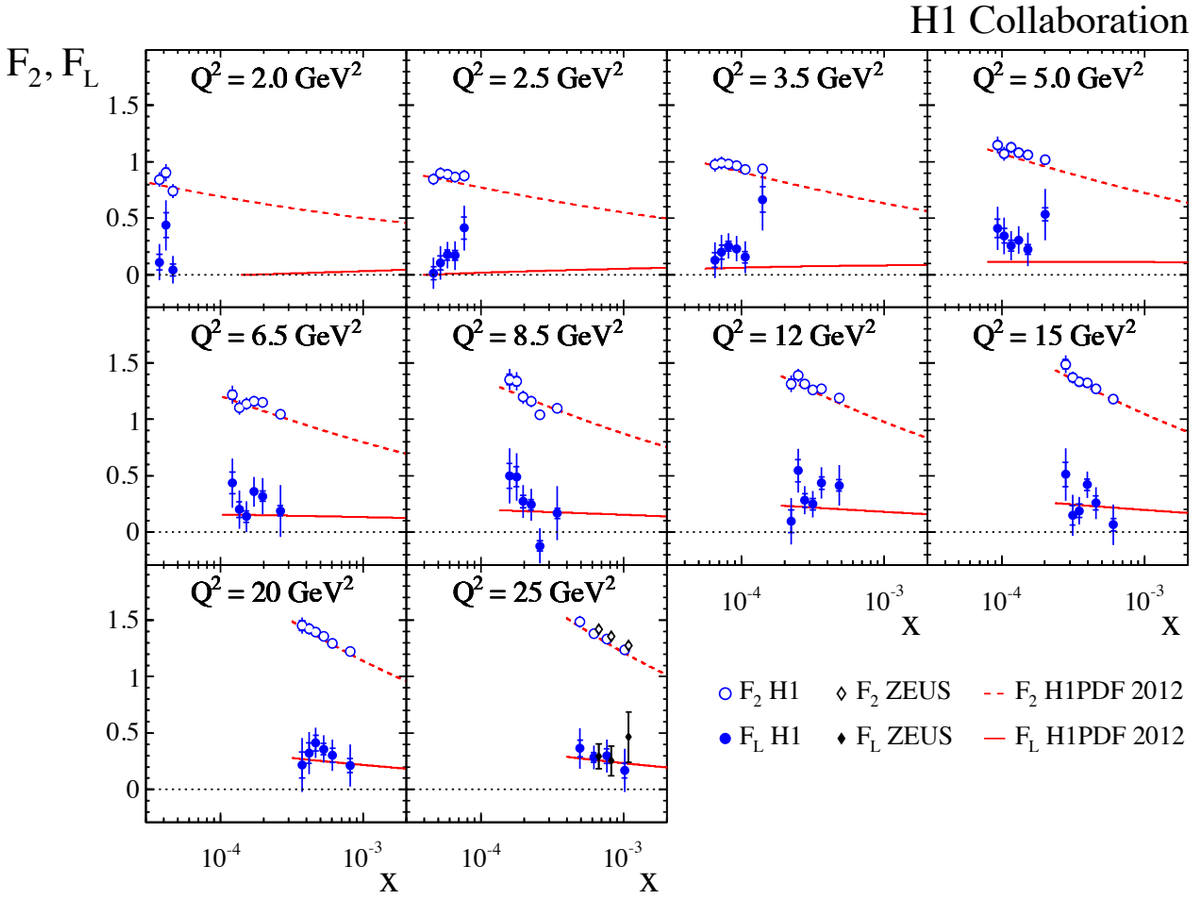


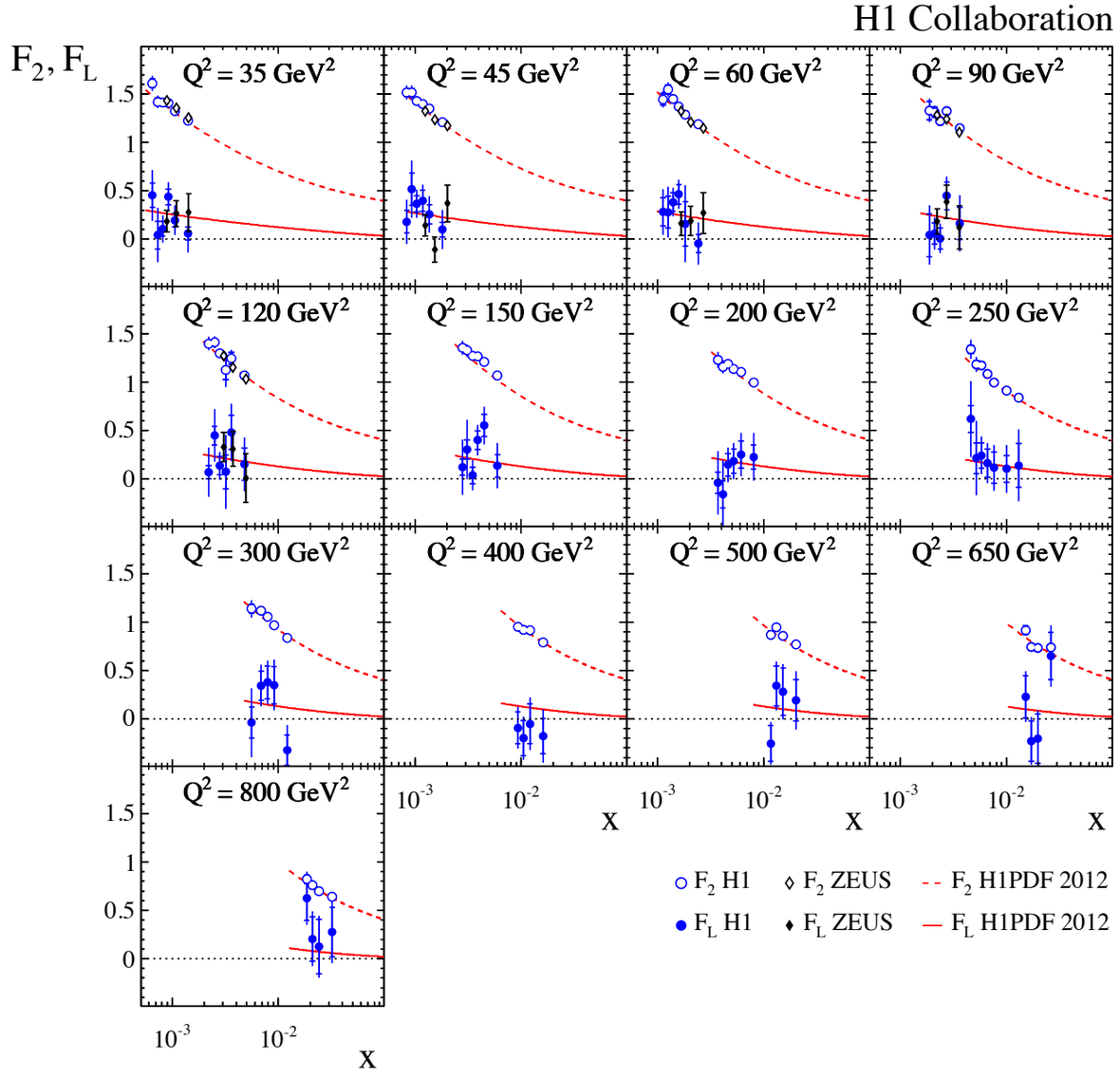


$F_L \ll F_2$ but non-negligible

Different sensitivity to the gluon density of both structure functions

# Ratio $R=F_L/F_T$

$$R = \frac{\sigma_L}{\sigma_T} = \frac{F_L}{F_2 - F_L}$$

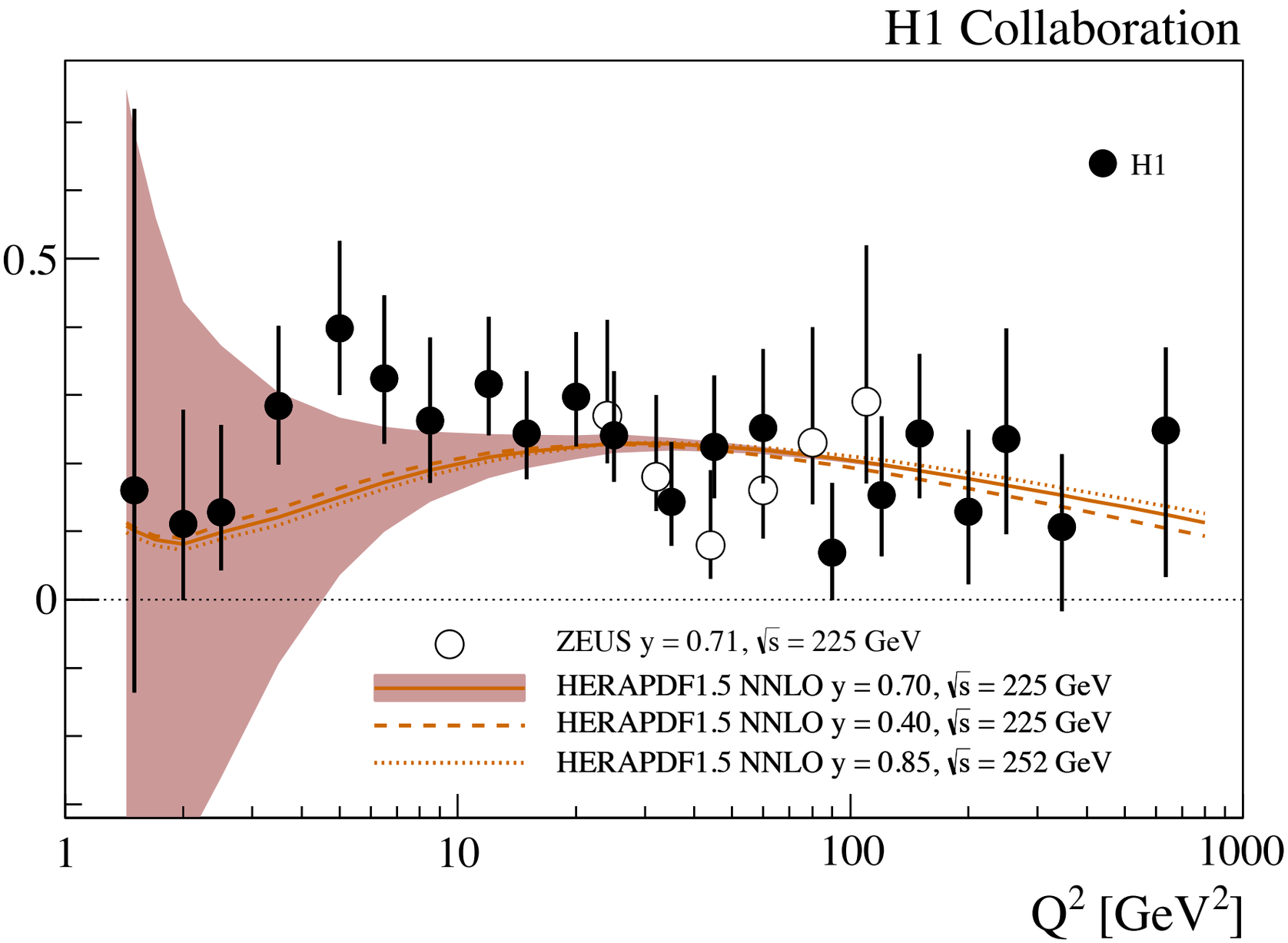


Ratio of cross sections with the exchange of the longitudinally polarized photons and transversely polarized photons. Should vanish as $\sim Q^2$.

# Prospects for measurements of $F_L$ at the EIC

EIC variable energies allow for extraction of $F_L$

Systematic errors on the reduced cross section

Conservative scenario: 3.9% sys. (HERA like)

Optimistic scenario: 1% sys.

Perform Rosenbluth separation to extract $F_L$

Final $F_L$ uncertainty comes from the fit

*Jimenez-Lopez, Newman, Wichmann*

| $e$-beam energy (GeV) | $p$-beam energy (GeV) | $\sqrt{s}$ (GeV) | Integrated lumi ($\text{fb}^{-1}$) |
|---|---|---|---|
| 18 | 275 | 141 | 15.4 |
| 10 | 275 | 105 | 100 |
| 10 | 100 | 63 | 79.0 |
| 5 | 100 | 45 | 61.0 |
| 5 | 41 | 29 | 4.4 |

Uncertainties in the simulated $F_L$

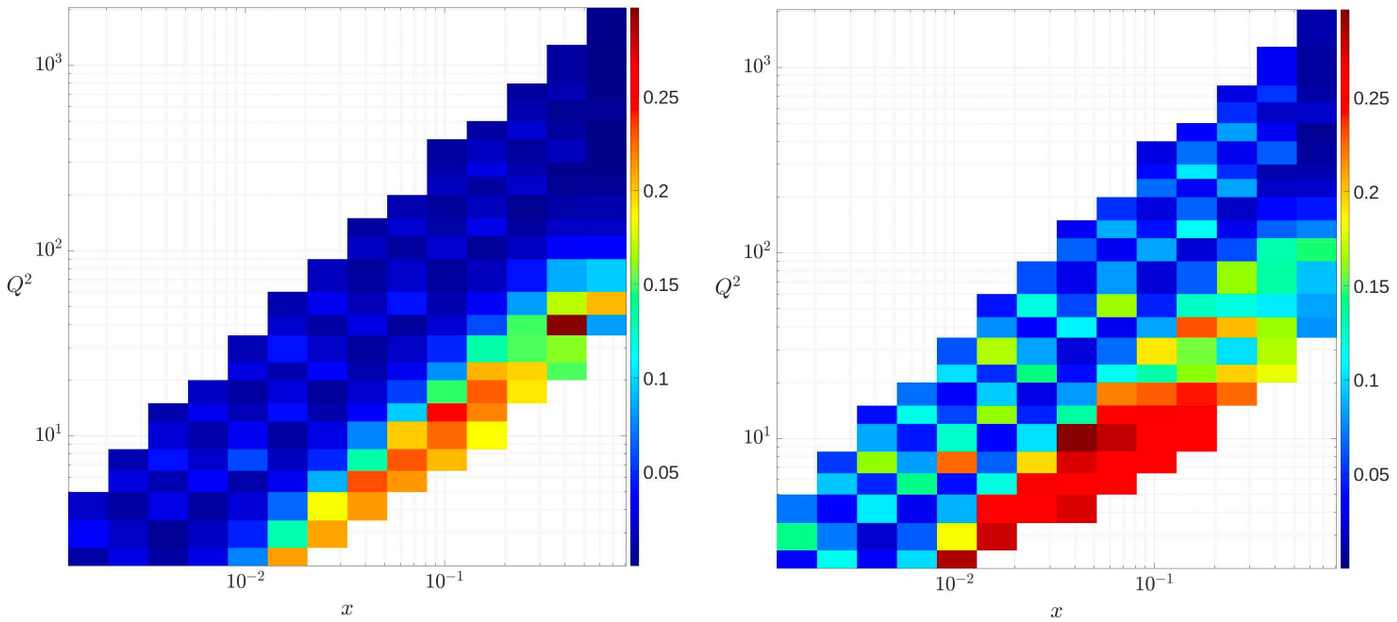


*optimistic* *conservative*

Examples of Rosenbluth fit

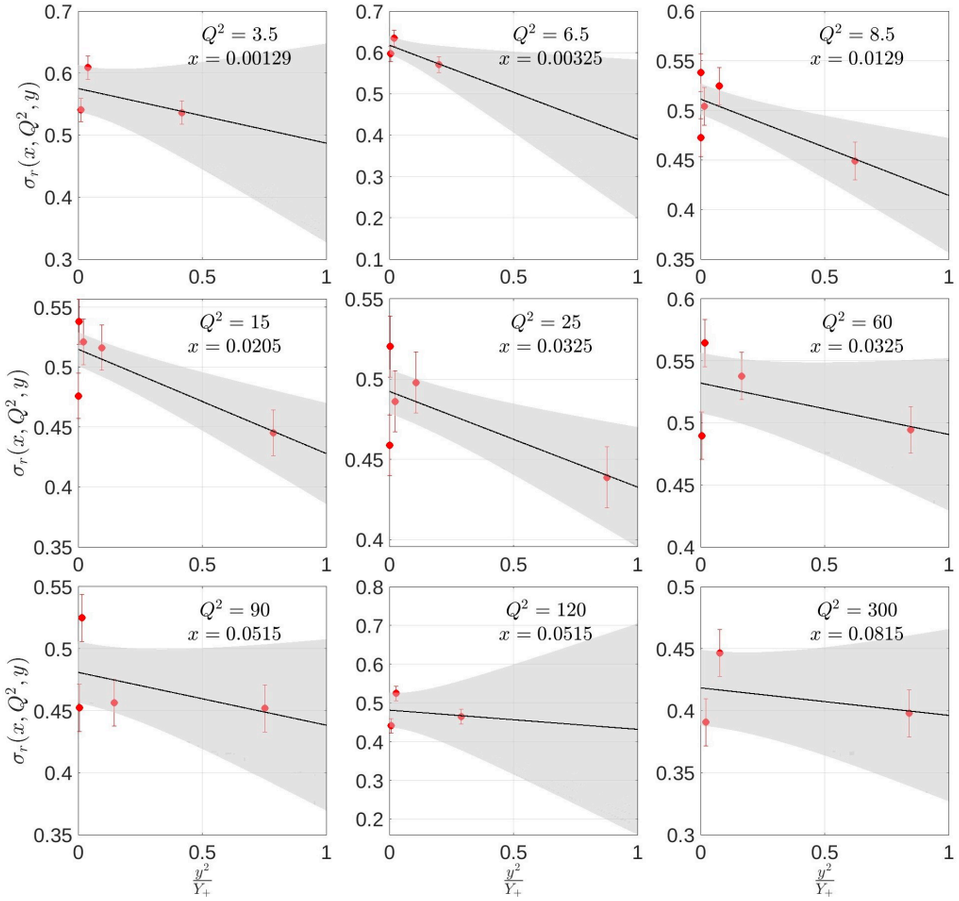

# Prospects for measurements of $F_L$ at the EIC

*Jimenez-Lopez, Newman, Wichmann*

*conservative*

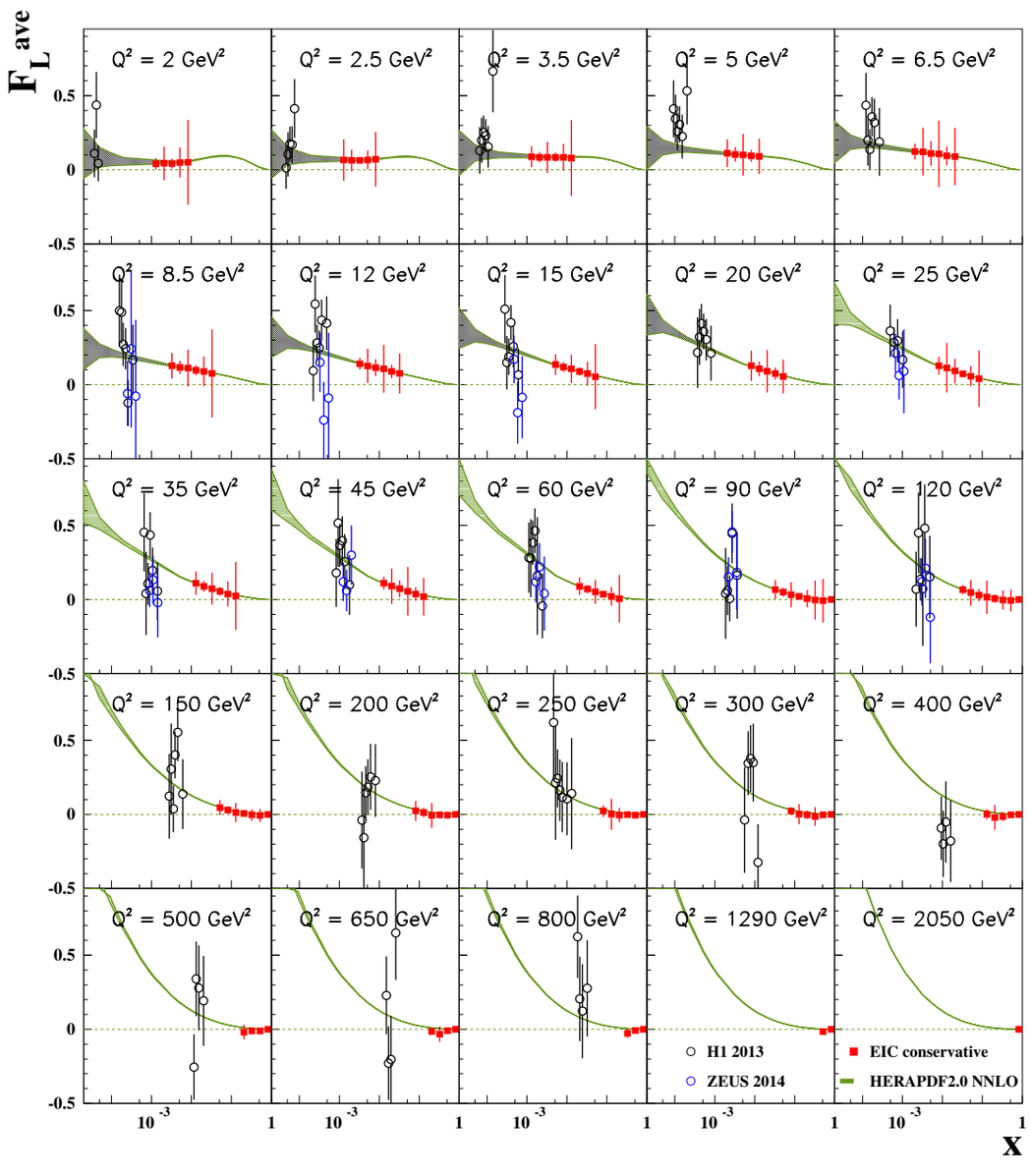


*optimistic*

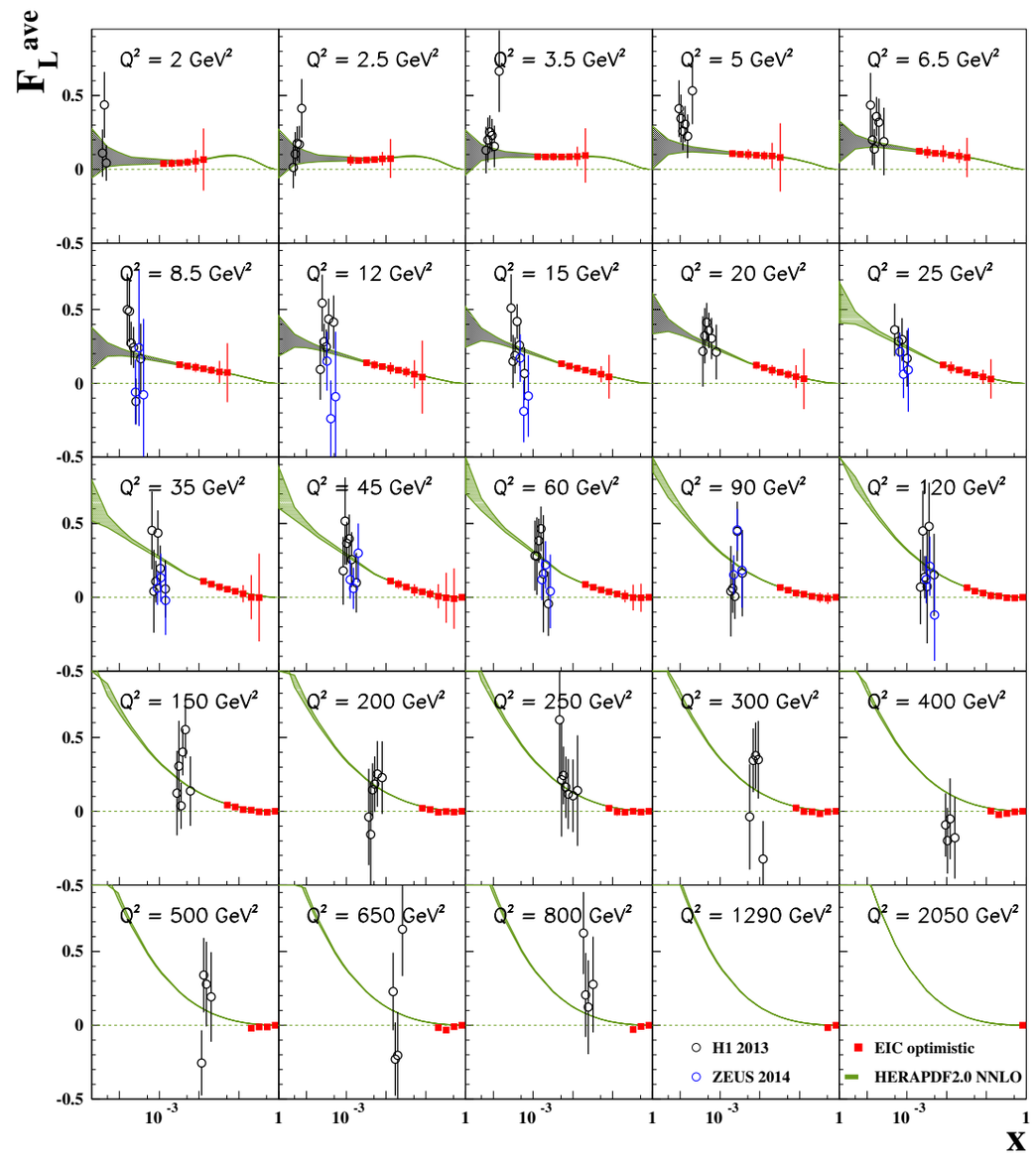

# Prospects for measurements of $F_L$ at the EIC

*Jimenez-Lopez, Newman, Wichmann*

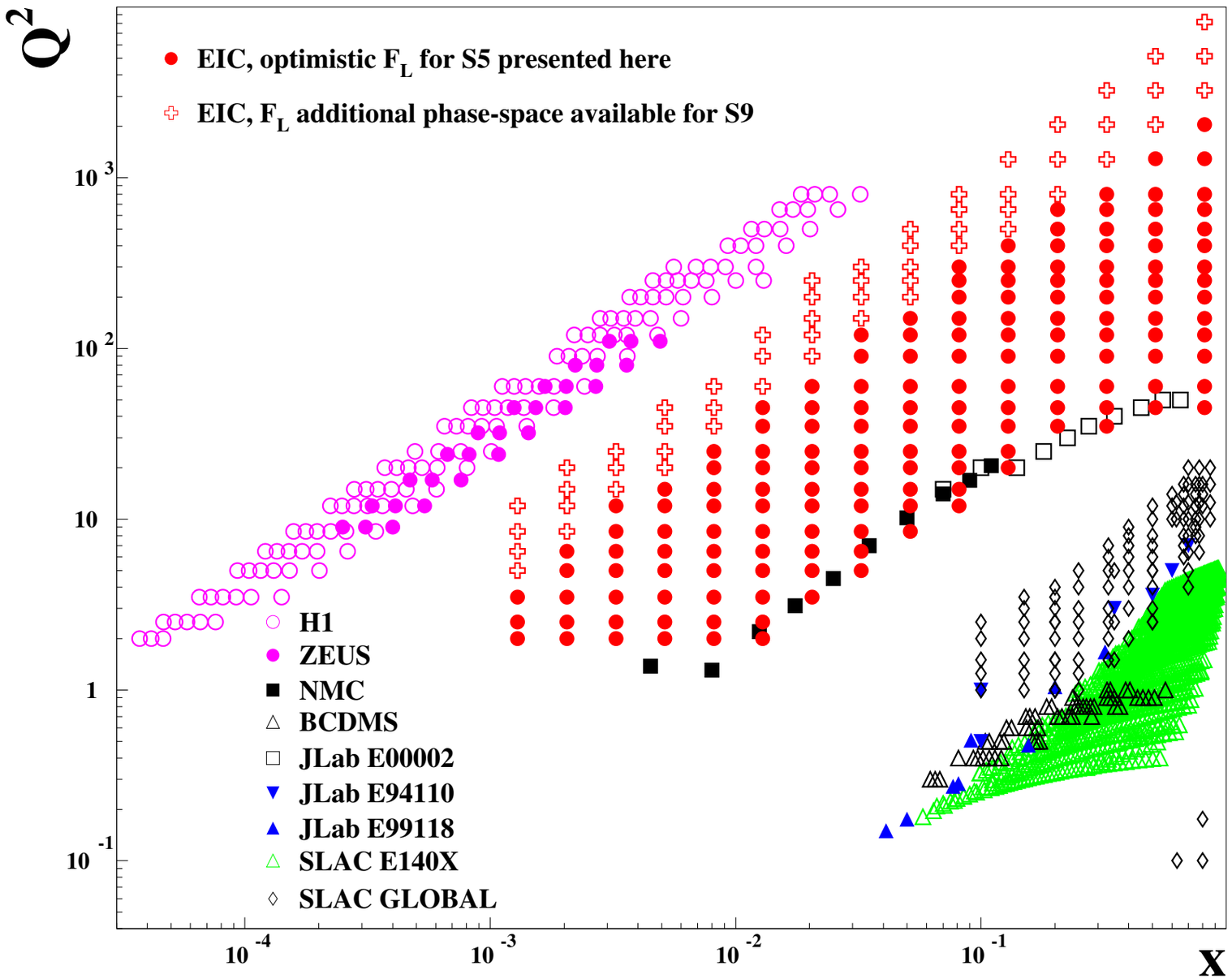


Kinematic region for $F_L$ for HERA, EIC and fixed target data

EIC data will close the large gap between the data from the fixed target and HERA

Already 5 energies give large span, 9 energies would enlarge the region towards higher $Q^2$

| | | $E_p$ [GeV] | | | | | |
|---|---|---|---|---|---|---|---|
| | | 41 | 100 | 120 | 165 | 180 | 275 |
| $E_e$ [GeV] | 5 | **29** | **45** | 49 | **57** | 60 | 74 |
| | 10 | 40 | **63** | 69 | **81** | (85) | **105** |
| | 18 | 54 | **85** | 93 | **109** | 114 | **141** |

*'EIC has potential to transform the knowledge on $F_L$. Large potential impact onto the precision of the proton PDFs and constraining models.'*

# DIS with nuclei

- What happens when the lepton scatters off a nucleus instead of nucleon?
- How the presence of a nuclear target modifies cross sections and structure functions?

| | |
|---|---|
| **Typical distance between nucleons** | $d \simeq 1.9\,\mathrm{fm}$ |
| **Baryon density** | $\rho_0 \simeq 0.15\,\mathrm{fm}^{-3}$ |
| **Fermi momentum** | $p_F \simeq 0.26\,\mathrm{GeV}$ |

**Incoherent scattering** from A nucleons but with their structure modified by the presence of nuclear medium. For example, mean field that nucleon experiences in the presence of other nucleons, Fermi motion of nucleons in the nucleus.

**Coherent scattering** which involve more than one nucleon at a time. Such effects arise when the hadronic  fluctuations produced by the photon propagate over the distance (in laboratory frame) which are longer than the characteristic length scale between nucleons, d=2 fm. An example of such effect is shadowing.

# DIS with nuclei

Similarly to the DIS on nucleons the information about the nuclear structure is encoded in the hadronic tensor.

$$W_{\mu\nu}(p,q) = -W_1(g_{\mu\nu} - \frac{q_\mu q_\nu}{q^2}) + \frac{W_2}{M^2}(p_\mu - \frac{p\cdot q}{q^2}q_\mu)\cdot(p_\nu - \frac{p\cdot q}{q^2}q_\nu)$$

Unpolarized case

**Nuclear structure functions:**

$$F_{1,2}^A(x_A, Q^2)$$

$P$ 4-mom of nucleus
$p$ 4-mom of nucleon

$$x_A = \frac{Q^2}{2P\cdot q} \qquad 0 < x_A \leq 1$$

Typically the quantity studied is the structure function as a function on Bjorken x on a single nucleon:

$$F_{1,2}^A(x, Q^2)$$

$$x = \frac{Q^2}{2p\cdot q} = x_A A$$

Note that: $0 < x \leq A$

# DIS kinematics: nuclei

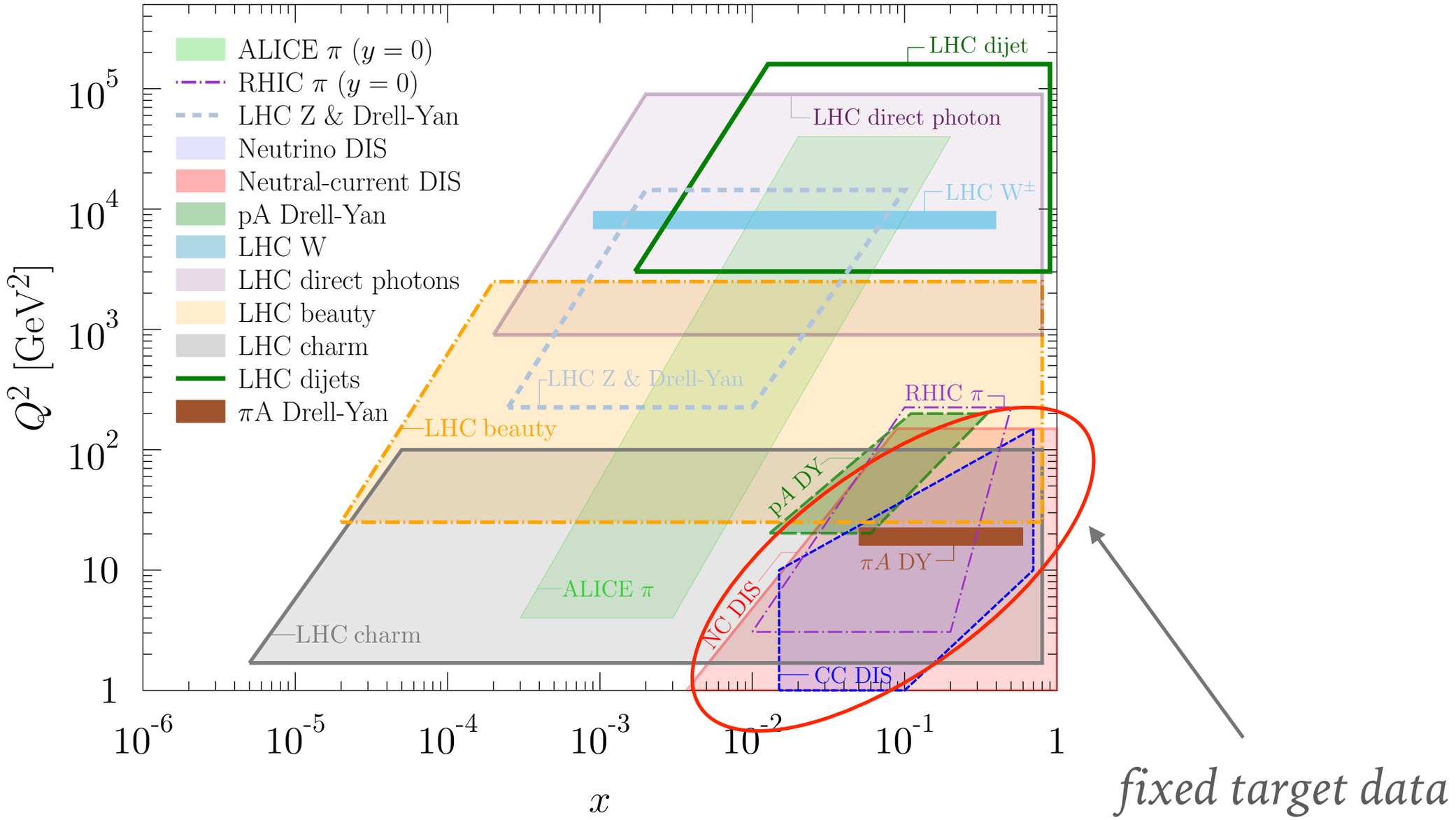


DIS nuclear data limited to fixed target: large $x$

LHC and RHIC extended kinematic regime for nPDFs for Au,Pb to low $x$ and high $Q^2$

# Nuclear structure

Nuclear ratio:

$$R^A_{F_2}(x,Q^2) = \frac{F_2^A(x,Q^2)}{A\,F_2^{\text{nucleon}}(x,Q^2)}$$

Ratio of cross section on a nucleus to the proton (scaled by mass number A)

Nuclear effects: $R^A \neq 1$

Schematic picture

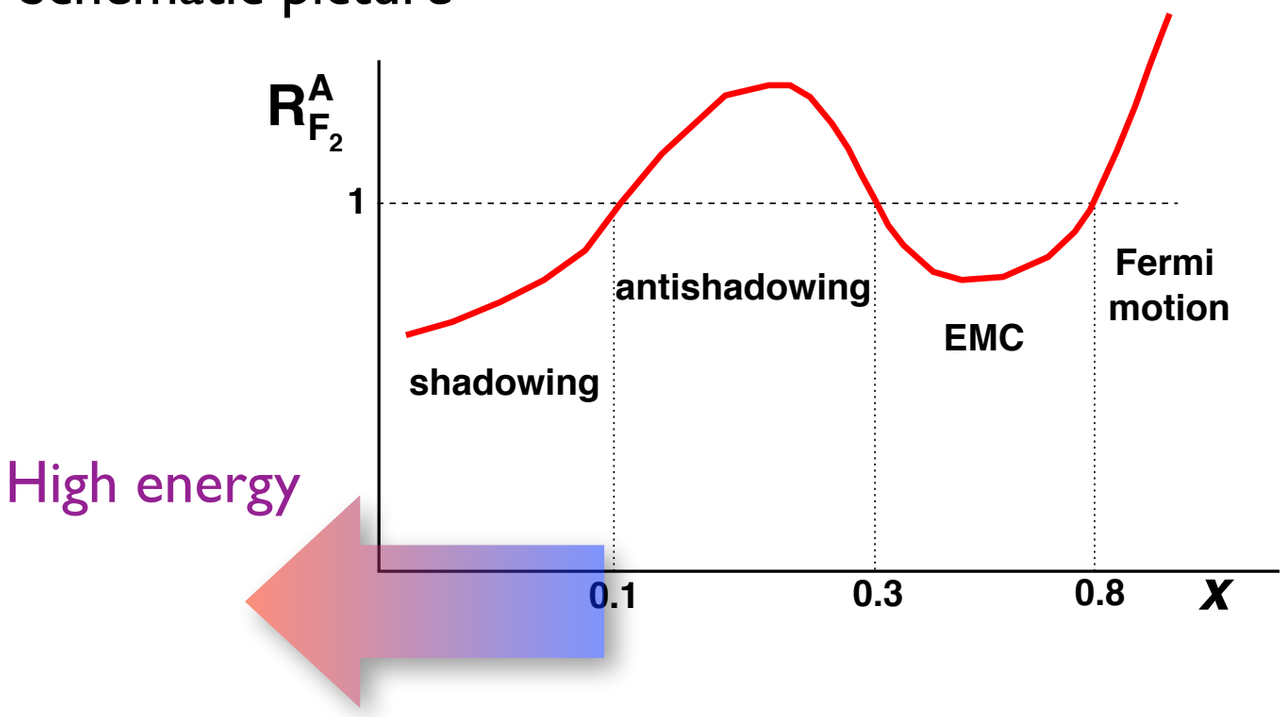


- Fermi motion

$$x \geq 0.8$$

- EMC region

$$0.25 - 0.3 \leq x \leq 0.8$$

- Antishadowing region

$$0.1 \leq x \leq 0.25 - 0.3$$

- Shadowing region

$$x \leq 0.1$$

# Nuclear structure

- Fermi motion:  ratio >1 for x>0.8. Due to motion of bound nucleons inside the nucleus.
- EMC region: EMC collaboration discovered large deviation of the ratio from 1 in the region of 0.3<x<0.8. Usually referred as the EMC effect.
- There exist several explanations. Mean field modification: nucleon structure  is modified by presence of nuclear matter. Possible explanation: Short range correlations between nucleons, most nucleons are not modified but some experiencing SRC are modified (about 20%).

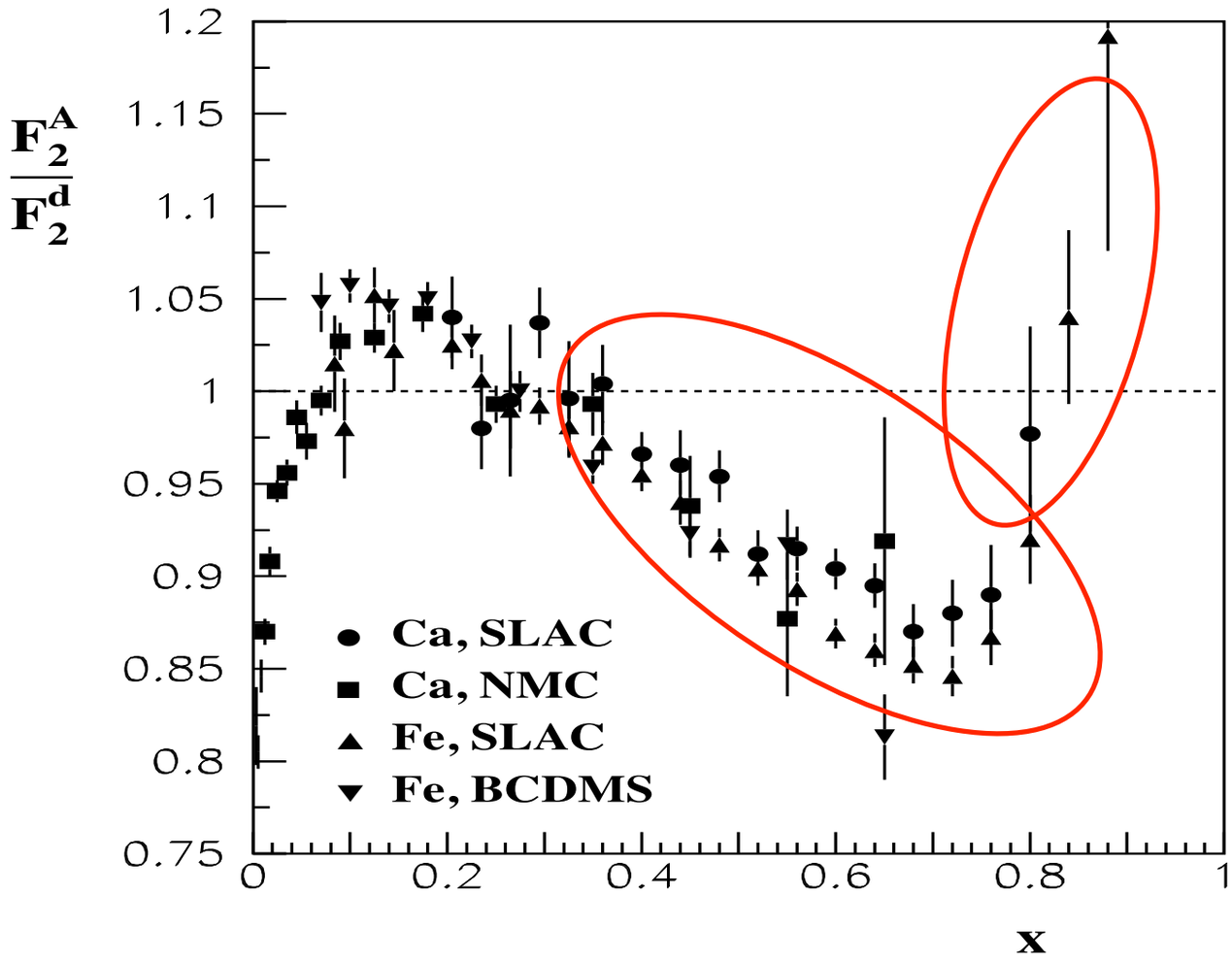

# Nuclear structure

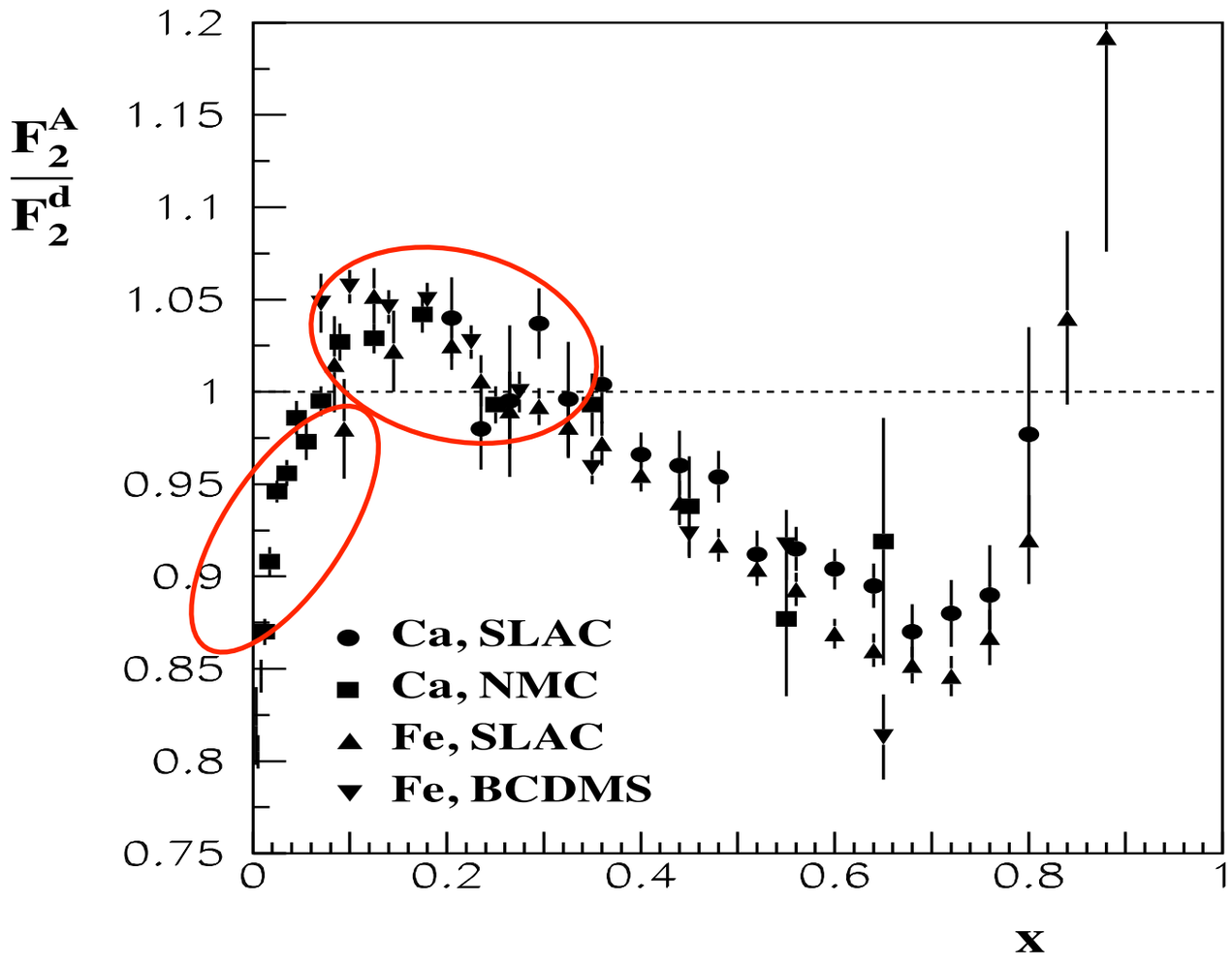


- Antishadowing: Ratio > 1 for 0.1<x<0.3. Momentum sum rule (?)
- Shadowing: ratio < 1 for small x, x<0.1.

# What nuclear data tell us about nuclear shadowing?

## Shadowing increases with A and increases with decreasing x

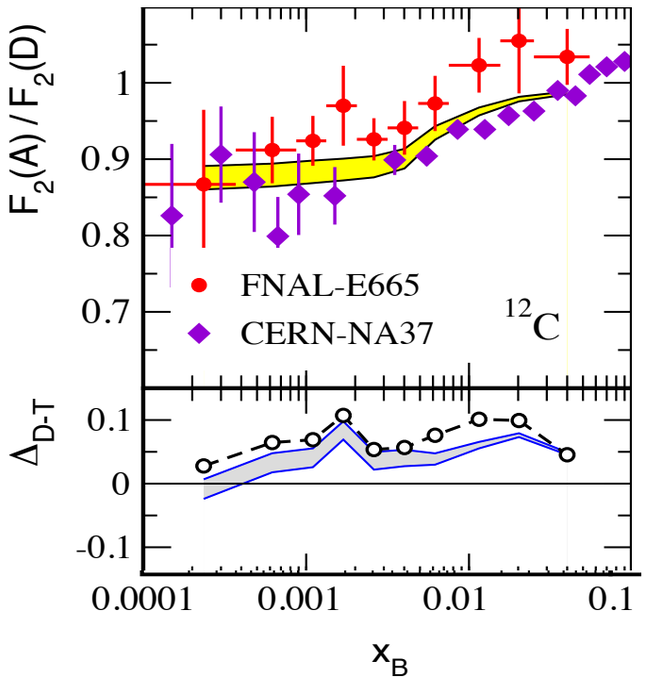


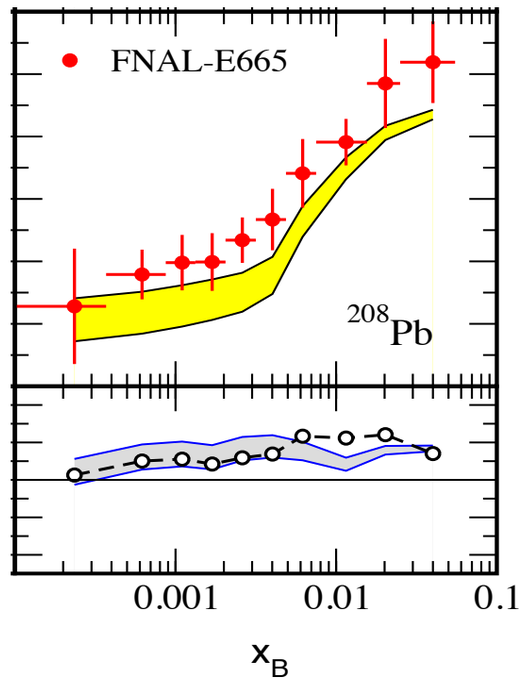


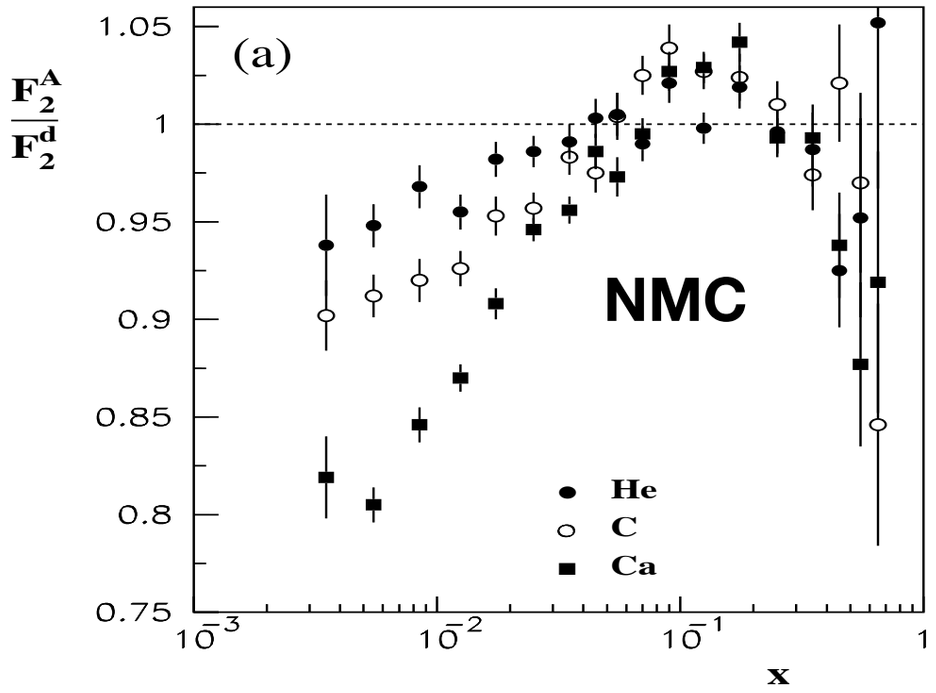


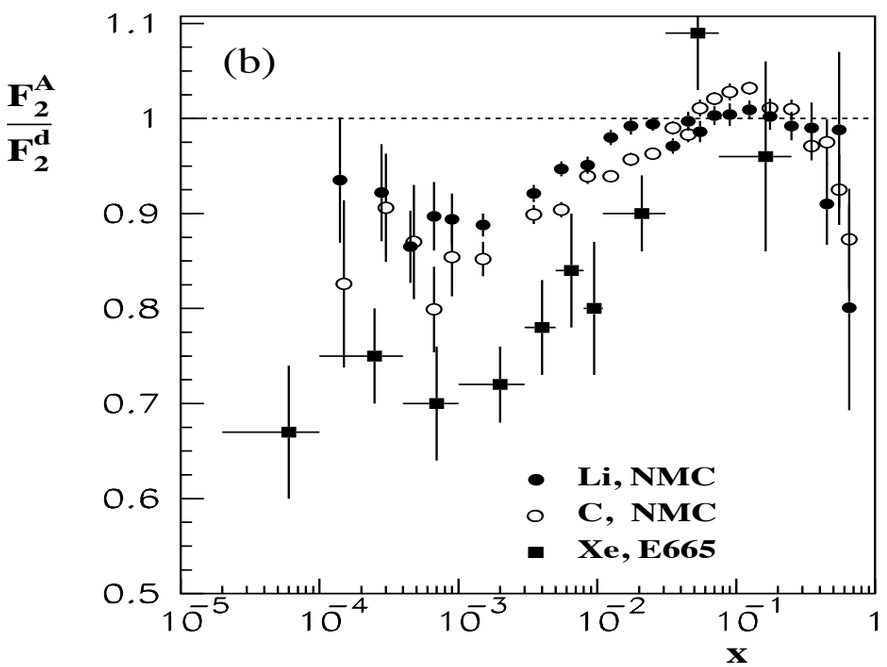


## Shadowing decreases with increasing Q

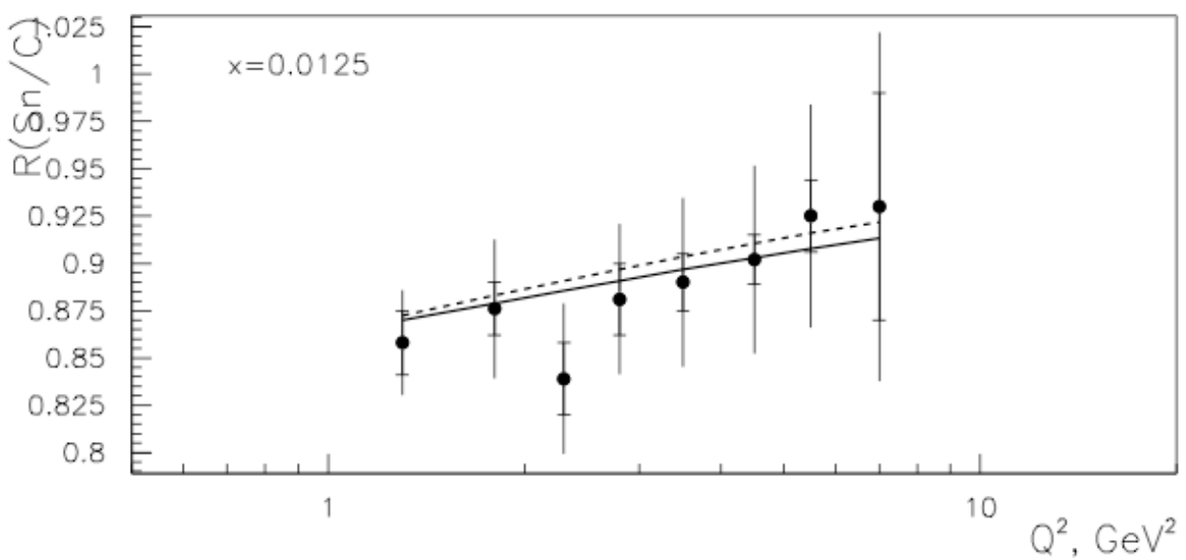

# Approaches to nuclear shadowing

The usual approach to nuclear shadowing is based on multiple scattering.
Models differ significantly.

✦**Glauber rescattering**.

✦Gribov shadowing: relation to **diffraction**.

✦High energy approaches: parton **saturation**.

- There are also approaches which do not try to provide physical explanation of shadowing but rather are based on parametrization.
- **DGLAP** fits to nuclear structure functions resulting in **nuclear PDFs** similar in spirit to the parametrization of proton PDFs.
- The idea behind is that nuclear effects are of **non-perturbative** origin which needs to be parametrized but at high $Q^2$ the DIS on nuclei is fundamentally the same as the DIS on a proton.

$$F_i(x,Q^2) = \sum_j \int_x^1 dy\, C_i^j(x/y, Q^2, \alpha_s)\, f_j(y,Q^2) + \mathcal{O}(\frac{\Lambda^2}{Q^2})$$

$f_j(y,\mu^2)$ Obeys DGLAP evolution

# Comparison of global analyses of nuclear PDFS

Table 1: Key features of recent global analyses of nuclear PDFs.

| Analysis | nCTEQ15HQ (50) | EPPS21 (51) | nNNPDF3.0 (52) | TUJU21 (80) | KSASG20 (81) |
|---|---|---|---|---|---|
| Theoretical input: | | | | | |
| Perturbative order | NLO | NLO | NLO | NNLO | NNLO |
| Heavy-quark scheme | SACOT$-\chi$ | SACOT$-\chi$ | FONLL | FONLL | FONLL |
| Value of $\alpha_s(M_Z)$ | 0.118 | 0.118 | 0.118 | 0.118 | 0.118 |
| Charm mass $m_c$ | 1.3 GeV | 1.3 GeV | 1.51 GeV | 1.43 GeV | 1.3 GeV |
| Bottom mass $m_b$ | 4.5 GeV | 4.75 GeV | 4.92 GeV | 4.5 GeV | 4.75 GeV |
| Input scale $Q_0$ | 1.3 GeV | 1.3 GeV | 1.0 GeV | 1.3 GeV | 1.3 GeV |
| Data points | 1484 | 2077 | 2188 | 2410 | 4353 |
| Independent flavors | 5 | 6 | 6 | 4 | 3 |
| Parameterization | Analytic | Analytic | Neural network | Analytic | Analytic |
| Free parameters | 19 | 24 | 256 | 16 | 18 |
| Error analysis | Hessian | Hessian | Monte Carlo | Hessian | Hessian |
| Tolerance | $\Delta\chi^2 = 35$ | $\Delta\chi^2 = 33$ | N/A | $\Delta\chi^2 = 50$ | $\Delta\chi^2 = 20$ |
| Proton PDF | ∼CTEQ6.1 | CT18A | ∼NNPDF4.0 | ∼HERAPDF2.0 | CT18 |
| Proton PDF correlations | | ✓ | ✓ | | |
| Deuteron corrections | (✓)[a,b] | ✓[c] | ✓ | ✓ | ✓ |
| Fixed-target data: | | | | | |
| SLAC/EMC/NMC NC DIS | ✓ | ✓ | ✓ | ✓ | ✓ |
| – Cut on $Q^2$ | 4 GeV$^2$ | 1.69 GeV$^2$ | 3.5 GeV$^2$ | 3.5 GeV$^2$ | 1.2 GeV$^2$ |
| – Cut on $W^2$ | 12.25 GeV$^2$ | 3.24 GeV$^2$ | 12.5 GeV$^2$ | 12.0 GeV$^2$ | |
| JLab NC DIS | (✓)[a] | ✓ | | | ✓ |
| CHORUS/CDHSW CC DIS | (✓/-)[b] | ✓/- | ✓/- | ✓/✓ | ✓/✓ |
| NuTeV/CCFR 2$\mu$ CC DIS | (✓/✓)[b] | | ✓/- | | |
| $pA$ DY | ✓ | ✓ | ✓ | | ✓ |
| $\pi A$ DY | | ✓ | | | |
| Collider data: | | | | | |
| $Z$ bosons | ✓ | ✓ | ✓ | ✓ | |
| $W^{\pm}$ bosons | ✓ | ✓ | ✓ | ✓ | |
| Light hadrons | ✓ | ✓[d] | | | |
| – Cut on $p_T$ | 3 GeV | 3 GeV | | | |
| Jets | | ✓ | ✓ | | |
| Prompt photons | | | ✓ | | |
| Prompt D$^0$ | ✓ | ✓ | ✓[e] | | |
| – Cut on $p_T$ | 3 GeV | 3 GeV | 0 GeV | | |
| Quarkonia ($J/\psi$, $\psi'$, $\Upsilon$) | ✓ | | | | |

[a] nCTEQ15HIX (26); [b] nCTEQ15$\nu$ (114); [c] through CT18A; [d] only $\pi^0$ in DAu; [e] only forward ($y > 0$).

*Klasen, Paukkunen, 2311.00450*

# EPPS21 example

Bound proton PDF for species i and nucleus with mass number A: $f_i^{\mathrm{p}/A}(x, Q^2)$

Defined relative to the free proton PDF:

$$f_i^{\mathrm{p}/A}(x, Q^2) = R_i^A(x, Q^2) f_i^{\mathrm{p}}(x, Q^2)$$

**Nuclear modification factor** $R_i^A(x, Q^2)$

Free proton PDF baseline CT18ANLO

$$R_i^A(x, Q_0^2) =$$

$$\begin{cases} a_0 + a_1(x - x_a)\left[e^{-xa_2/x_a} - e^{-a_2}\right], & x \le x_a \\ b_0 x^{b_1}(1-x)^{b_2} e^{xb_3}, & x_a \le x \le x_e \\ c_0 + c_1(c_2 - x)(1-x)^{-\beta}, & x_e \le x \le 1. \end{cases}$$

Parameters a,b,c fixed by the requirement of continuity of function and derivative and the following constraints:

$y_0 = R_i^A(x \to 0, Q_0^2)$ **Small x shadowing**

$y_a = R_i^A(x_a, Q_0^2)$ **Antishadowing max.**

$y_e = R_i^A(x_e, Q_0^2)$ **EMC min.**

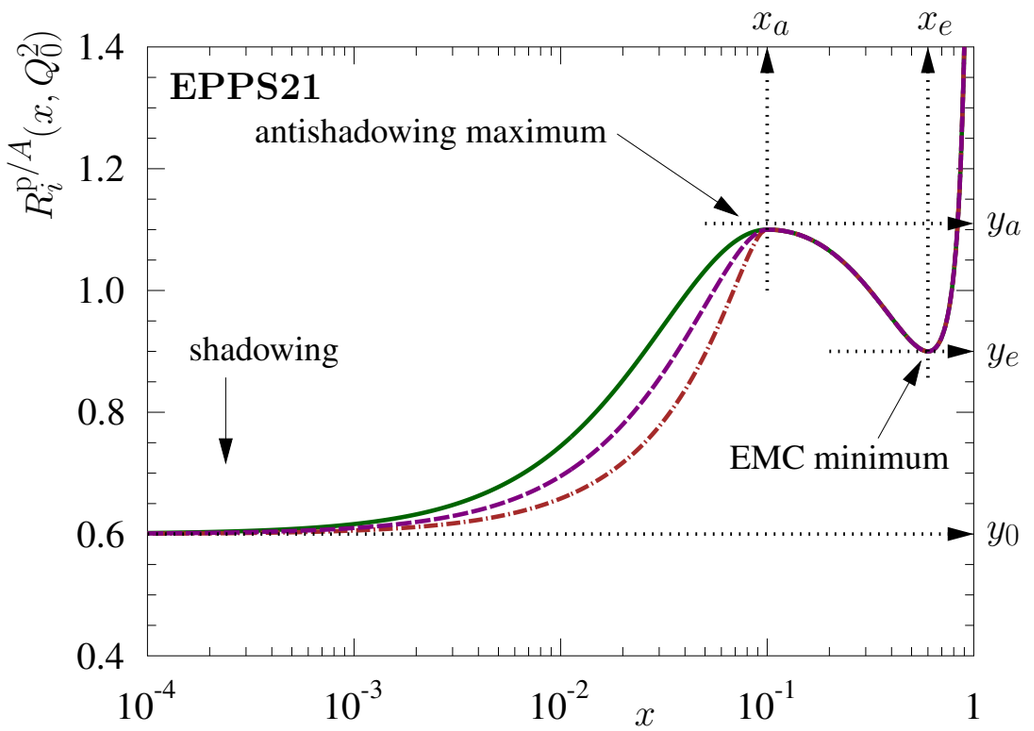


**Fig. 1** Prototype of the EPPS21 fit functions $R_i^A(x, Q_0^2)$. The solid green line corresponds to $a_2 = 2$, the dashed purple line to $a_2 = 0$, and the brown dotted-dashed line to $a_2 = -3$.

# EPPS21 example

A dependence of the height parameters:

$$y_i(A) = 1 + \Big[y_i(A_{\rm ref}) - 1\Big] \left(\frac{A}{A_{\rm ref}}\right)^{\gamma_i}$$

$$A_{\rm ref} = 12$$

$$\int_0^1 dx f_{u_{\rm V}}^{{\rm p}/A}(x, Q_0^2) = 2,$$

$$\int_0^1 dx f_{d_{\rm V}}^{{\rm p}/A}(x, Q_0^2) = 1,$$

Valence quark sum rules

$$\int_0^1 dx x \sum_i f_i^{{\rm p}/A}(x, Q_0^2) = 1,$$

Momentum sum rule

Deuteron A=2 is assumed to be free from nuclear effects

Bound neutron PDFs are determined from bound proton PDFs through isospin symmetry.

$$f_{u,\overline{u}}^{{\rm n}/A}(x, Q^2) = f_{d,\overline{d}}^{{\rm p}/A}(x, Q^2),$$
$$f_{d,\overline{d}}^{{\rm n}/A}(x, Q^2) = f_{u,\overline{u}}^{{\rm p}/A}(x, Q^2),$$
$$f_i^{{\rm n}/A}(x, Q^2) = f_i^{{\rm p}/A}(x, Q^2) \quad \text{for other flavours.}$$

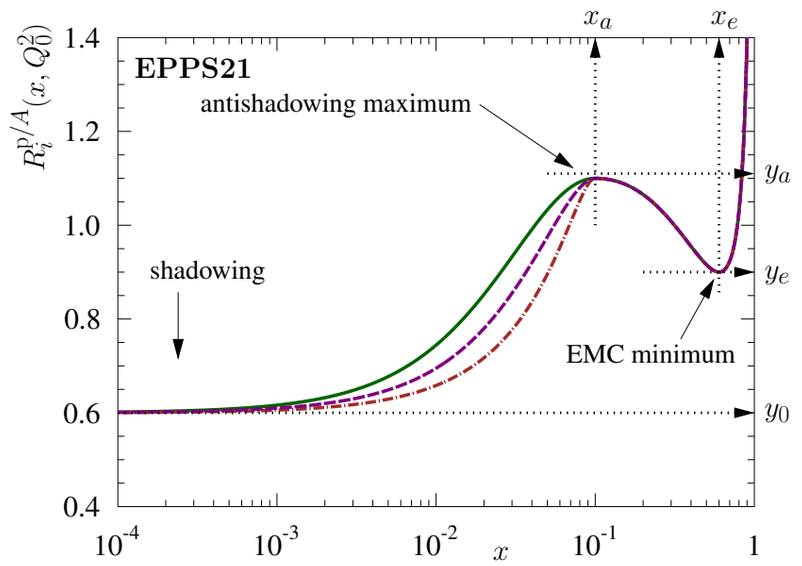


**Fig. 1** Prototype of the EPPS21 fit functions $R_i^A(x, Q_0^2)$. The solid green line corresponds to $a_2 = 2$, the dashed purple line to $a_2 = 0$, and the brown dotted-dashed line to $a_2 = -3$.

# EPPS21 example: data used

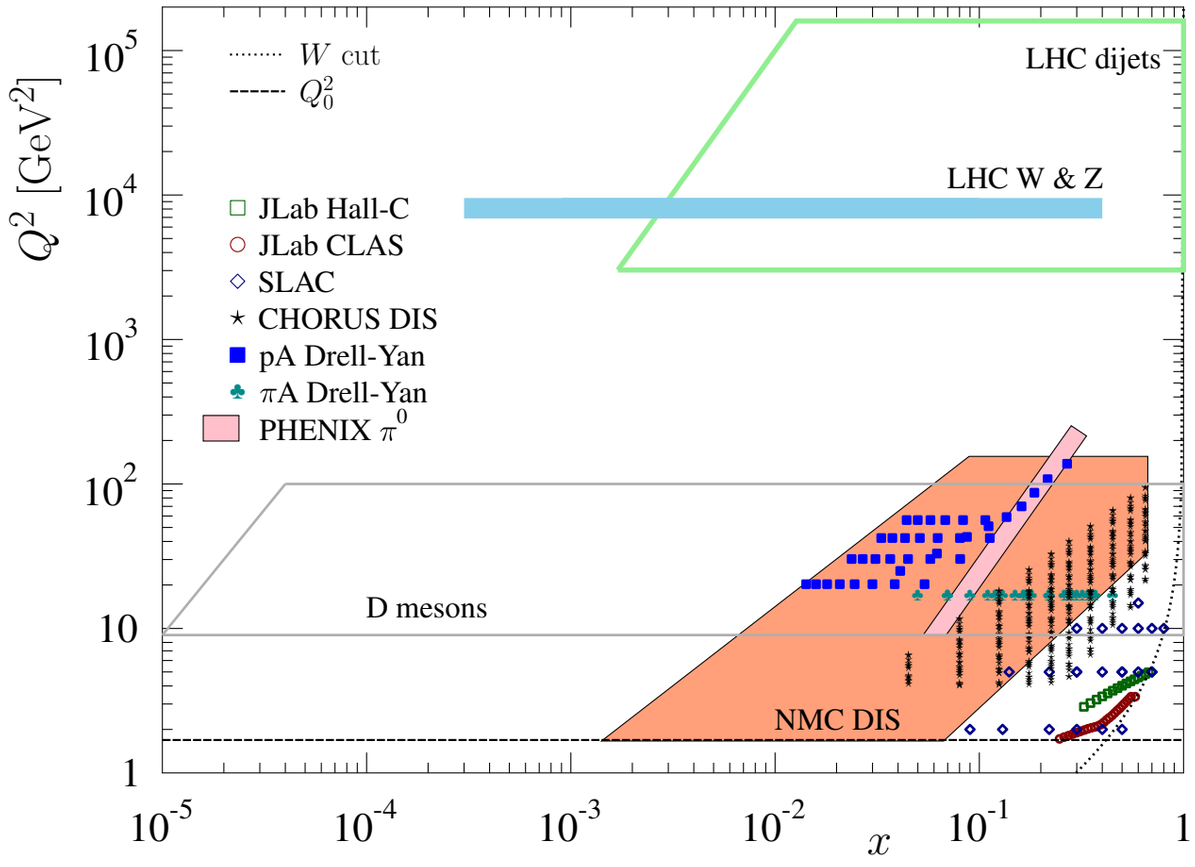


- Fixed target eA DIS and pA Drell-Yan
- Neutrino data
- Pion data from dA
- LHC data from dijets and electroweak W,Z boson production, D meson

**Table 2** The data used in the EPPS21 analysis. The new data with respect to the EPPS16 analysis are marked with a star.

| Experiment | Observable | Collisions | Data points | $\chi^2$ | Normalization | Ref. |
|---|---|---|---|---|---|---|
| JLab Hall C★ | DIS | $e^-$He(3), $e^-$D | 15 | 4.47 | 1.027 | [13] |
| JLab Hall C★ | DIS | $e^-$He(4), $e^-$D | 15 | 4.33 | 0.985 | [13] |
| SLAC E139 | DIS | $e^-$He(4), $e^-$D | 16 | 7.75 | 0.997 | [43] |
| CERN NMC 95, re. | DIS | $\mu^-$He(4), $\mu^-$D | 16 | 17.90 | 1.000 | [44] |
| CERN NMC 95, $Q^2$ dep. | DIS | $\mu^-$Li(6), $\mu^-$D | 153 | 159.74 | 1.002 | [45] |
| JLab Hall C★ | DIS | $e^-$Be(9), $e^-$D | 15 | 4.72 | 0.971 | [13] |
| SLAC E139 | DIS | $e^-$Be(9), $e^-$D | 15 | 15.19 | 0.990 | [43] |
| CERN NMC 96 | DIS | $\mu^-$Be(9), $\mu^-$C | 15 | 4.84 | 1.000 | [46] |
| JLab Hall C★ | DIS | $e^-$C(12), $e^-$D | 15 | 2.58 | 0.981 | [13] |
| SLAC E139 | DIS | $e^-$C(12), $e^-$D | 6 | 4.89 | 0.998 | [43] |
| CERN NMC 95, $Q^2$ dep. | DIS | $\mu^-$C(12), $\mu^-$D | 165 | 131.25 | 0.997 | [45] |
| CERN NMC 95, re. | DIS | $\mu^-$C(12), $\mu^-$D | 16 | 16.99 | 0.998 | [44] |
| CERN NMC 95, re. | DIS | $\mu^-$C(12), $\mu^-$Li(6) | 20 | 16.27 | 0.997 | [44] |
| JLab CLAS★ | DIS | $e^-$C(12), $\mu^-$D(6) | 25 | 19.41 | 0.996 | [14] |
| FNAL E772 | DY | pC(12), pD | 9 | 8.20 | - | [56] |
| SLAC E139 | DIS | $e^-$Al(27), $e^-$D | 15 | 10.58 | 0.994 | [43] |
| CERN NMC 96 | DIS | $\mu^-$Al(27), $\mu^-$C(12) | 15 | 7.02 | 1.000 | [46] |
| JLab CLAS★ | DIS | $e^-$Al(27), $e^-$D | 25 | 20.68 | 1.004 | [14] |
| SLAC E139 | DIS | $e^-$Ca(40), $e^-$D | 6 | 3.91 | 0.989 | [43] |
| CERN NMC 95, re. | DIS | $\mu^-$Ca(40), $\mu^-$D | 15 | 30.45 | 1.004 | [44] |
| CERN NMC 95, re. | DIS | $\mu^-$Ca(40), $\mu^-$Li(6) | 20 | 17.08 | 0.998 | [44] |
| CERN NMC 96 | DIS | $\mu^-$Ca(40), $\mu^-$C(12) | 15 | 8.35 | 1.001 | [46] |
| FNAL E772 | DY | pCa(40), pD | 9 | 2.59 | - | [56] |
| SLAC E139 | DIS | $e^-$Fe(56), $e^-$D | 20 | 23.86 | 1.002 | [43] |
| CERN NMC 96 | DIS | $\mu^-$Fe(56), $\mu^-$C(12) | 15 | 11.11 | 1.001 | [46] |
| JLab CLAS★ | DIS | $e^-$Fe(56), $e^-$D | 25 | 26.74 | 1.005 | [14] |
| FNAL E772 | DY | $e^-$Fe(56), $e^-$D | 9 | 2.03 | - | [56] |
| FNAL E866 | DY | pFe(56), pBe(9) | 28 | 21.04 | - | [57] |
| CERN EMC | DIS | $\mu^-$Cu(64), $\mu^-$D | 19 | 15.13 | - | [48] |
| SLAC E139 | DIS | $e^-$Ag(108), $e^-$D | 6 | 8.13 | 0.990 | [43] |
| CERN NMC 96 | DIS | $\mu^-$Sn(117), $\mu^-$C(12) | 15 | 10.90 | 0.999 | [46] |
| CERN NMC 96, $Q^2$ dep. | DIS | $\mu^-$Sn(117), $\mu^-$C(12) | 144 | 84.44 | 0.999 | [47] |
| FNAL E772 | DY | pW(184), pD | 9 | 5.93 | - | [56] |
| FNAL E866 | DY | pW(184), pBe(9) | 28 | 25.82 | - | [57] |
| CERN NA10 | DY | $\pi^-$W(184), $\pi^-$D | 10 | 10.87 | 1.040(h.e), 1.116(l.e) | [89] |
| FNAL E615 | DY | $\pi^+$W(184), $\pi^-$W(184) | 11 | 13.26 | - | [87] |
| CERN NA3 | DY | $\pi^-$Pt(195), $\pi^-$H | 7 | 4.70 | - | [88] |
| SLAC E139 | DIS | $e^-$Au(197), $e^-$D | 16 | 19.70 | 0.999 | [43] |
| RHIC PHENIX | $\pi^0$ | dAu(197), pp | 17 | 6.68 | 1.008 | [80] |
| CERN NMC 96 | DIS | $\mu^-$Pb(207), $\mu^-$C(12) | 15 | 4.29 | 1.000 | [46] |
| JLab CLAS★ | DIS | $e^-$Pb(208), $e^-$D | 25 | 15.39 | 0.994 | [14] |
| CERN CHORUS | DIS | $\nu$Pb(208), $\bar{\nu}$Pb(208) | 824 | 990.95 | - | [49] |
| CERN CMS 5TeV | $W^\pm$ | pPb(208) | 10 | 11.82 | - | [60] |
| CERN CMS 8TeV★ | $W^\pm$ | pPb(208), pp | 44 | 41.30 | 0.996 | [9] |
| CERN CMS | Z | pPb(208) | 6 | 6.80 | - | [61] |
| CERN ATLAS | Z | pPb(208) | 7 | 8.91 | - | [62] |
| CERN CMS★ | dijet | pPb(208) | 83 | 123.81 | - | [58] |
| CERN LHCb★ | D meson | pPb(208) | 48 | 45.71 | 0.999(fwd.), 1.010(bwd.) | [4] |
| Total | | | 2077 | 2058.5 | | |

# Nuclear PDFs: EPPS21 carbon

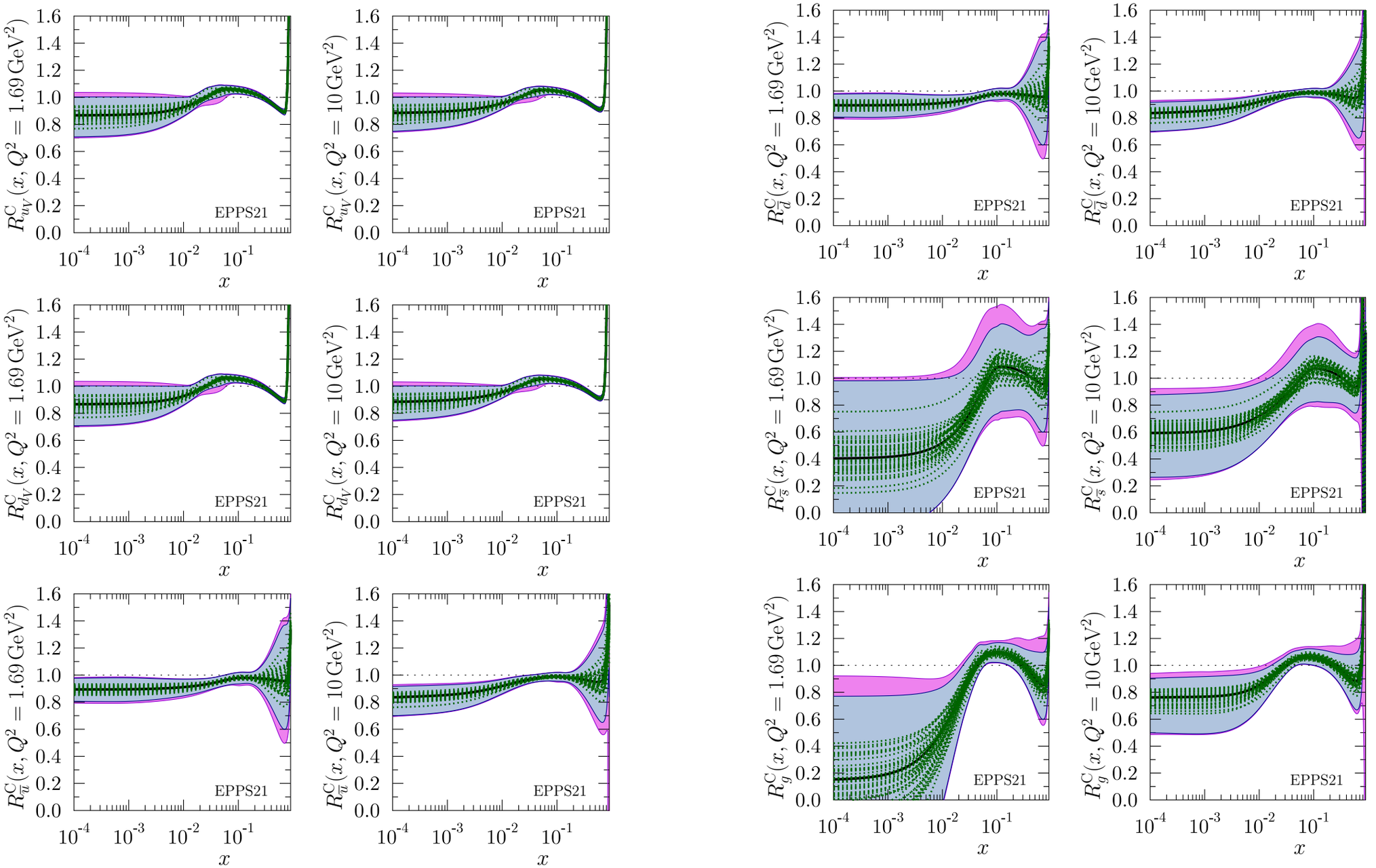


Nuclear modification for carbon for various flavors and gluons, at two scales $Q^2 = 1.69,10\ \mathrm{GeV}^2$

# Nuclear PDFs: EPPS21 lead

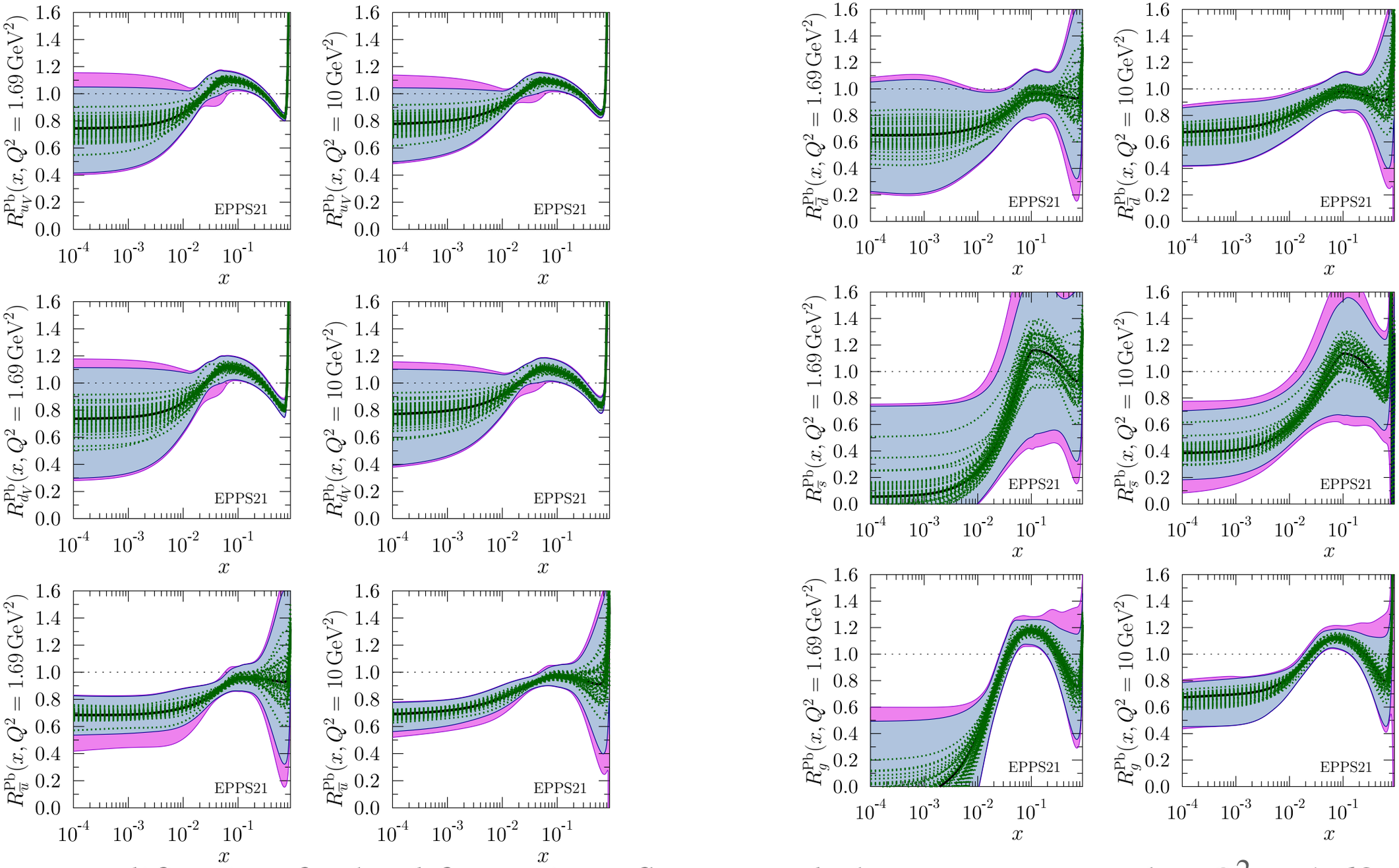


Nuclear modification for lead for various flavors and gluons, at two scales $Q^2 = 1.69,10\ \mathrm{GeV}^2$

Large uncertainties, particularly at low values of x

# Comparison of various nuclear PDFs

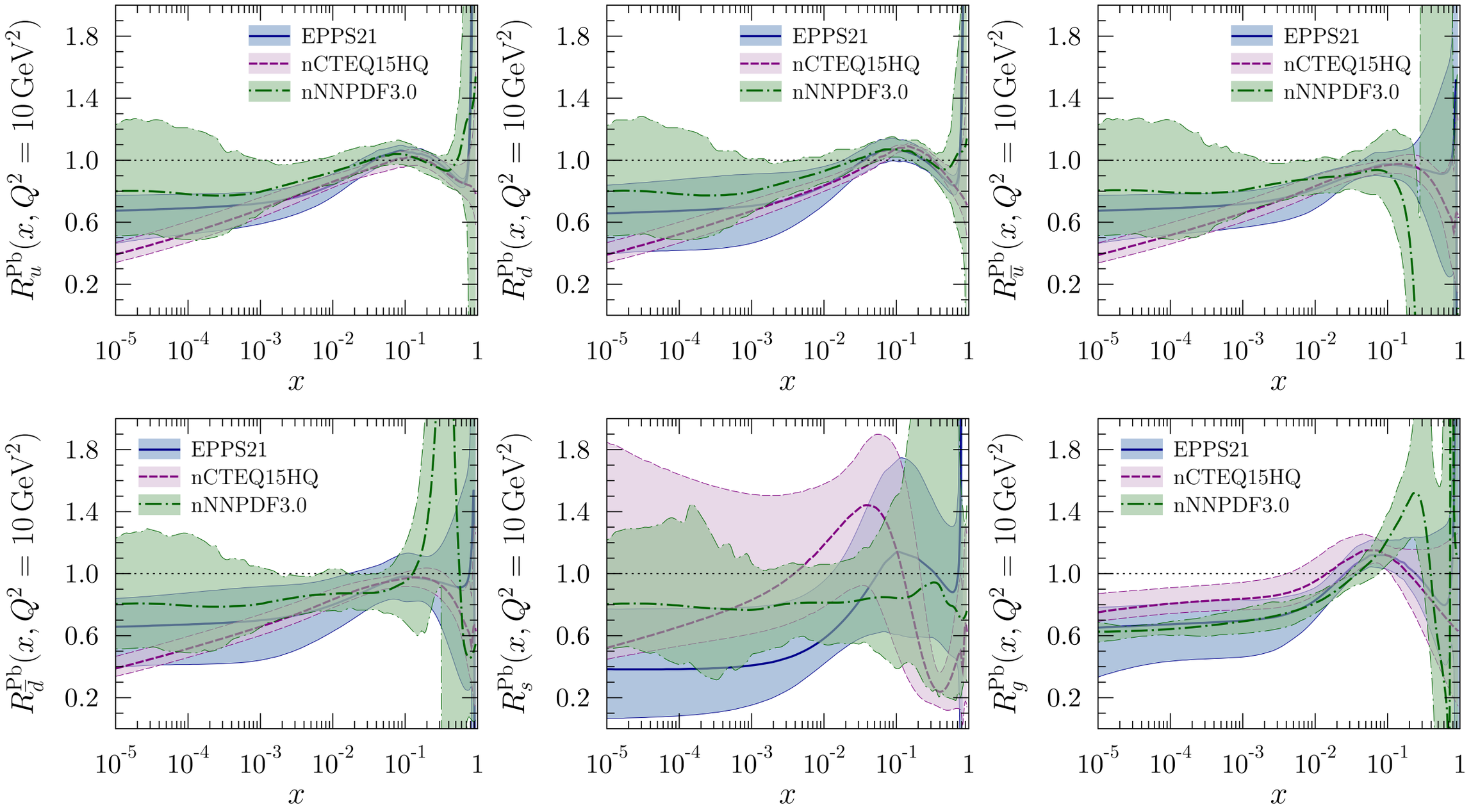

# Prospects at EIC

*kinematic plane EIC*

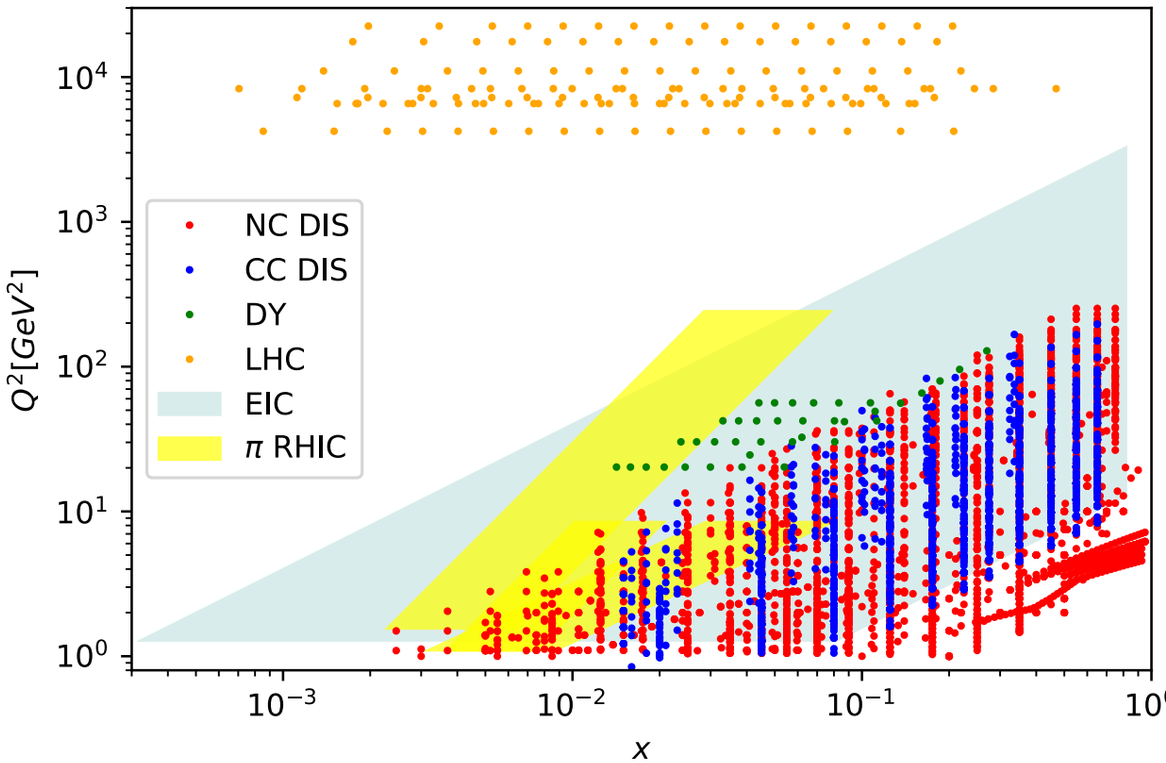


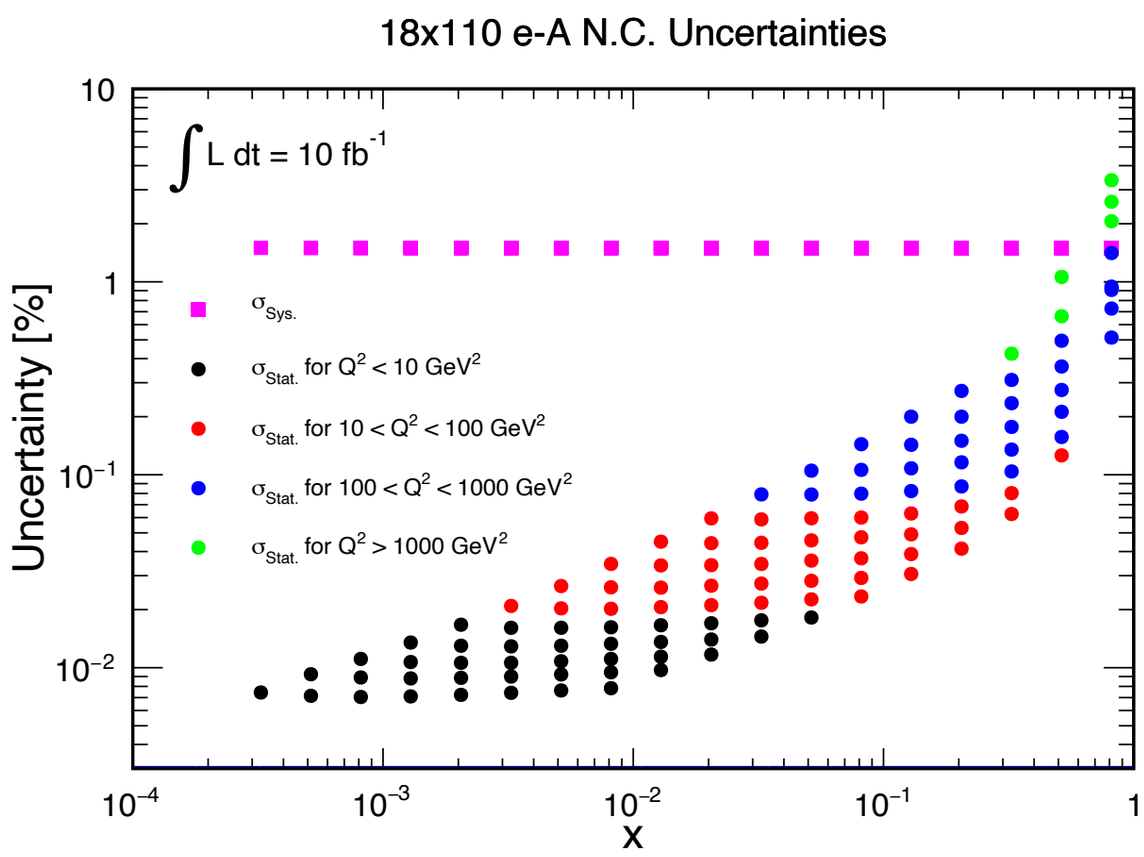


- Precise measurement of **nuclear structure functions** for wide range of nuclei and **wide kinematic range**
- Sys. uncertainties at most few %, stat. negligible
- Proton, deuteron and wide range nuclei structure function within **one facility:** reduction of uncertainties

# Global nuclear structure: structure functions

*Aschenauer, Fazio, Lamont, Paukkunen, Zurita*

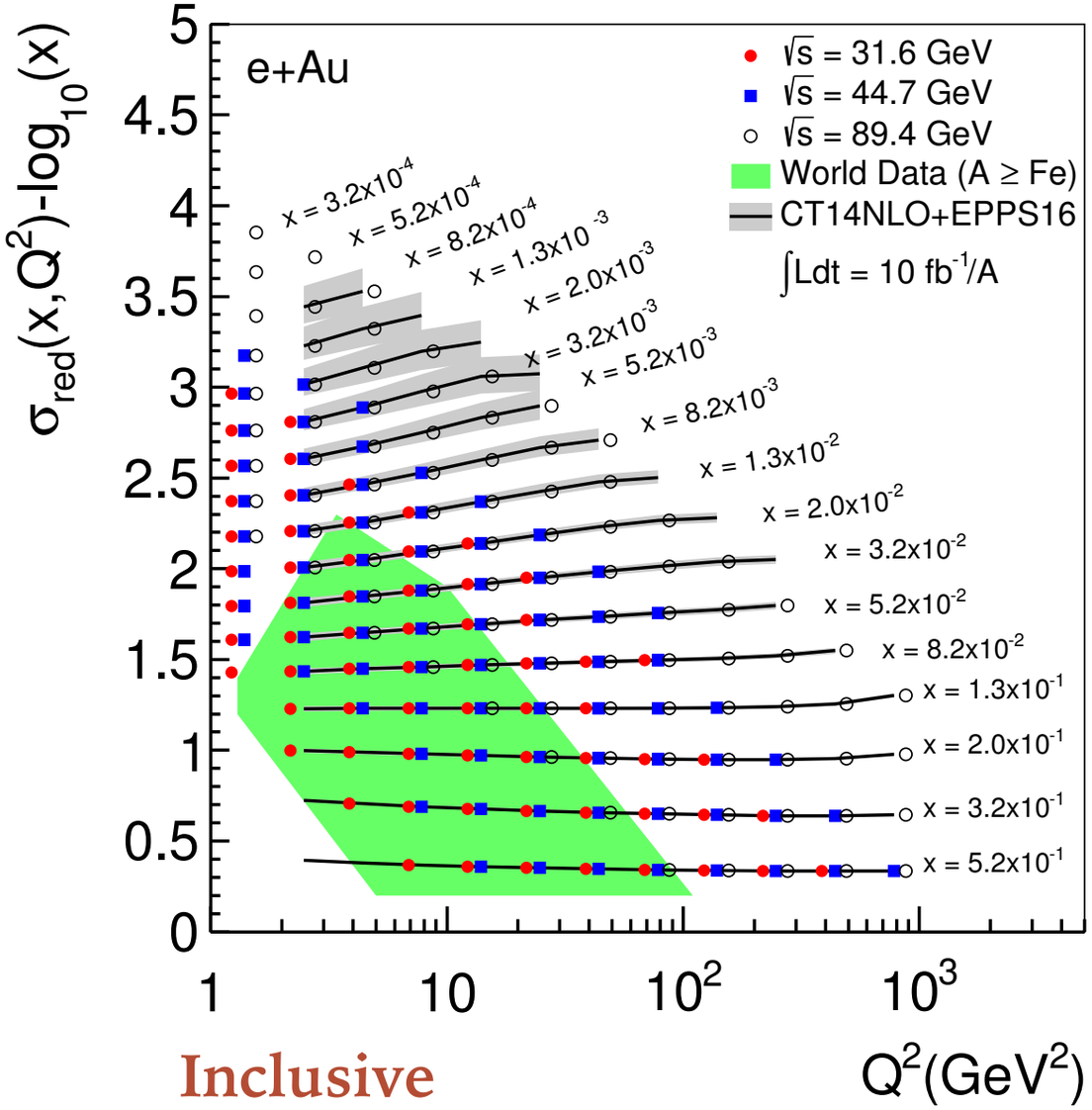


Inclusive

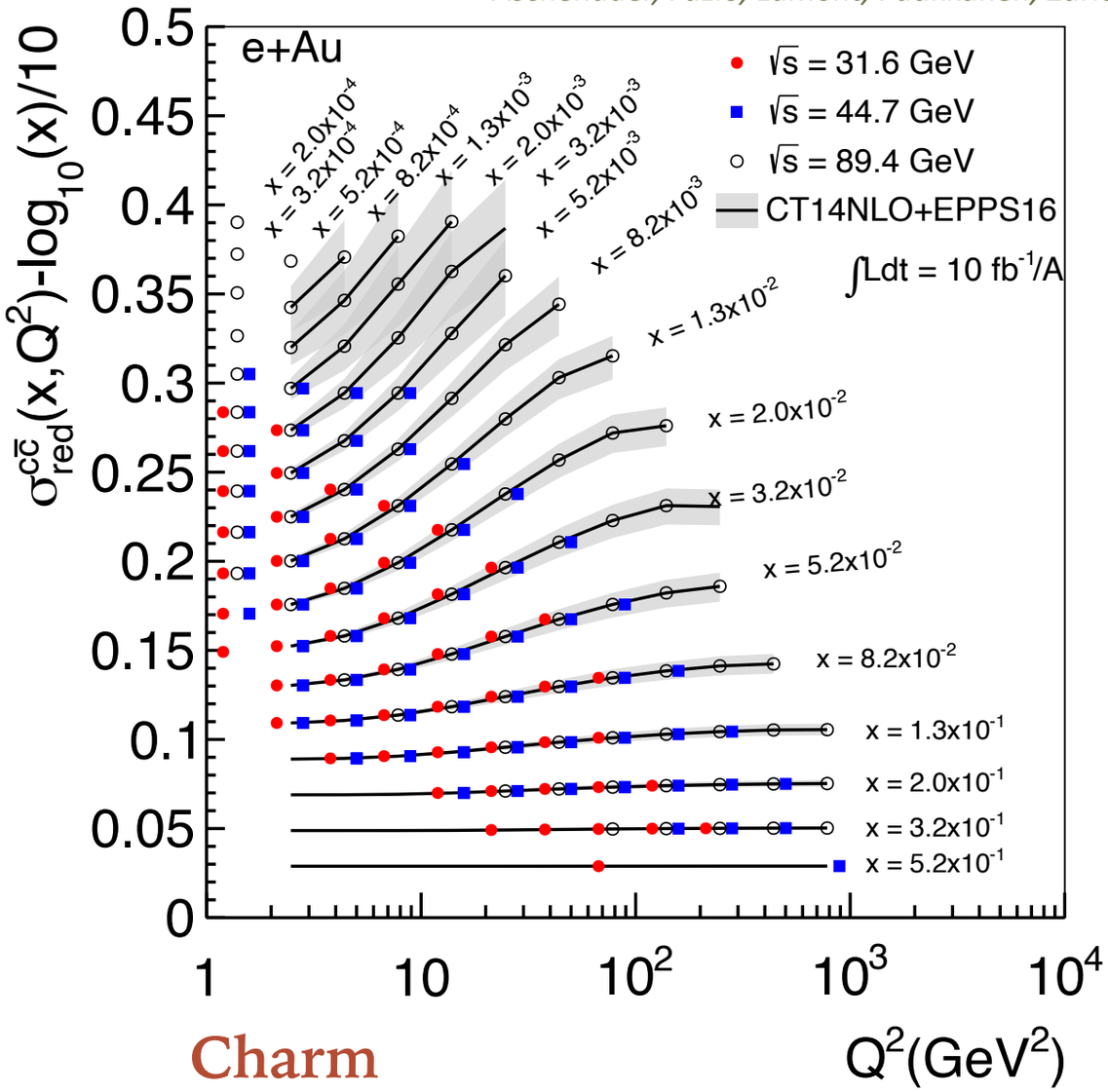


Charm

- Precision measurements of the reduced cross section
- Charm component in nuclei
- Errors much smaller than the uncertainties of QCD predictions

# Impact of EIC on nuclear PDFs

## Collinear factorization

$$F_{2,L}(x,Q^2) = \sum_j \int_x^1 dz\, C_{2,L}(Q/\mu, x/z; \alpha_s)\, f_j(z,\mu) + \ldots$$

Nuclear modification in this framework:

**initial condition** at low scales, **linear evolution with scale**

- Impact of **charm cross section** on the gluon PDF at high x
- Charm is produced mainly in the photon-gluon fusion process
- Further constraints: $\mathbf{F_L}$

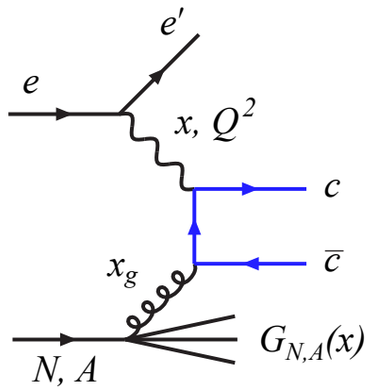


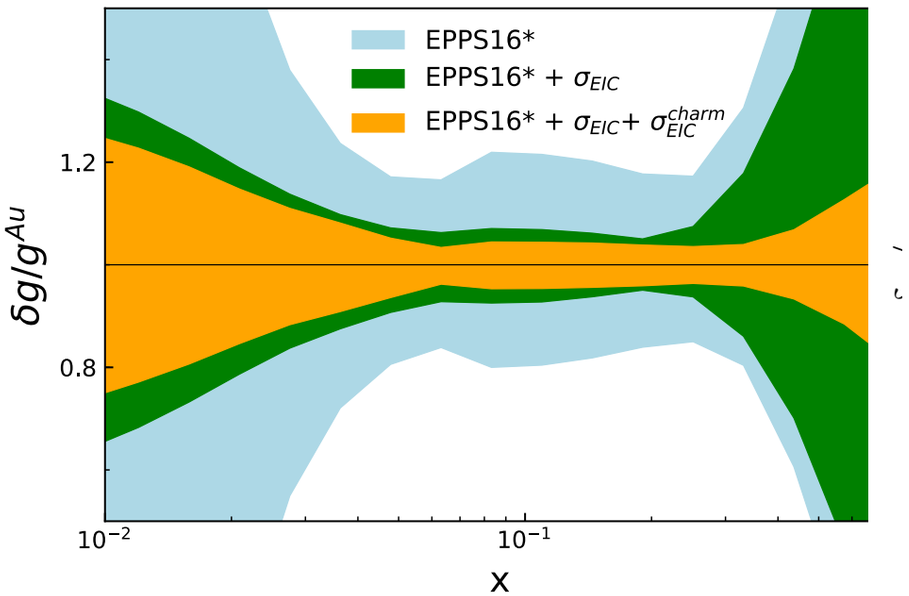


## DGLAP : linear evolution

$$\frac{d}{d\ln\mu^2} f_j(z,\mu) = \sum_k \int \frac{d\xi}{\xi} P_{jk}(\xi,\alpha_s) f_k(z/\xi,\mu)$$

*Yellow Report*

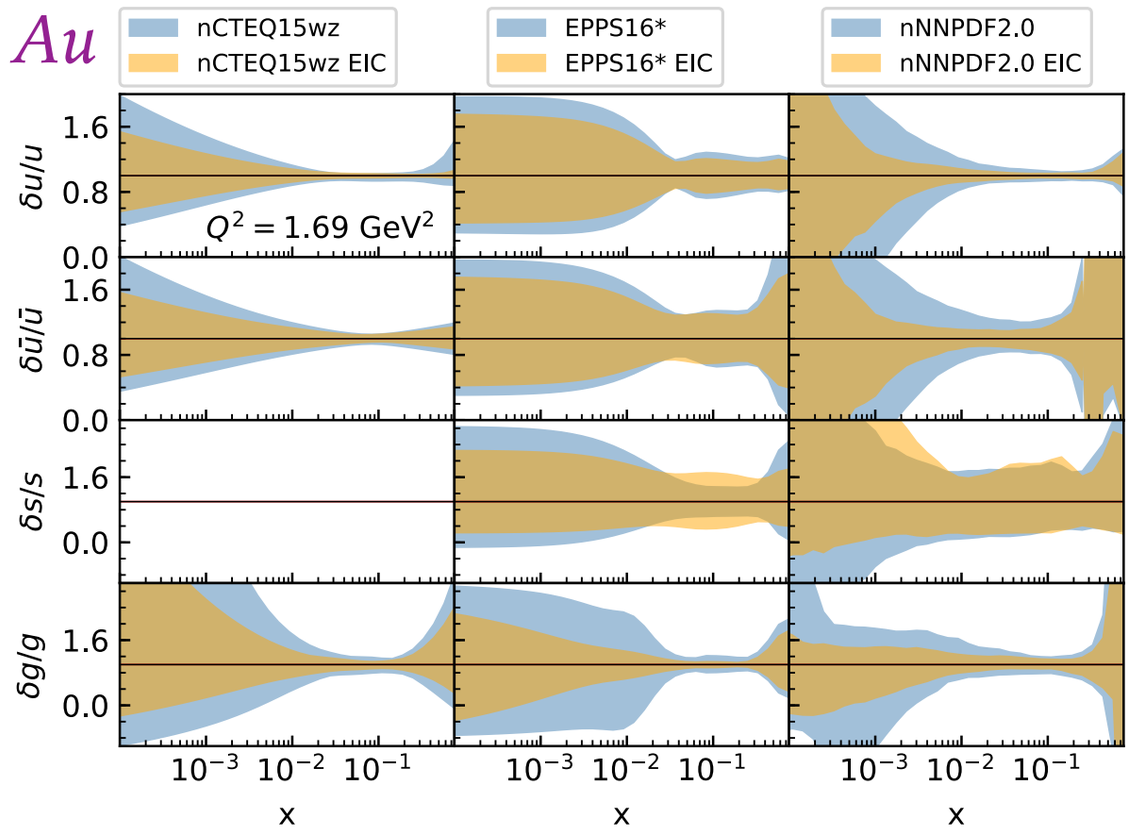


**Significant impact of EIC measurements on nuclear PDFs**